

MECHANISMS OF STRUCTURE DIRECTION
IN ZEOLITE SYNTHESIS

Thesis by
Sandra Louise Burkett

In Partial Fulfillment of the Requirements
for the Degree of
Doctor of Philosophy

California Institute of Technology
Pasadena, California

1995

(Submitted November 14, 1994)

To my parents

Acknowledgments

First and foremost, I would like to express my sincerest appreciation to Professor Mark Davis for his enthusiasm, guidance, and encouragement over the past four years. I have been fortunate to work with someone who has such a true appreciation of the “big picture” of chemistry as well as depth of understanding. I have the utmost respect for Mark as a scientist, an advisor, and a person.

The diversity of personalities and interests among the members of the Davis group has made for a dynamic and enjoyable learning environment. I would like to thank my colleagues, past and present, for their help and expertise. Special thanks go to Dr. Hong-Xin Li for teaching me the basics of solid state NMR and Dr. Hubert Koller for providing greater knowledge of the field. Chris Dartt has been a very helpful coworker as well as a close friend. I would also like to acknowledge Bog Kuszta and Tom Dunn of the division staff for their time and assistance in keeping the temperamental NMR instrument functioning.

I have enjoyed many discussions, both scientific and otherwise, with Dr. Stacey Zones of the Chevron Research and Technology Company. I appreciate his continued interest in this project, and I would like to acknowledge financial support of this research from the Chevron Research and Technology Company and from the Caltech Consortium in Chemistry and Chemical Engineering.

Outside of lab, there are several special people whose friendship and understanding have been invaluable. I will dearly miss Julia Hodge and our sporadically regular Sunday morning bikerides, innumerable Buster’s runs, and shared sense of humor. I have always looked forward to Friday

lunches with Susanne Lin, sharing stories and solving problems over pizza at Pinnochio's. Hali Forstner has also provided many welcome distractions. For the past year and a half, Suzanne D'Ascoli has been the best roommate one could ever hope to find, always with a tempting invitation and a funny story to make me smile. Another wonderful roommate, Brenda Fiala Stewart has already moved on to bigger and better things. I am grateful to Maureen Hughes MacAloon and Bryan Coughlin for their patience as ski instructors. I am indebted to Wayne Larson and Todd Richmond for introducing me to the thrills of mountain biking and the perils of Josephine Peak, and for welcoming me as softball Scum.

For the past three years, both in person and long-distance, Bryan Coughlin has been a source of seemingly infinite patience and understanding. Our truly special friendship has kept me going through the hills and valleys of my experience at Caltech.

Finally, I would like to thank my parents and my brother, Bill, for their unwavering support and encouragement through the years. Without their love, this journey would not have been possible.

Abstract

The mechanisms by which the geometries of organic structure-directing agents are translated into the product pore architectures in the synthesis of pure-silica and aluminosilicate zeolites are investigated by numerous spectroscopic techniques and variations in synthesis gel composition. For the tetrapropylammonium- and 1,6-hexanediamine-mediated syntheses of pure-silica ZSM-5 (Si-ZSM-5), ^1H - ^{29}Si CP MAS NMR is performed between the protons of the organic species and the silicon atoms of the zeolite framework precursors in a deuterated synthesis medium to probe the interactions between the organic and inorganic components. The origin of structural specificity in the synthesis of pure-silica zeolites in the presence of structure-directing agents is attributed to the formation of favorable intermolecular van der Waals interactions within inorganic-organic composite species that form the key components in zeolite self-assembly. Investigation of the ^1H - ^{29}Si CP MAS NMR profiles of silicate gels containing tetraalkylammonium cations that do not induce the formation of a crystalline zeolite product suggest the significance of hydrophobic hydration of the organic component in the formation of the inorganic-organic composite structures that is essential to the synthesis of pure-silica zeolites. For the syntheses of the hexagonal (EMT) and cubic (FAU) polymorphs of the aluminosilicate zeolite faujasite in the presence of 18-crown-6 and 15-crown-5, respectively, a combination of NMR and vibrational spectroscopic techniques and variations in the synthesis compositions are used to elucidate the structure-directing roles of the crown ethers. Sodium/crown ether complexes facilitate and direct the assembly of sodium-templated extended aluminosilicate structures via

ion–dipole interactions to form the EMT and FAU products. Thus, for the synthesis of Si–ZSM-5 and the synthesis of EMT and FAU, two different mechanisms of structure direction and self-assembly via the formation of extended inorganic or inorganic–organic composite species are proposed.

Table of Contents

Acknowledgments.....	iii
Abstract.....	v
List of Figures.....	x
List of Tables	xix
List of Abbreviations	xx

Chapter One

<i>Structure Direction in Zeolite Synthesis</i>	1
Introduction.....	2
Issues in Structure Direction and Zeolite Synthesis.....	3
References	15

Chapter Two

<i>Mechanism of Structure Direction in the TPA-Mediated Synthesis of Si-ZSM-5: An Investigation by ^1H-^{29}Si CP MAS NMR</i>	18
Abstract.....	19
Introduction.....	20
Experimental.....	26
Synthesis.....	26
Analysis	29
Results.....	31
Synthesis Profile	31
NMR Profiles	38
Silylation	54
Discussion	60

Table of Contents (continued)

Proposed Mechanism.....	67
References	73

Chapter Three*Hydrophobic Hydration and the Origin of Structural Specificity in the*

<i>Synthesis of Pure-Silica Zeolites.....</i>	<i>77</i>
Abstract.....	78
Introduction.....	79
Experimental.....	82
Synthesis.....	82
Analysis	85
Results.....	86
Structural Specificity.....	86
Hydrophobic Hydration.....	97
Crystallization Kinetics	103
Discussion	108
Proposed Mechanism.....	122
References	125

Chapter Four*Mechanism of Structure Direction in the Crown Ether-Mediated*

<i>Syntheses of FAU and EMT Zeolites</i>	<i>129</i>
Abstract.....	130
Introduction.....	131

Table of Contents (continued)

Experimental.....	135
Synthesis.....	135
Analysis.....	136
Results and Discussion.....	138
Chemical Composition of FAU and EMT.....	138
Raman Spectroscopy.....	139
Liquid-Phase Absorption of Crown Ethers.....	145
NMR Spectroscopy.....	146
Synthesis Variations.....	152
Proposed Mechanism.....	165
References.....	173

Chapter Five

<i>Towards the “Rational Synthesis” of Zeolites</i>	177
References.....	186

List of Figures

Chapter One

- Figure 1.1. Multiple zeolite structural types synthesized using tetraethylammonium as the organic space-filling agent..... 8
- Figure 1.2. Geometric correspondence between organic structure-directing agents and clathrasil and zeosil pore architectures synthesized from the same pure-silica synthesis composition. 10
- Figure 1.3. “Hand-in-glove” geometric correspondence between organic templates and the zeolite pore architecture of ZSM-18. 11

Chapter Two

- Figure 2.1 Proposed mechanism of structure direction in the TPA-mediated synthesis of ZSM-5. 22
- Figure 2.2 Effect of interatomic distance on the ^1H – ^{29}Si cross polarization efficiency between the protons of occluded *p*-xylene and the framework silicon atoms of Si-ZSM-5..... 25

List of Figures (continued)

- Figure 2.3 X-ray diffraction patterns of the D₂O-washed, freeze-dried samples collected during the TPA-mediated, sodium-containing synthesis of Si-ZSM-5. 32
- Figure 2.4. Crystallization profiles of TPA-mediated syntheses of Si-ZSM-5..... 33
- Figure 2.5. IR spectra of the D₂O-washed, freeze-dried samples collected during the TPA-mediated, sodium-containing synthesis of Si-ZSM-5. 35
- Figure 2.6. IR spectra of the D₂O-washed, freeze-dried samples collected during the TPA-mediated, sodium-free synthesis of Si-ZSM-5 using Cab-O-Sil. 36
- Figure 2.7. IR spectra of the D₂O-washed, freeze-dried samples collected during the TPA-mediated, sodium-free synthesis of Si-ZSM-5 using TEOS..... 37
- Figure 2.8. ²⁹Si MAS and ¹H-²⁹Si CP MAS NMR spectra of the freeze-dried samples collected during the TPA-mediated, sodium-containing synthesis of Si-ZSM-5. 39

List of Figures (continued)

- Figure 2.9. ^{29}Si MAS and ^1H - ^{29}Si CP MAS NMR spectra of the freeze-dried samples collected during the TPA-mediated, sodium-free synthesis of Si-ZSM-5 using Cab-O-Sil. 40
- Figure 2.10. ^{29}Si MAS and ^1H - ^{29}Si CP MAS NMR spectra of the freeze-dried samples collected during the TPA-mediated, sodium-free synthesis of Si-ZSM-5 using TEOS..... 41
- Figure 2.11. Origin of Q^3 defect sites in as-synthesized, pure-silica zeolites. 43
- Figure 2.12. ^{29}Si MAS and ^1H - ^{29}Si CP MAS NMR spectra of the freeze-dried samples of the synthesis gel containing TMA in lieu of TPA..... 45
- Figure 2.13. ^1H - ^{13}C CP MAS NMR spectra of TPABr, TPA occluded in Si-ZSM-5, and TPA- d_{28} occluded in Si-ZSM-5..... 47
- Figure 2.14. ^1H - ^{13}C CP MAS NMR spectra of the freeze-dried samples collected during the TPA-mediated, sodium-containing synthesis of Si-ZSM-5..... 49
- Figure 2.15. ^1H - ^{13}C CP MAS NMR spectra of the D_2O -washed, freeze-dried samples collected during the TPA-mediated, sodium-containing synthesis of Si-ZSM-5..... 50

List of Figures (continued)

- Figure 2.16. ^1H - ^{13}C CP MAS NMR spectra of the D_2O -washed, freeze-dried samples collected during the TPA-mediated, sodium-free synthesis of Si-ZSM-5 using Cab-O-Sil. 52
- Figure 2.17. ^1H - ^{13}C CP MAS NMR spectra of the D_2O -washed, freeze-dried samples collected during the TPA-mediated, sodium-free synthesis of Si-ZSM-5 using TEOS..... 53
- Figure 2.18. IR spectrum of the sample collected by trimethylsilylation of the unheated, TEOS-containing synthesis mixture..... 55
- Figure 2.19. ^{29}Si MAS and ^1H - ^{29}Si CP MAS NMR spectra of the sample collected by trimethylsilylation of the unheated, TEOS-containing synthesis mixture..... 56
- Figure 2.20. ^1H -decoupled and ^1H - ^{13}C CP MAS NMR spectra of the sample collected by trimethylsilylation of the unheated, TEOS-containing synthesis mixture..... 58
- Figure 2.21. Proposed mode of interaction of silicate and TPA within inorganic-organic composite species. 62

List of Figures (continued)

- Figure 2.22. Proposed mechanism of structure direction and crystal growth involving inorganic–organic composite species in the TPA-mediated synthesis of Si–ZSM-5..... 70

Chapter Three

- Figure 3.1. Location of TPA occluded in Si–ZSM-5..... 87
- Figure 3.2. X-Ray diffraction patterns of the D₂O-washed, freeze-dried samples collected during the hexanediamine-mediated synthesis of Si–ZSM-5..... 88
- Figure 3.3. IR spectra of the D₂O-washed, freeze-dried samples collected during the hexanediamine-mediated synthesis of Si–ZSM-5. 89
- Figure 3.4. Proposed location of hexanediamine occluded in Si–ZSM-5 and Si–ZSM-48..... 91
- Figure 3.5. X-Ray diffraction patterns of the D₂O-washed, freeze-dried samples collected during the hexanediamine-mediated synthesis of Si–ZSM-48..... 92

List of Figures (continued)

- Figure 3.6. IR spectra of the D₂O-washed, freeze-dried samples collected during the hexanediamine-mediated synthesis of Si-ZSM-48. 93
- Figure 3.7. ²⁹Si MAS and ¹H-²⁹Si CP MAS NMR spectra of the freeze-dried samples collected during the hexanediamine-mediated synthesis of Si-ZSM-5. 94
- Figure 3.8. ²⁹Si MAS and ¹H-²⁹Si CP MAS NMR spectra of the freeze-dried samples collected during the hexanediamine-mediated synthesis of Si-ZSM-48. 96
- Figure 3.9. IR spectra of Si-ZSM-5 synthesized in the presence of hexanediamine and H₂O. 98
- Figure 3.10. ²⁹Si MAS and ¹H-²⁹Si CP MAS NMR spectra of Cab-O-Sil and of the freeze-dried samples collected from synthesis gels containing TMA and TEA. 100
- Figure 3.11. ²⁹Si MAS and ¹H-²⁹Si CP MAS NMR spectra of the freeze-dried samples collected from synthesis gels containing TPA and TBA. 101

List of Figures (continued)

- Figure 3.12. ^{29}Si MAS and ^1H - ^{29}Si CP MAS NMR spectra of the freeze-dried samples collected from synthesis gels containing TPenA and TEOA. 102
- Figure 3.13. Crystallization profiles of TPA-mediated syntheses of Si-ZSM-5..... 104
- Figure 3.14. Crystallization profiles of TPA- d_{28} -mediated syntheses of Si-ZSM-5..... 105
- Figure 3.15. Crystallization profiles of hexanediamine-mediated syntheses of Si-ZSM-5..... 106
- Figure 3.16. Crystallization profiles of hexanediamine-mediated syntheses of Si-ZSM-48..... 107
- Figure 3.17. Proposed mechanism of formation of inorganic-organic composite species from hydrophobically-hydrated TPA and silicate species..... 110
- Figure 3.18. Proposed mechanism of structure direction in the TPA-mediated synthesis of Si-ZSM-5..... 111

List of Figures (continued)

Figure 3.19. Proposed structure-directing (a) and space-filling (b) roles of hexanediamine in the syntheses of Si-ZSM-5 and Si-ZSM-48.....	113
Figure 3.20. Differences in hydration of tetraalkylammonium cations.....	116
 Chapter Four	
Figure 4.1. Structure of FAU.....	133
Figure 4.2. Structure of EMT.....	134
Figure 4.3. Raman spectra of 18-crown-6 in various environments.....	140
Figure 4.4. Raman spectra of 15-crown-5 in various environments.....	141
Figure 4.5. Static ^1H - ^{13}C CP NMR spectra of crown ethers.....	148
Figure 4.6. Static ^1H - ^{13}C CP NMR spectra of 18-crown-6 in dehydrated EMT and FAU.....	149
Figure 4.7. Static ^1H - ^{13}C CP NMR spectra of 15-crown-5 in dehydrated EMT and FAU.....	150

List of Figures (continued)

Figure 4.8. Raman spectra of Kryptofix 2.2.2 in various environments..... 161

Figure 4.9. Sodium/18-crown-6 complex in the smaller supercage of EMT..... 170

Chapter Five

Figure 5.1. Proposed mechanism of structure direction in the synthesis of Si-ZSM-5 using siloxane-functionalized tetrabutylammonium..... 181

Figure 5.2. Representation of how a diquatery ammonium propellane species might disrupt the formation of a linear channel structure in SSZ-26..... 183

List of Tables

Chapter Four

Table 4.1.	Variations of Crown Ether Concentrations in the Synthesis of FAU and EMT Zeolites	154
Table 4.2.	Synthesis of Intergrowth Structures.....	156
Table 4.3.	Syntheses Involving Organic Components	159
Table 4.4.	Structure-Directing Effects of Sodium and Crown Ethers.....	163
Table 4.5.	Structure-Directing Effects of Alkali Metal Ions and Crown Ethers.....	166

List of Abbreviations

Å	angstrom
C	Celsius
CP	cross polarization
cm ⁻¹	wavenumber
15-crown-5	1,4,7,10,13-pentaoxacyclopentadecane
18-crown-6	1,4,7,10,13,16-hexaoxacyclooctadecane
d	day
deg	degree
dibenzo-18-crown-6	2,3,11,12-dibenzo-1,4,7,10,13,16-hexaoxacyclooctadeca-2,11-diene
DMF	<i>N,N</i> -dimethylformamide
EMT	hexagonal polymorph of faujasite
FAU	cubic polymorph of faujasite
FT	Fourier transform
g	gram
h	hour
HXN	1,6-hexanediamine
Hz	hertz
IR	infrared
kcal	kilocalorie
kHz	kilohertz
Kryptofix 2.2.2	4,7,13,16,21,24-hexaoxa-1,10-diazabicyclo[8.8.8]hexacosane
M	molar
(m)	multiplet

List of Abbreviations (continued)

MAS	magic angle spinning
mbar	millibar
mg	milligram
MHz	megahertz
min	minute
mm	millimeter
mW	milliwatt
mol	mole
ms	millisecond
μs	microsecond
nm	nanometer
NMR	nuclear magnetic resonance
N ₂ -18-crown-6	1,4,10,13-tetraoxa-7,16-diazacyclooctadecane
N ₆ -18-crown-6	1,4,7,10,13,16-hexaazacyclooctadecane
PEG	pentaethylene glycol
ppm	parts per million
Q ⁿ	Si(OSi) _n (OH) _{4-n} or Si(OSi) _n (OD) _{4-n} (n=0-4)
s	second
(s)	singlet
SANS	small-angle neutron scattering
SAXS	small-angle X-ray scattering
Si-ZSM-5	pure-silica ZSM-5
Si-ZSM-48	pure-silica ZSM-48
S ₆ -18-crown-6	1,4,7,10,13,16-hexathiacyclooctadecane
T	tetrahedral atom (Si or Al)

List of Abbreviations (continued)

(t)	triplet
TAA	tetraalkylammonium
TBA	tetrabutylammonium
TEA	tetraethylammonium
TEG	tetraethylene glycol
TEGDME	2,5,8,11,14-pentaoxapentadecane (tetraethylene glycol dimethyl ether)
TEOA	tetraethanolammonium
TEOS	tetraethylorthosilicate
TGA	thermogravimetric analysis
TMA	tetramethylammonium
TPA	tetrapropylammonium
TPA- <i>d</i> ₂₈	tetrapropylammonium- <i>d</i> ₂₈ (perdeuterated tetrapropylammonium)
TPenA	tetrapentylammonium
wt %	weight percent
XRD	X-ray diffraction

Chapter One

Structure Direction in Zeolite Synthesis

Reprinted in part with permission from *Comprehensive Supramolecular Chemistry*, Vol. 7; J. -M. Lehn, Ed.; Elsevier: Oxford, in press.

Copyright 1995 Elsevier Science Ltd.

Introduction

The unique feature of zeolites and crystalline molecular sieves is that they contain void spaces of a uniform size and regularly-ordered arrangement within the crystals. In these microporous materials, the sizes of the void spaces are on the order of small molecules (≤ 20 Å). There is considerable interest in the design and synthesis of novel molecular sieves containing void spaces with particular features such as shape, size, and connectivity. An understanding of the variables that affect which zeolite is crystallized from a given synthesis mixture is essential to the goal of being able to control the synthesis of a new material such that the desired structural features appear in the product. The potential variables that can be adjusted in the synthesis of an aluminosilicate or silicate molecular sieve are limited for a purely inorganic system: these include the ratio of silicon to aluminum (Si/Al) in the gel, the type and concentration of alkali metal ions, the concentration of hydroxide or fluoride ions (mineralizing agent), the amount of water in the gel, the presence of potential framework heteroatoms (Be, B, Mg, P, Ti, V, Cr, Mn, Fe, Co, Zn, Ga),¹ and the synthesis temperature. These parameters are discussed in detail in numerous reviews.¹⁻⁵

One of the most significant structure-directing influences on zeolite synthesis is the effect of alkali metal ions on the chemistry of the inorganic gel, in part due to the water structure-altering behavior of these cations.⁶⁻⁸ Recognizing the analogy between the tetramethylammonium (TMA) ion and alkali metal ions,⁹⁻¹¹ Barrer and Denny in 1961 used tetramethylammonium hydroxide in the synthesis of zeolite A (LTA framework topology) in place of sodium hydroxide.¹² A material with the

LTA structure containing occluded TMA ions and a higher framework Si/Al ratio than is normally found in zeolite A was produced. The increase in framework Si/Al ratio is related to the larger size of the TMA cation relative to the sodium ion: because each cation present in the product balances the anionic charge introduced by a framework aluminum atom, the number of aluminum sites ($\text{Si/Al} \geq 1$)¹³ is limited (due to size considerations) by the maximum number of cations that can be accommodated within the zeolite void space. Since the groundbreaking work of Barrer and Denny on organic-mediated zeolite synthesis, the possibilities of producing known zeolite topologies with new chemical compositions and of synthesizing novel zeolite structures through the use of cationic or neutral organic additives have attracted considerable attention.^{1,3,4,14,15} However, because the influence of organic species on zeolite crystallization can be very weak relative to other factors, these are not straightforward tasks.

At the present time, the synthesis of new zeolites and molecular sieves relies on a heuristic approach.¹ However, an understanding of the mechanisms by which the transformation from an amorphous gel to a crystalline solid takes place will be a key to the synthesis of new materials. Recent efforts have focused on elucidating crystallization mechanisms, with particular attention to the interactions between the organic and inorganic components during synthesis.

Issues in Structure Direction and Zeolite Synthesis

Crystallization is the result of supramolecular self-assembly with

specific molecular recognition events occurring throughout the entire nucleation and crystal growth processes. However, the routes by which a zeolite synthesis gel is transformed from a mixture of numerous silicon oxide and aluminum oxide species (which vary depending on the concentration and nature of the aqueous alkali metal hydroxide solution present) into a crystalline product are very complex. Little is known about the molecular-scale mechanisms of self-assembly that occur during synthesis. Unlike organic synthesis, in which the product molecule is made by series of discrete, well-defined reactions through which one functional group transformation is achieved in each step, the gel chemistry and crystallization process in zeolite synthesis involve numerous simultaneous, interdependent equilibria and condensation steps.^{1,5,16} A multitude of reactions must occur in order for the product to form. The alteration of one synthesis variable influences other parameters, rendering systematic study difficult. An additional complication is that zeolites are metastable materials and thus their formation is kinetically controlled; a thermodynamically-controlled synthesis would produce quartz or other dense phases.^{1,15} The challenge presented by zeolite synthesis is fundamentally one of molecular recognition and self-assembly: the composition of the synthesis gel must be such that the various molecular species can spontaneously and specifically organize and assemble into a single, highly-ordered, covalently-bonded macrostructure, with no additional products being formed.

It appears that there is not a universal mechanism for zeolite crystallization. The mechanism depends instead on the nature and concentrations of the inorganic reactants and organic species present.

Two limiting cases have been identified: the solution-mediated transport mechanism, in which small inorganic species diffuse through the solution phase to the site of nucleation and growth; and the solid hydrogel transformation mechanism, whereby an amorphous solid phase rearranges to form the crystalline product.^{1,2} It appears that most syntheses occur by a combination of the two pathways.¹⁷ In addition, it has been proposed that extended silicate and aluminosilicate structures ($\approx 10\text{--}200$ Å length scale) may be involved during the crystallization of some zeolites:¹⁸⁻²⁴ these structures form initially and then condense to create the long-range order of the zeolite crystals. This description is conceptually analogous to the hierarchy of structures in biological systems; for example, in the synthesis of folded protein structures, the formation of secondary and tertiary structure (via folding) occurs subsequently to the linkage of amino acid units to form polypeptides.¹ The precise atomic arrangements in structures on the length scale of $10\text{--}200$ Å cannot be determined by conventional spectroscopic techniques (^{29}Si and ^{27}Al magic angle spinning NMR; Raman and IR spectroscopy).²⁰ Small-angle neutron and small-angle X-ray scattering experiments demonstrate the existence of extended structures^{18,20-24} but cannot be used to characterize their molecular composition or structure. These extended structures may be related to the hydrophilic hydration spheres of aqueous alkali metal ions and the hydrophobic hydration spheres of tetraalkylammonium ions in aqueous solution,⁶⁻¹¹ with subsequent replacement of water molecules by silicate species.^{1,25} However, it should be emphasized that these extended structures are not equivalent to the "structural building units" that are used in topological classification,^{5,26-28} despite evidence from ^{29}Si NMR and Raman spectroscopy of zeolite synthesis gels for the presence of anionic

silicate oligomers that resemble some of these units.²⁹⁻³⁴

Based on the pioneering work of Barrer and Denny, the observation that TMA ions were occluded into the cages of the zeolite product suggested that other organic cations might be used to influence the void space architecture, perhaps creating novel framework topologies. Although numerous previously-known and novel structures have been synthesized in the presence of organic additives,¹⁵ the functions of these so-called organic templates during zeolite crystallization are not well understood. In general, these species do not function as templates in the highly-specific manner implied by analogy with biological templates or template polymerization since there is not a one-to-one correspondence between the organic compound used and the product obtained.^{1,3,4,14,15} In many instances, the structure-directing capability of the organic species is weak relative to other factors that influence structure formation, e.g., high pH, high concentration of alkali metal ions or framework heteroatoms. A change in the inorganic composition of the synthesis gel may mask, alter, or eliminate the structure-influencing ability of the organic species.³⁵

The organic species that have been used in zeolite synthesis fall into two general categories: singly- or multiply-charged cationic molecules, e.g., alkylammonium ions and alkali metal ion complexes of crown ethers, and weakly hydrogen-bonding moieties, e.g., amines (which may be protonated in the synthesis mixture) and alcohols.^{1,5,14,15} Organic compounds must be stable at the severe conditions of synthesis, i.e., strongly alkaline media (pH typically greater than 10), temperatures of up to 200 °C, and reaction times of up to several months. A combination of hydrophobic and hydrophilic properties appears to be a requisite property;^{35,36} hydrophilicity is required for solubility in an aqueous

synthesis medium, whereas some hydrophobic character is necessary for interaction with the silicate species that form the zeolite framework.³⁷ Finally, the geometry of the organic molecules is of primary importance, since it is this characteristic that will hopefully be translated into the pore architecture. The relationships between organic geometries and inorganic structural features will be discussed in detail for two examples of organic-mediated zeolite synthesis.

Three roles have been proposed for organic species in zeolite synthesis: space-filling agents, structure-directing agents, and templates.^{1,3,4,14,15} The latter two are most important to the synthesis of new materials with controlled pore properties. Organic molecules that function as space-filling species are occluded into the void space of the product, but do not influence the pore architecture that is formed (Figure 1.1). In the product, there is not a tight fit of the organic guest molecules within the void space of the host, and the occluded guest molecules exhibit substantial rotational and perhaps translational mobility.³⁸ In this case, the organic species may be adsorbed into the zeolite void space due to entropic considerations and may inhibit dissolution of the metastable, growing crystallites in the alkaline synthesis medium. However, a material of the same structural type generally can be synthesized by an organic-free route; the inorganic gel chemistry apparently determines which structure is formed. Thus, these systems do not appear to offer any means to control the product pore architectures, but only the product Si/Al ratio (*vide supra*) or the kinetics of crystallization.

Alternatively, the organic species may function as a structure-directing agent, which implies that there is a closer correspondence between the structure of the organic molecule and the product structure,

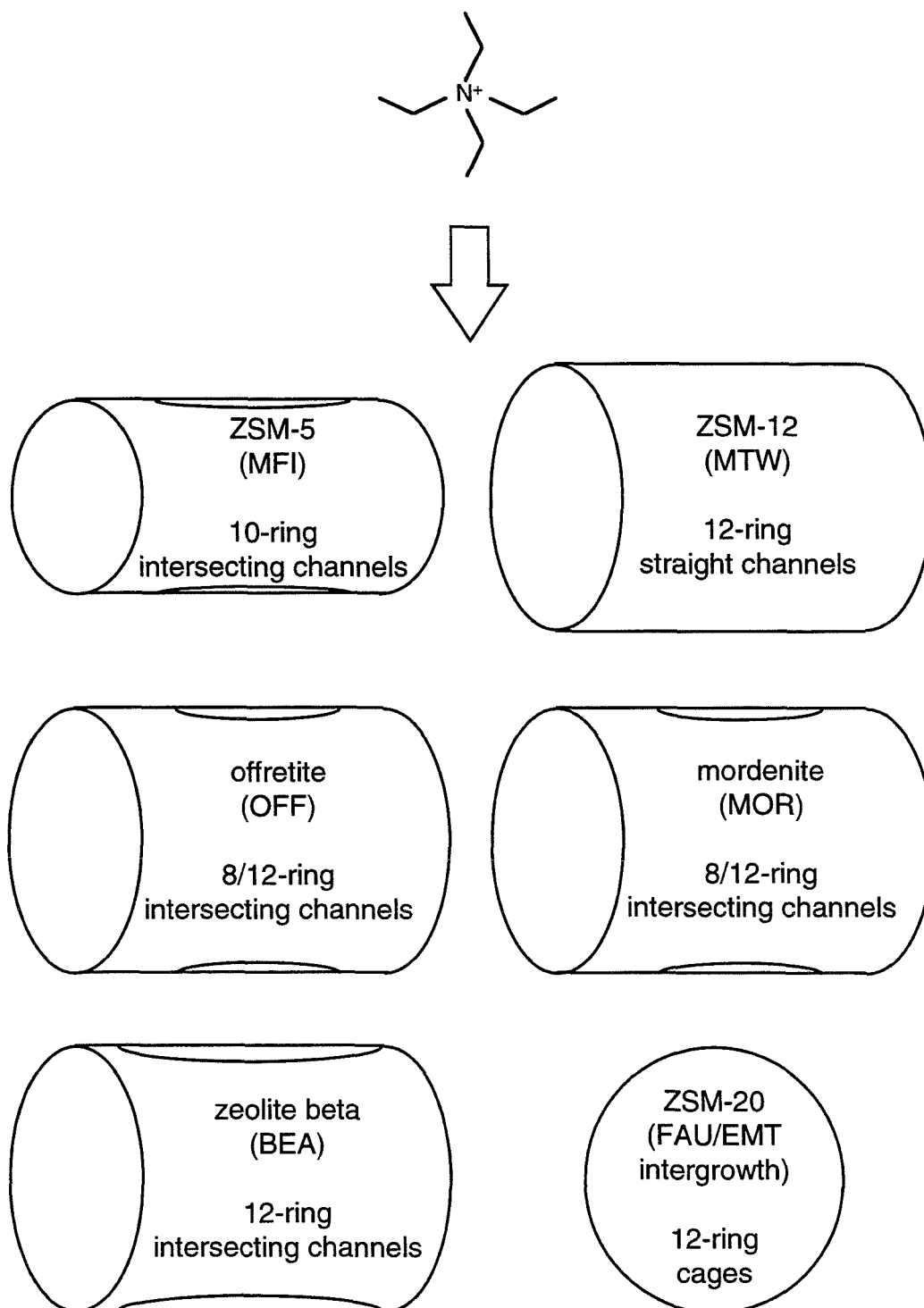


Figure 1.1. Multiple zeolite structural types synthesized using tetraethylammonium as the organic space-filling agent.¹⁵

such as in the synthesis of zeosils and clathrasils (pure-silica zeolites) (Figure 1.2),³⁷ or that the synthesis of the zeolite structure is accessible through the use of only one particular organic species.¹ The organic molecules may participate in nucleation, perhaps via orientation or organization of the inorganic components prior to crystallite formation. However, the intermolecular interactions present both during and after crystallization are weak, and molecules of the structure-directing agent may still demonstrate rotational mobility within the pores of the crystalline host.^{35,38}

Finally, templating differs from structure direction in the degree of structural similarity between the organic guest and the zeolite host. The “hand-in-glove” analogy for templating implies that the zeolite cavity conforms closely to the shape and contour of the rotationally- and translationally-immobilized organic template; after calcination to remove the organic species, the zeolite retains the geometric imprint of the template molecule.^{1,14} There is a close correspondence between the shape of the zeolite void space and the geometry of the template molecule, although more than one organic species may exhibit the appropriate geometry, as demonstrated by the example of ZSM-18 (Figure 1.3).³⁹⁻⁴¹ Immobilization of the organic molecule implies that there is a high degree of specificity in the molecular recognition interactions between the organic and inorganic species occurring during synthesis. Although examples of the templating phenomenon are few, there are several examples of structure direction, including the syntheses of pure-silica ZSM-5 and the hexagonal polymorph of faujasite (EMT).

Knowledge of the mechanisms by which structure direction and templating occur is of critical importance to the goal of using of tailor-

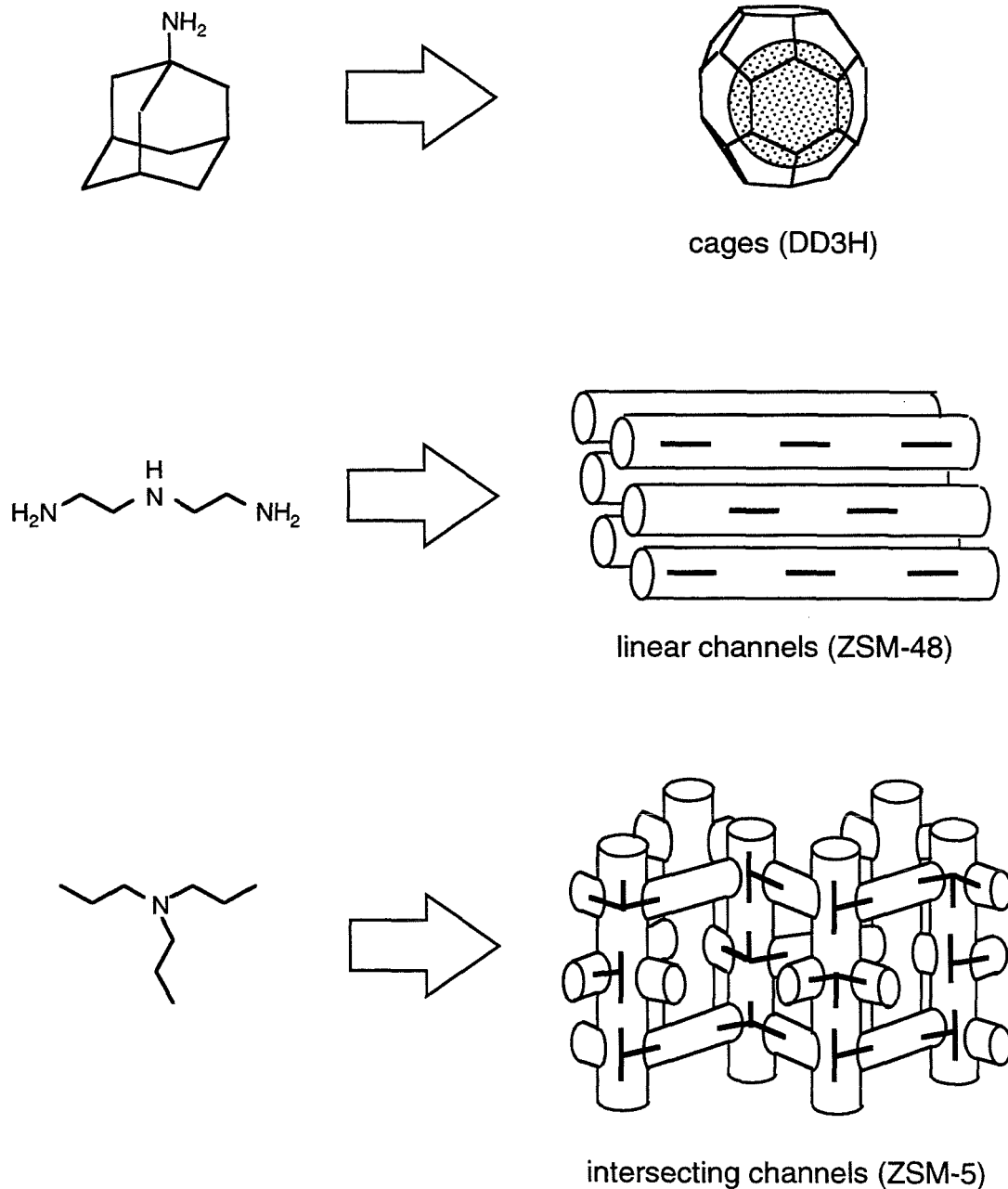


Figure 1.2. Geometric correspondence between organic structure-directing agents and clathrasil and zeosil pore architectures synthesized from the same pure-silica synthesis composition.³⁷

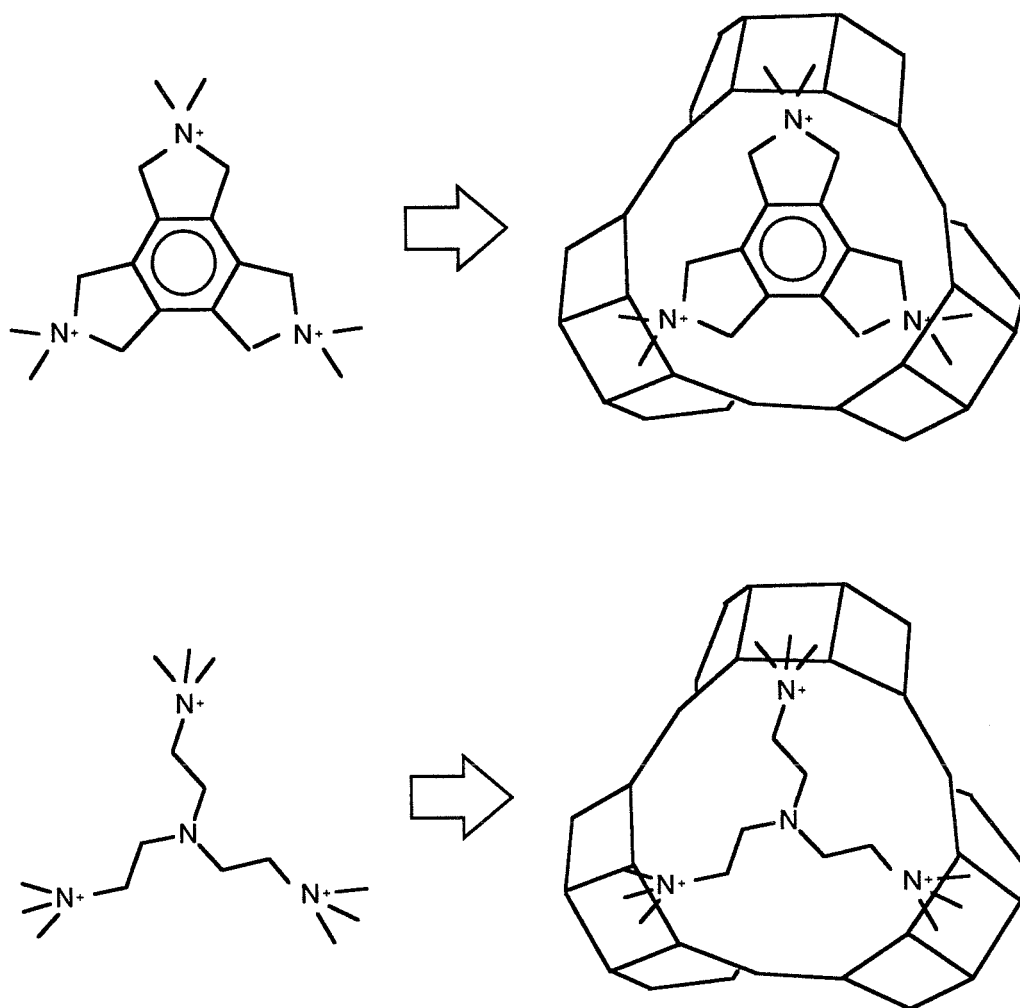


Figure 1.3. "Hand-in-glove" geometric correspondence between organic templates and the zeolite pore architecture in ZSM-18.³⁹⁻⁴¹

made organic moieties to synthesize new materials which incorporate the desired structural features. In order to understand how the shape of the organic molecule is translated into the zeolite pore architecture, the types of interactions between the organic and inorganic components must be considered at the molecular level, even though the synthesis mechanisms of purely inorganic systems are not fully understood. Two different classes of materials can be considered: pure- or high-silica molecular sieves and aluminum-rich zeolites.

Pure-silica molecular sieves and zeolites that contain a high silica content ($5 < \text{Si}/\text{Al} < \infty$)¹ are the simplest systems in which to assess organic structure-directing effects, for two reasons. First, in these systems there is a limited number of synthetic variables: silica, water, organic species, and low concentrations of alkali metal hydroxides (small amounts of alkali metal ions may enhance the crystallization kinetics of some syntheses,⁴² but high concentrations of alkali metal ions exhibit a strong structure-directing influence). Second, the pure-silica product is hydrophobic and uncharged (except for non-surface $\text{Si}(\text{OSi})_3(\text{O}^-)$ defect sites which can balance the charge of a cationic structure-directing agent),^{36,43} and thus the predominant interactions between the organic molecules and the silicate species should be van der Waals forces.^{16,37} During synthesis, hydrophobic silicate species may interact preferentially with organic moieties rather than water, resulting in enclathration of the organic molecules in a configuration in which intramolecular and intermolecular van der Waals interactions are optimized for all species in the system.³⁷ Thus, the influence of the geometry of the organic moiety on the shape and size of void spaces within the product structure should be apparent in a pure-silica or high-silica system. The role of inorganic-organic

intermolecular interactions in the synthesis of pure-silica ZSM-5 is discussed in detail in Chapters Two and Three.

The syntheses of aluminum-rich zeolites ($1 \leq \text{Si}/\text{Al} \leq 5$)¹ are less amenable to structure direction by organic species than high-silica syntheses. Alkali metal ions are necessary to balance the negative charges introduced by framework aluminum, because even if organic cations are present, the zeolite typically cannot accommodate a sufficient number of organic cations in the void space to balance the framework charges. The high concentrations of alkali metal hydroxides that are thus usually used in these syntheses can strongly influence the inorganic gel chemistry and subsequent structure formation.^{1-4,35} Organic structure-directing effects are weak relative to these influences, perhaps in part because the interactions between organic molecules and the inorganic species are primarily electrostatic in nature (perhaps with a contribution from van der Waals forces). As a result, organic structure-directing effects appear in a much narrower range of synthesis conditions as the aluminum concentration is increased. Although aluminosilicate syntheses are a more complicated system in which to discern structure-directing effects, there are examples of structure direction in aluminosilicate zeolite syntheses, including the synthesis of the hexagonal (EMT) and cubic (FAU) polymorphs of faujasite described in Chapter Four.

Thus, the theme of this thesis is the role of organic molecules as structure-directing agents in the self-assembly processes which constitute zeolite synthesis. The objective is to elucidate the mechanisms by which the shapes of the organic species are translated into the pore architectures of the pure-silica molecular sieve ZSM-5 and the aluminosilicate zeolite EMT. A combination of solid state NMR and vibrational spectroscopic

techniques and systematic variations of the synthesis compositions is used to probe the relationships between the inorganic and organic components during and after synthesis and to demonstrate the types and strengths of inorganic–organic intermolecular interactions that give rise to structural specificity.

References

- (1) Davis, M. E.; Lobo, R. F. *Chem. Mater.* **1992**, *4*, 756.
- (2) Flanigen, E. M. In *Molecular Sieves*; W. M. Meier and J. B. Uytterhoeven, Eds.; American Chemical Society: Washington, DC, 1973; pp 119.
- (3) Barrer, R. M. *Zeolites* **1981**, *1*, 130.
- (4) Barrer, R. M. In *Zeolites: Synthesis, Structure, Technology and Application*; B. Drzaj, S. Hocevar and S. Pejovnik, Eds.; Elsevier: Amsterdam, 1985; pp 1.
- (5) Gilson, J. -P. In *Zeolite Microporous Solids: Synthesis, Structure, and Reactivity*; E. G. Derouane, F. Lemos, C. Naccache and F. R. Ribeiro, Eds.; Kluwer Academic: Dordrecht, 1992; pp 19.
- (6) Gabelica, Z.; Blom, N.; Derouane, E. G. *Appl. Catal.* **1983**, *5*, 227.
- (7) Aiello, R.; Crea, F.; Nastro, A.; Subotic, B.; Testa, F. *Zeolites* **1991**, *11*, 767.
- (8) de Ruiter, R.; Jansen, J. C.; van Bekkum, H. *Zeolites* **1992**, *12*, 56.
- (9) Nakayama, H.; Kuwata, H.; Yamamoto, N.; Akagi, Y.; Matsui, H. *Bull. Chem. Soc. Jpn.* **1989**, *62*, 985.
- (10) Mootz, D.; Seidel, R. *J. Inclusion Phenom. Mol. Recognit. Chem.* **1990**, *8*, 139.
- (11) Ratcliffe, C. I.; Garg, S. K.; Davidson, D. W. *J. Inclusion Phenom. Mol. Recognit. Chem.* **1990**, *8*, 159.
- (12) Barrer, R. M.; Denny, P. J. *J. Chem. Soc.* **1961**, 971.
- (13) Loewenstein, W. *Am. Mineralogist* **1954**, *39*, 92.
- (14) Lok, B. M.; Cannan, T. R.; Messina, C. A. *Zeolites* **1983**, *3*, 282.

- (15) Szostak, R. *Handbook of Molecular Sieves*; Van Nostrand Reinhold: New York, 1992, pp 584.
- (16) Davis, M. E. In *Interfacial Design and Chemical Sensing*; T. E. Mallouk and D. J. Harrison, Eds.; American Chemical Society: Washington, DC, 1994; Vol. 561; pp 27.
- (17) Bodart, P.; Nagy, J. B.; Gabelica, Z.; Derouane, E. G. *J. Chim. Phys.* **1986**, *83*, 777.
- (18) Henderson, S. J.; White, J. W. *J. Appl. Cryst.* **1988**, *21*, 744.
- (19) Vaughan, D. E. W. In *Catalysis and Adsorption by Zeolites*; G. Ohlmann, Ed.; Elsevier: Amsterdam, 1991; pp 275.
- (20) Iton, L. E.; Trouw, F.; Brun, T. O.; Epperson, J. E.; White, J. W.; Henderson, S. J. *Langmuir* **1992**, *8*, 1045.
- (21) Wijnen, P. W. J. G.; Beelen, T. P. M.; van Santen, R. A. In *Expanded Clays and Other Microporous Solids*; M. L. Occelli and H. E. Robson, Eds.; Van Nostrand Reinhold: New York, 1992; pp 341.
- (22) Regev, O.; Cohen, Y.; Kehat, E.; Talmon, Y. *J. Phys. IV (Orsay, Fr.)* **1993**, *C8*, 397.
- (23) Dokter, W. H.; Beelen, T. P. M.; van Garderen, H. F.; Rummens, C. P. J.; van Santen, R. A.; Ramsay, J. D. F. *Colloids Surfaces A* **1994**, *85*, 89.
- (24) Regev, O.; Cohen, Y.; Kehat, E.; Talmon, Y. *Zeolites* **1994**, *14*, 314.
- (25) Wiebcke, M. *J. Chem. Soc., Chem. Commun.* **1991**, 1507.
- (26) Keijsper, J. J.; Post, M. F. M. In *Zeolite Synthesis*; M. L. Occelli and H. E. Robson, Eds.; American Chemical Society: Washington, DC, 1989; pp 28.
- (27) McCormick, A. V.; Bell, A. T. *Catal. Rev. Sci. Eng.* **1989**, *31*, 97.
- (28) Knight, C. T. G. *Zeolites* **1990**, *10*, 140.

- (29) Guth, J. L.; Caullet, P.; Wey, R. In *Fifth International Conference on Zeolites*; Heyden: Naples, 1980; pp 30.
- (30) Boxhoorn, G.; Sudmeijer, O.; van Kasteren, P. H. G. *J. Chem. Soc., Chem. Commun.* **1983**, 1416.
- (31) Groenen, E. J. J.; Kortbeek, A. G. T. G.; Mackay, M.; Sudmeijer, O. *Zeolites* **1986**, 6, 403.
- (32) Dutta, P. K.; Shieh, D. C.; Puri, M. *J. Phys. Chem.* **1987**, 91, 2332.
- (33) Twu, J.; Dutta, P. K.; Kresge, C. T. *J. Phys. Chem.* **1991**, 95, 5267.
- (34) Dutta, P. K.; Rao, K. M.; Park, J. Y. *Langmuir* **1992**, 8, 722.
- (35) Burkett, S. L.; Davis, M. E. *Microporous Mater.* **1993**, 1, 265.
- (36) Lobo, R. F.; Zones, S. I.; Davis, M. E. In *Inclusion Chemistry with Zeolites: Nanoscale Materials by Design*; N. Herron and D. Corbin, Eds.; in press.
- (37) Gies, H.; Marler, B. *Zeolites* **1992**, 12, 42.
- (38) Hong, S. B.; Cho, H. M.; Davis, M. E. *J. Phys. Chem.* **1993**, 97, 1622.
- (39) Ciric, J. (Mobil Oil Corp.). U. S. Patent 3 950 496, 1976; *Chem. Abstr.* **1976**, 85, P23253d.
- (40) Lawton, S. L.; Rohrbaugh, W. J. *Science* **1990**, 247, 1319.
- (41) Schmitt, K. D.; Kennedy, G. J. *Zeolites*, in press.
- (42) Goepper, M.; Li, H. -X.; Davis, M. E. *J. Chem. Soc., Chem. Commun.* **1992**, 1665.
- (43) Dessau, R. M.; Schmitt, K. D.; Kerr, G. T.; Woolery, G. L.; Alemany, L. *B. J. Catal.* **1987**, 104, 484.

Chapter Two

Mechanism of Structure Direction in the TPA-Mediated Synthesis of Si-ZSM-5: An Investigation by ^1H - ^{29}Si CP MAS NMR

Reprinted in part with permission from *J. Phys. Chem.* **1994**, *98*, 4647.

Copyright 1994 American Chemical Society.

Abstract

The role of tetrapropylammonium (TPA) as a structure-directing agent in the synthesis of pure-silica ZSM-5 (Si-ZSM-5) is investigated by solid state NMR. It has previously been proposed that the mechanism of structure direction involves preorganization of silicate species around the TPA ions with subsequent assembly of these inorganic-organic composite structures to yield crystalline Si-ZSM-5 with occluded TPA molecules. However, such structures have not been directly observed. Here, ^1H - ^{29}Si CP MAS NMR is performed between the protons of TPA and the silicon atoms of the zeolite framework precursors in a deuterated synthesis medium to probe the relationship between the organic and inorganic components. The ^1H - ^{29}Si CP MAS NMR results indicate that short-range intermolecular interactions, i.e., on the order of van der Waals interactions ($\approx 3.3 \text{ \AA}$ for $\text{H}\cdots\text{Si}$), are established during the heating of the zeolite synthesis gel prior to the development of long-range order indicative of the ZSM-5 structure. The nature of these interactions is independent of the presence of sodium in the gel or the silica source used. An attempt to isolate the relevant composite species by trimethylsilylation of the synthesis mixture was somewhat successful. These results thus provide the first direct evidence for the existence of preorganized inorganic-organic composite structures during the synthesis of Si-ZSM-5. They also demonstrate the relevance of van der Waals interactions to the occurrence of an organic structure-directing effect. A modified mechanism of structure direction and crystal growth of Si-ZSM-5 is proposed.

Introduction

The routes by which crystalline zeolites are produced from an amorphous aluminosilicate or silicate gel are complex self-assembly processes that involve numerous simultaneous and interdependent equilibria and condensation steps. Consequently, zeolite crystallization is not well understood, except in that there does not appear to be a universal mechanism to describe all zeolite syntheses.¹ The addition of organic molecules such as amines and alkylammonium ions to zeolite synthesis gels can affect the rate at which a particular material is formed, or can make new structures or framework chemical compositions accessible. However, the exact role of the organic species and the mechanism by which it affects the formation of the product structure remain to be elucidated.^{1,2} In particular, the nature and extent of interactions between the organic and inorganic components of a zeolite synthesis gel are not well defined. These interactions may be the key to understanding why in some zeolite syntheses there is a strong correlation between the geometry of the organic molecule and the zeolite pore architecture (the organic species serves as a structure-directing agent) while in other syntheses no such relationship is observed (the organic species serves as a space-filling agent).

ZSM-5 (MFI topology) is one of the most widely studied and commercially important zeolites. The MFI structure consists of parallel, linear, 10-ring channels intersected by 10-ring sinusoidal channels. ZSM-5 can be synthesized at a wide variety of framework silicon-to-aluminum ratios via numerous synthetic routes, both with and without organic species present.³ Several of these syntheses, including that of silicalite or

pure-silica ZSM-5 (Si-ZSM-5),⁴ involve the tetrapropylammonium (TPA) cation; Si-ZSM-5 has not been synthesized in the absence of an organic structure-directing agent.³ In the resulting materials, the TPA molecules are located at the channel intersections with the propyl chains extending into both the linear and sinusoidal channels.^{5,6} The molecules are held tightly at these sites and can be removed only by calcination; they cannot diffuse into or out of the structure. Tight enclathration of the TPA molecules suggests that they must be incorporated into the silicate structure during the process of crystal growth. Based on this observation and on the close geometric correspondence between the TPA molecule and the channel intersections of ZSM-5, a structure-directing role has been proposed for TPA in the synthesis of Si-ZSM-5 (or aluminosilicate ZSM-5).^{4,7,8} An understanding of the mechanism by which the shape and contour of the organic species are translated to the zeolite pore architecture is of particular interest because such examples are rare, e.g., ZSM-18.⁹

In the original report of the synthesis of Si-ZSM-5,⁴ a mechanism of structure direction by TPA involving preorganization of silicate species around the organic cations to form the zeolite channel intersections was postulated based on geometric considerations (Figure 2.1). Subsequent studies have relied on bulk properties such as the degree of silicate condensation (by ²⁹Si MAS NMR)^{7,8} and the organic content in the solid phase of the synthesis mixture (by ion exchange of [Pt(NH₃)₄]²⁺ followed by elemental analysis to determine Si/Pt ratio)⁸ to evaluate the proposed mechanism, but such techniques cannot probe the relevant inorganic-organic intermolecular interactions. The existence of ordered structures on the length scale of 40–50 Å during the synthesis of

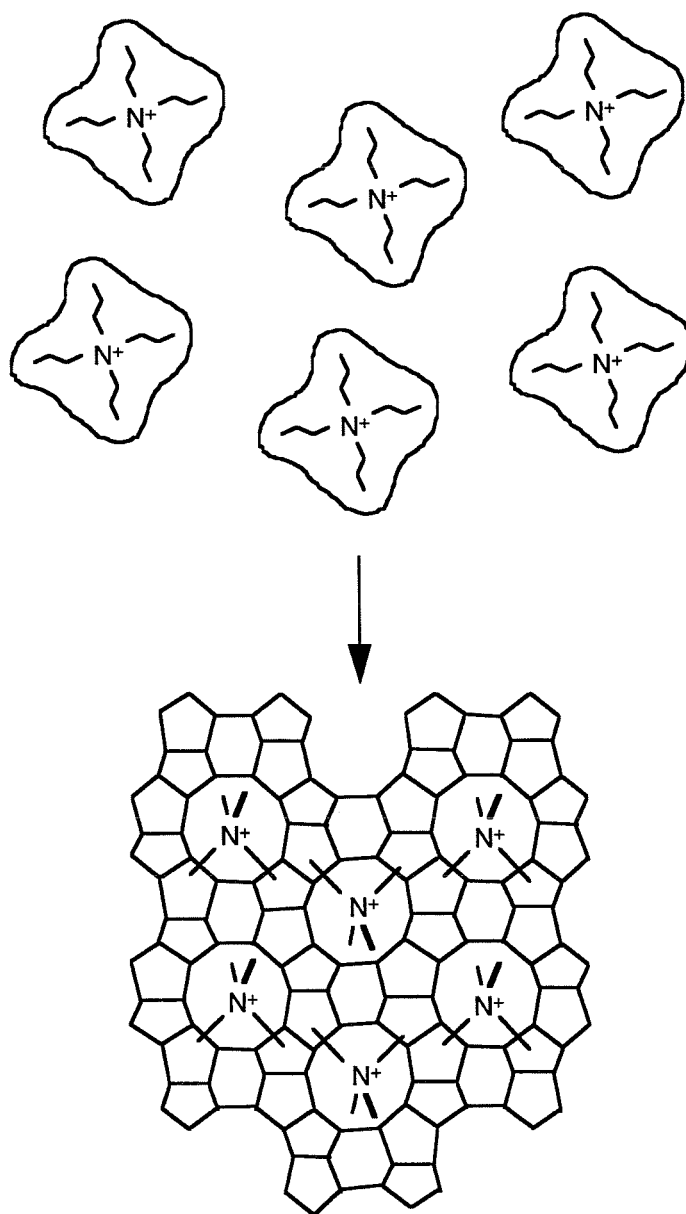


Figure 2.1. Proposed mechanism of structure direction in the TPA-mediated synthesis of ZSM-5. Inorganic-organic composite structures that resemble the channel intersections of the product are formed and subsequently assemble to yield ZSM-5.^{4,8}

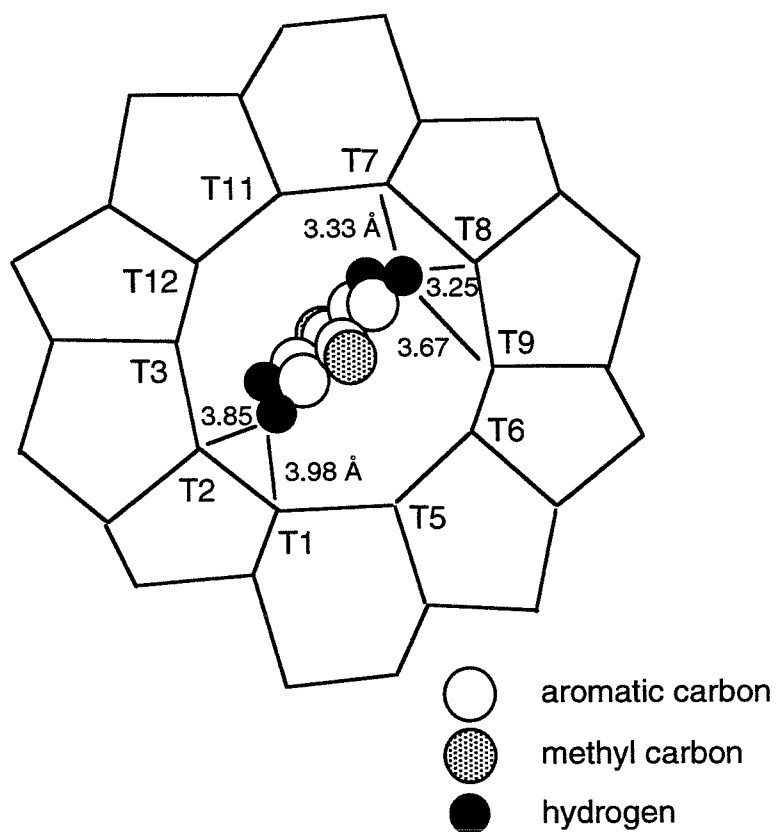
aluminosilicate¹⁰⁻¹² and pure-silica¹³ ZSM-5 (and other zeolites)¹⁴ is suggested by small-angle neutron scattering data, small-angle X-ray scattering data, and cryo-transmission electron microscopy, but the precise atomic arrangements within these extended structures cannot be ascertained using these techniques. It has been proposed that the interactions between organic molecules and silicate species in a pure-silica zeolite synthesis mixture result primarily from van der Waals contacts.¹⁵ However, direct evidence for such interactions has not previously been observed. In the present chapter, solid state cross polarization, magic angle spinning NMR is used to probe these interactions.

The technique of cross polarization (CP) is applied in conjunction with magic angle spinning (MAS) in solid state NMR to enhance the signal obtained for low-abundant isotopes such as ¹³C and ²⁹Si.^{16,17} The efficiency of polarization transfer from an abundant nucleus such as ¹H to the nucleus of interest is determined by the internuclear dipole interactions. Because the strength of the dipole interactions is directly related to internuclear distance (r^{-6}), polarization transfer studies can provide information regarding the proximity of particular nuclei as well as the presence of molecular motion. CP MAS NMR usually involves intramolecular polarization transfer. However, if the molecules are sufficiently close and immobilized, intermolecular cross polarization can be achieved. Intermolecular ¹H-¹³C CP MAS NMR studies have been used to study polymer miscibility in partially deuterated systems, in which polarization is transferred from the protons of one polymer to the carbon atoms of the other, deuterated polymer.¹⁸⁻²⁰

In the study of zeolites, the primary application of ¹H-²⁹Si CP MAS

NMR (with intramolecular cross polarization) is in the detection of framework Si–OH sites in organic-free materials.²¹ However, there are a few reports of polarization transfer between the protons of occluded organic molecules and silicon atoms in the zeolite framework.²²⁻²⁴ Mentzen and coworkers have described a striking example of the distance dependence of polarization transfer for cross polarization between the aromatic protons of immobilized, occluded *p*-xylene and the framework silicon atoms of Si–ZSM-5, which are well resolved in the ²⁹Si MAS and ¹H–²⁹Si CP MAS NMR spectra of this sample.²⁵ In this case, cross polarization is most efficient between protons and silicon atoms that are separated by a crystallographically-determined distance of approximately 3.3 Å or less. An increase in interatomic distance to 3.7 Å or greater results in a dramatic decrease in cross polarization efficiency (Figure 2.2). Mentzen and coworkers point out that the 3.3 Å threshold is approximately equal to the distance of a H···Si van der Waals contact. These results demonstrate the critical importance of interatomic distance to polarization transfer and suggest that cross polarization from the protons of organic molecules to the zeolite structures in which they are occluded occurs only when the appropriate atoms are in van der Waals contact.

In the present chapter, the technique of intermolecular cross polarization is applied to an investigation of the mechanism of synthesis of Si–ZSM-5. In particular, ¹H–²⁹Si CP is used to probe the interactions between the TPA cation and the silicate species that ultimately form the zeolite framework. It is anticipated that organization of silicate by the organic molecules should require close contact between these species, which should be indicated by efficient ¹H–²⁹Si polarization transfer. A control experiment is performed using tetramethylammonium (TMA) in



Tetrahedral Site	Enhanced By ^1H - ^{29}Si CP
T1	no
T2	no
T7	yes
T8	yes
T9	no

Figure 2.2. Effect on interatomic distance on the ^1H - ^{29}Si cross polarization efficiency between the protons of occluded *p*-xylene and the framework silicon atoms of Si-ZSM-5.²⁵

lieu of TPA in the synthesis gel in order to observe the effect on the ^1H - ^{29}Si CP profile of an organic species which does not serve as a structure-directing agent for Si-ZSM-5³ or any other crystalline, pure-silica product. The issues of whether organic-mediated preorganization of silicate occurs in the TPA-mediated synthesis of Si-ZSM-5 and at what stage during the synthesis these organized, X-ray amorphous species are formed are of primary concern. The influence of the inorganic components of the synthesis mixture, e.g., the presence of sodium or the use of different silica sources, on the mechanism of structure direction and the kinetics of product formation is also investigated. Finally, an attempt to isolate the relevant preorganized, intermediate species by capping the Si-OH groups of the silicate species in solution with trimethylsilane is described.

Experimental

Synthesis

A synthesis procedure for Si-ZSM-5 was developed in which the only source of protons is the tetrapropylammonium cation; all other reagents were used in their deuterated forms. The gel composition was 0.5 TPA₂O: 3 Na₂O: 10 SiO₂: 2.5 D₂SO₄: 380 D₂O. In a typical synthesis, 2.76 g TPABr (Aldrich) was dissolved in a solution of 6.38 g 40 wt % NaOD in D₂O (Aldrich, 99+ atom % D) and 75 g D₂O (Cambridge Isotope Laboratories, 99.9 atom % D). To the clear solution was added 6.25 g fumed SiO₂ (Cab-O-Sil, Grade M-5), and the mixture was stirred for 15 min. To adjust the pH of the gel, 2.63 g D₂SO₄ (Aldrich, 98 wt % in D₂O, 99.5+ atom % D)

was added and the final gel was stirred for 3 h. The gel was heated statically at 110 °C and autogenous pressure in Teflon-lined, stainless steel reactors for 10 d. Samples were collected from the unheated gel, and after 1, 2, 3, and 10 days of heating. The samples were freeze-dried by immediate quenching of the hot gels in liquid N₂, with subsequent removal of D₂O by sublimation at -4 °C in vacuo. The freeze-dried samples were stored in a N₂ atmosphere. Spectral analyses were performed on freeze-dried samples both before and after washing with D₂O to remove non-occluded TPA.

In order to perform syntheses of Si-ZSM-5 in the absence of sodium, an approximately 0.5 M solution of TPAOH in D₂O was prepared using Amberlite IRA-400 (OH) anion exchange resin (Aldrich) and TPABr in D₂O; the exact concentration of TPAOH was determined by titration with 0.096 N HCl (Aldrich). Gels were prepared with a composition of 0.5 TPA₂O: 10 SiO₂: 380 D₂O. In a typical sodium-free synthesis of Si-ZSM-5, a gel containing 5.23 g TPAOH solution, 14.22 g D₂O, and 1.5 g fumed SiO₂ was stirred for 3 h. The fluid gel was heated statically at 110 °C and autogenous pressure in Teflon-lined, stainless steel reactors for 20 d. Samples were collected from the unheated gel and after 1, 10, and 15 days of heating, as described above; sample collection was difficult since some nucleation occurred on the surface of the Teflon liner, rendering the crystalline solid difficult to isolate. When tetraethylorthosilicate (TEOS) (Aldrich) was instead used as the silica source, the synthesis mixture was a clear solution. Samples were collected from the unheated solution and after 1, 4, and 7 days of heating; crystallization was complete in 7 days.

A sample of Si-ZSM-5 was also prepared using deuterated TPA (TPA-*d*₂₈) and TEOS using a gel composition of 0.5 (TPA-*d*₂₈)₂O: 10 SiO₂:

380 H₂O. (TPA-*d*₂₈)Br was purchased from Isotec (custom synthesis) and converted to the hydroxide form using Amberlite IRA-400 (OH) anion exchange resin, as described above. Zeolite crystallization was complete after 7 days of heating at 110 °C.

A gel similar in composition to the initial, sodium-containing synthesis gel for Si-ZSM-5 but containing 1.14 g TMACl (Aldrich) in lieu of TPABr was prepared for comparison in the ²⁹Si NMR studies. As expected, this synthesis gel did not give any crystalline product after heating at 110 °C for 60 days.

Silylation of the silicate species in the unheated, TEOS-containing synthesis mixture was performed according to the procedure of Agaskar.²⁶ An aged synthesis mixture prepared from 0.84 g 40 wt % TPAOH in H₂O (Johnson Matthey), 10.9 g H₂O, and 3.5 g TEOS was added dropwise to a solution containing 2.34 g hexamethyldisiloxane (Aldrich), 18.1 g 2,2-dimethoxypropane (Aldrich), and 1.10 g concentrated HCl (Fisher) and stirred for 1 h at room temperature. After concentration in vacuo at room temperature to remove the volatile components of the silylation reaction mixture, a solution containing 2.34 g hexamethyldisiloxane, 5.8 g *N,N*-dimethylformamide (DMF) (Aldrich), and 1.31 g trimethylchlorosilane (Aldrich) was added and stirred for 1 h to complete the silylation process. *n*-Pentane and water were added to the resulting solution and stirred for 5 min. The two-phase mixture contained a white solid suspended in the organic phase. The aqueous phase was extracted four times with *n*-pentane. Filtration of the combined organic phases yielded a fine, white powder.

Analysis

Solid state NMR studies were performed on a Bruker AM 300 spectrometer equipped with a Bruker dual channel MAS probe, a Bruker solid state CP MAS accessory, and high-power proton and X-channel amplifiers. Samples were packed under a dry N₂ or Ar atmosphere into 7 mm ZrO₂ rotors and spun at 1–3 kHz. ²⁹Si spectra (59.63 MHz) were collected using MAS (8 s recycle time) or ¹H–²⁹Si CP MAS with ¹H decoupling (4 s recycle time; 2–8 ms contact time) and were referenced to a tetrakis(trimethylsilyl)silane external standard (downfield resonance at –10.05 ppm vs. tetramethylsilane). Exponential line broadening of 50 Hz was applied to the data. ¹³C spectra of TPA-containing samples (75.47 MHz) were obtained using ¹H–¹³C CP MAS with ¹H decoupling (2 s recycle time; 2 ms contact time) and were referenced to an adamantane external standard (downfield resonance at 38.4 ppm vs. tetramethylsilane). ¹³C spectra of TMA-containing or silylated samples were obtained using ¹H decoupling only (2 s recycle time). Exponential line broadening of 20 Hz (unwashed samples) or 100 Hz (washed samples) was applied to the data. Spectral fitting was performed using Bruker LINESIM software.

Solution phase ¹H (300.10 MHz) and ¹³C (75.47 MHz) NMR spectroscopy of the silylated samples was performed using a General Electric QE 300 spectrometer. ¹H spectra were obtained using a 10 μs 90° pulse and a 4 s recycle time. ¹³C spectra were obtained with ¹H decoupling using a 30° pulse of 3.47 μs and a recycle time of 1 s. Chemical shifts were referenced to tetramethylsilane. Solution phase ²⁹Si NMR (99.36 MHz) was performed using a Bruker AM 400 spectrometer. ¹H-decoupled spectra were obtained using a 90° pulse of

13.5 μ s and a recycle time of 5 s. Chromium (III) acetylacetonate was added as a relaxation agent.

X-ray powder diffraction (XRD) data were collected on a Scintag XDS-2000 diffractometer using $\text{CuK}\alpha$ radiation. As a qualitative assessment of the amount of crystalline material present, the percent crystallinity of each sample was determined from the ratio of height of the most intense reflection in the XRD pattern ($23.19^\circ 2\theta$; (501) reflection) to the height of the 501 reflection of the Si-ZSM-5 sample prepared using Cab-O-Sil, sodium, and D_2O . Because the choice of reference sample (assigned as 100% crystallinity) is somewhat arbitrary, it is possible that a product may have a percent crystallinity value greater than 100%. For amorphous samples, the intensity of the 501 reflection and the percent crystallinity are zero.

IR spectroscopy was performed on a Nicolet System 800 FTIR Instrument. IR samples were prepared as KBr pellets. Raman spectroscopy was performed using the Fourier Transform Raman Accessory (Nd-YAG laser; $\lambda=1064$ nm; 600 mW) for the Nicolet System 800 FTIR.

Thermogravimetric analyses (TGA) were performed on a DuPont 951 Thermogravimetric Analyzer. Approximately 10 mg of sample were heated at a rate of 5°C min^{-1} to 600°C . Elemental analysis (C, H, N, Si, Na) was performed at Galbraith Laboratories, Knoxville, Tennessee. Time-of-flight mass spectrometry was performed by Jane Sanders at the California Institute of Technology.

Results

Synthesis Profile

X-ray powder diffraction data for the washed, freeze-dried samples collected from the unheated, sodium-containing gel and at various time intervals during the synthesis show that crystalline order observable by XRD (on the order of approximately 4–5 unit cells, or 80–100 Å)²⁷ is present after two days of heating, and that crystallization is complete after ten days (Figure 2.3). The crystallization profiles for the three syntheses of Si-ZSM-5 (sodium/Cab-O-Sil; no sodium/Cab-O-Sil; no sodium/TEOS) are compared in Figure 2.4. Crystallization of Si-ZSM-5 from a condensed silica precursor (Cab-O-Sil) in the absence of sodium involves a 2–4 day induction period before crystalline material is detected by XRD; crystallization is slower than from the sodium-containing gel. However, when a monomeric silica source (TEOS) is used, nucleation and crystal growth occur more rapidly than when a highly condensed source of silica such as Cab-O-Sil is used, even in the absence of sodium. For the synthesis using TEOS, crystallization begins in less than 1 day of heating and is essentially complete after 3 days of heating.

The IR spectrum of Si-ZSM-5 is characterized by two structural vibrational bands in the spectral region of 400–700 cm⁻¹: one at 550–560 cm⁻¹,²⁷ which has not been conclusively assigned but may be a stretching mode of structural silicate double -ring units,²⁸ and one at 440–470 cm⁻¹, which is a Si–O bending mode observed in many polymorphs of SiO₂.²⁹ The appearance of the 550–560 cm⁻¹ band is indicative of the atomic ordering of Si-ZSM-5 and is not observed in amorphous silica, TEOS, or TEOS hydrolyzed in the presence of sodium hydroxide. This

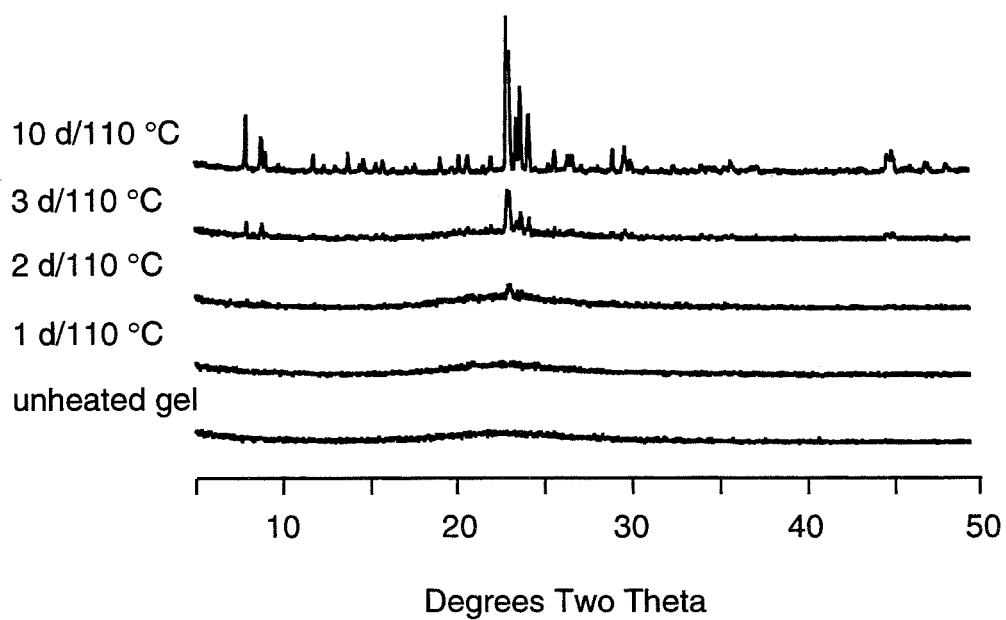


Figure 2.3. X-ray diffraction patterns of the D₂O-washed, freeze-dried samples collected during the TPA-mediated, sodium-containing synthesis of Si-ZSM-5.

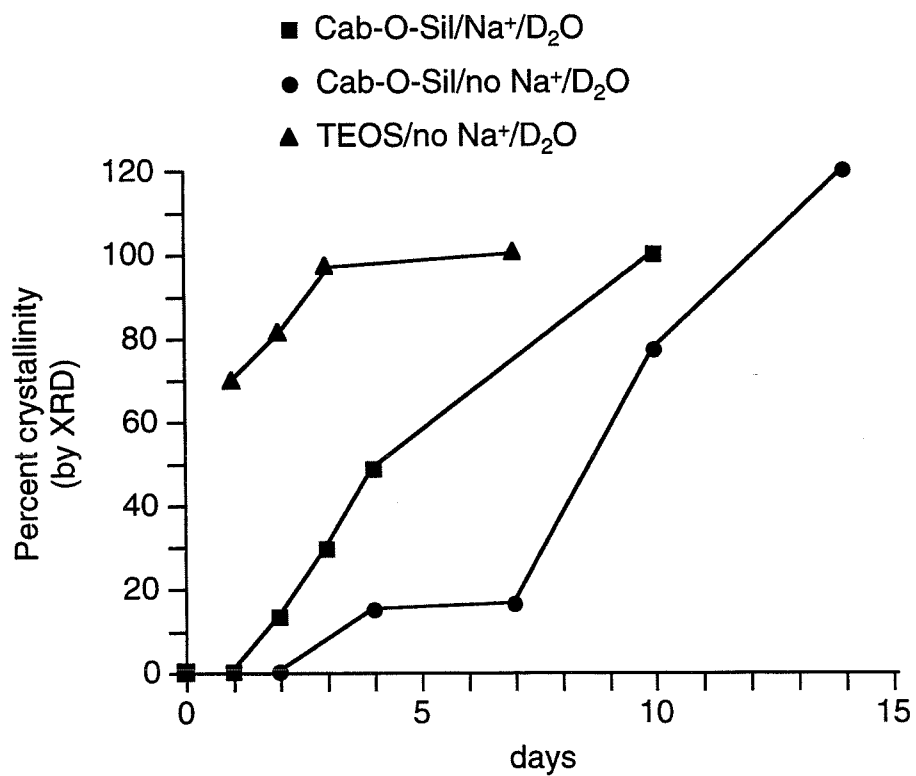


Figure 2.4. Crystallization profiles of TPA-mediated syntheses of Si-ZSM-5.

spectroscopic signature is apparent even in samples that are apparently amorphous by conventional X-ray techniques and most likely contain domains of Si-ZSM-5 that are on the order of only a few unit cells (length scale $<80 \text{ \AA}$).²⁷ For the syntheses using condensed silica, the appearance of the $550\text{--}560 \text{ cm}^{-1}$ band in the spectrum of the washed, freeze-dried samples is concurrent with the development of peaks in the XRD pattern, i.e., after two days of heating of the sodium-containing sample (Figure 2.5) and after 5–10 days of heating of the sodium-free sample (Figure 2.6). However, in the IR spectra obtained during the synthesis of Si-ZSM-5 using TEOS, a band is apparent at 560 cm^{-1} in the spectrum of the X-ray amorphous, freeze-dried, unheated synthesis mixture as well as in those of all of the partially- or fully-crystalline samples obtained after heating (Figure 2.7).

TGA of the crystalline products indicates two stages of weight loss: the first, from $25 \text{ }^\circ\text{C}$ to $345 \text{ }^\circ\text{C}$ corresponds to desorption of water, and the second, from $345 \text{ }^\circ\text{C}$ to $600 \text{ }^\circ\text{C}$, corresponds primarily to combustion of TPA, with perhaps some additional desorption of water due to silanol group condensation; calculation of the weight percent of TPA from the weight loss above $345 \text{ }^\circ\text{C}$ may thus overestimate the TPA content. Based on TGA data, the crystalline products in all cases have similar unit cell compositions (4.4 TPA: 0.40 Na^+ : 96 SiO_2 : $7.7 \text{ D}_2\text{O}$ for the synthesis with sodium (sodium content determined by elemental analysis); 4.6 TPA: 96 SiO_2 : $1.5 \text{ D}_2\text{O}$ for the sodium-free synthesis from Cab-O-Sil; 4.4 TPA: 96 SiO_2 : $2.3 \text{ D}_2\text{O}$ for the synthesis using TEOS). With four intersections per unit cell, Si-ZSM-5 thus contains one TPA molecule per channel intersection, and TPA completely fills the available void space of the ZSM-5 structure (ZSM-5 cannot contain more than 4 TPA molecules per 96 SiO_2).

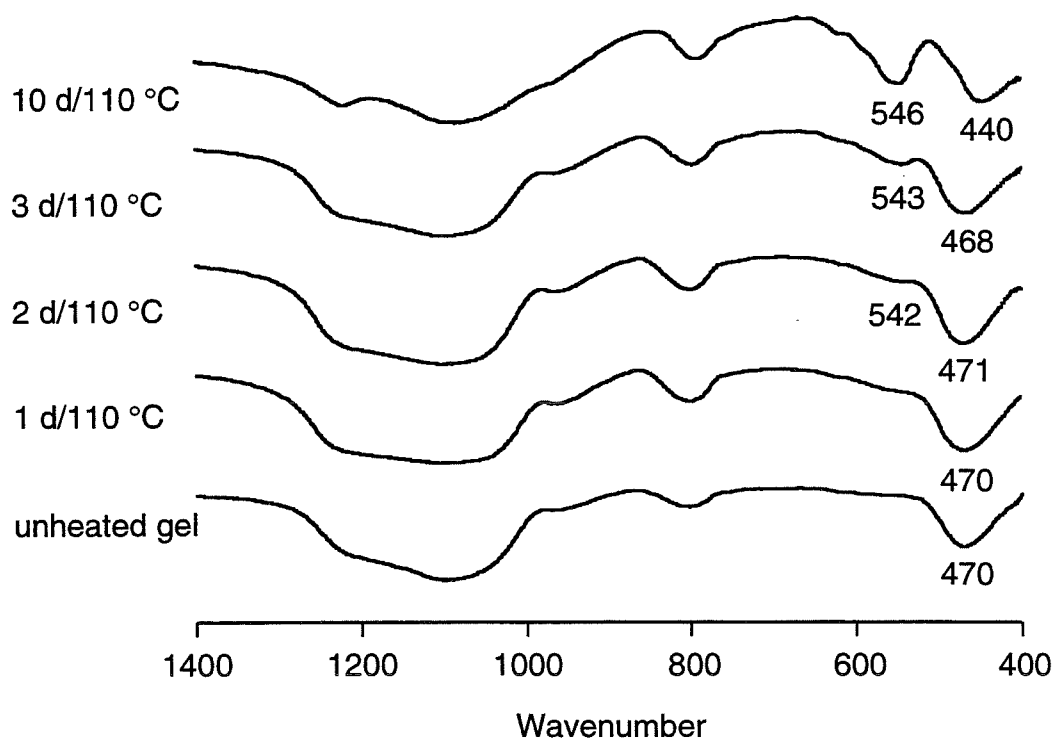


Figure 2.5. IR spectra of the D₂O-washed, freeze-dried samples collected during the TPA-mediated, sodium-containing synthesis of Si-ZSM-5.

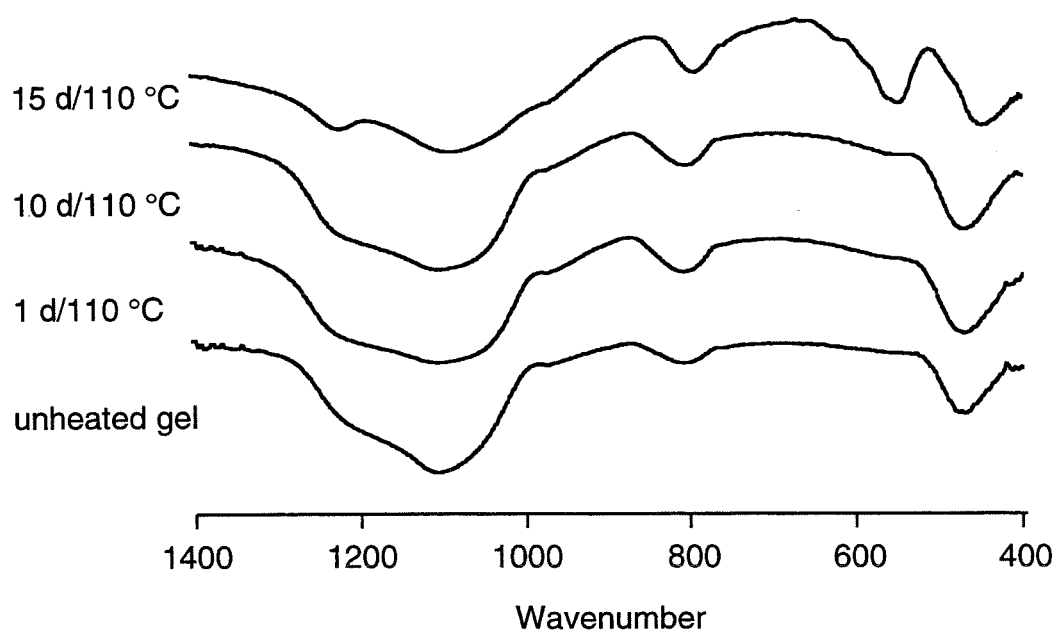


Figure 2.6. IR spectra of the D₂O-washed, freeze-dried samples collected during the TPA-mediated, sodium-free synthesis of Si-ZSM-5 using Cab-O-Sil.

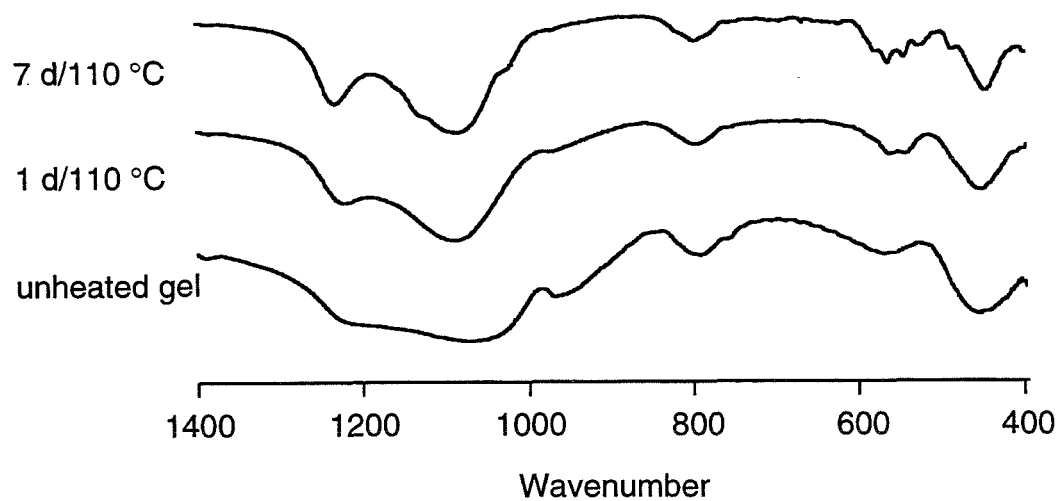


Figure 2.7. IR spectra of the D₂O-washed, freeze-dried samples collected during the TPA-mediated, sodium-free synthesis of Si-ZSM-5 using TEOS.

NMR Profiles

The ^{29}Si MAS and ^1H - ^{29}Si CP MAS NMR spectra of the freeze-dried samples from the three syntheses of Si-ZSM-5 are presented in Figures 2.8–2.10. An in situ ^1H - ^{29}Si CP MAS NMR study was not possible for this system because of the large amount of water (D_2O) present; the species within the system are too mobile to permit efficient cross polarization. The freeze-dry technique was employed in order to preserve the silicate structures that are present at synthesis conditions and to avoid the appearance of structural artifacts that may result from slow cooling of the sample and filtration to collect the solid phase.³⁰ Subsequent washing of the freeze-dried samples with D_2O did not significantly alter the cross polarization profiles. ^1H - ^{29}Si CP MAS NMR spectra are shown at two different contact times to demonstrate the degree of molecular motion within the samples. For relatively immobilized systems and short contact times (≤ 10 ms), a greater extent of polarization transfer is achieved with increasing contact time because polarization is transferred to more distant nuclei as well as to nuclei within the van der Waals contact distance; however, spin-lattice relaxation of the spin-locked protons becomes significant at long contact times (> 10 ms), thus reducing the extent of polarization transfer.²⁰

The two resonances observed in Figures 2.8–2.10 correspond to Q^3 (downfield resonance) and Q^4 (upfield resonance) species (Q^n represents $\text{Si}(\text{OSi})_n(\text{OD})_{4-n}$). During the course of the synthesis, the overall intensities of the spectra obtained without CP remain constant (note the different intensity scale for highly crystalline samples) but show an increase in the number of Q^4 sites relative to Q^3 . The positions of the Q^3 and Q^4 signals shift from -100 to -102 ppm and from -110 to -112 ppm, respectively, during

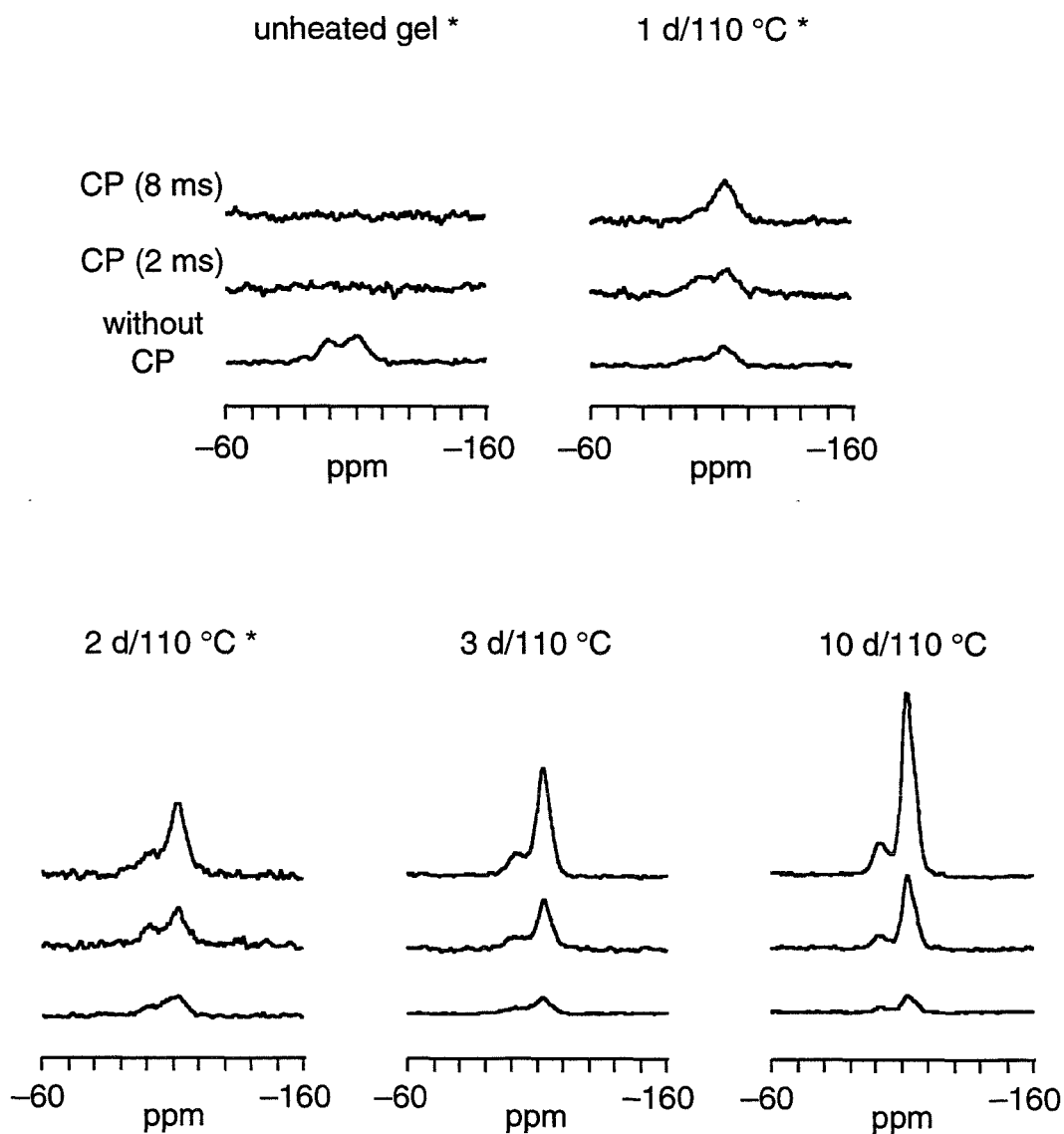


Figure 2.8. ^{29}Si MAS and ^1H - ^{29}Si CP MAS NMR spectra of the freeze-dried samples collected during the TPA-mediated, sodium-containing synthesis of Si-ZSM-5 (CP contact times as indicated; * indicates an expanded intensity scale (x5)).

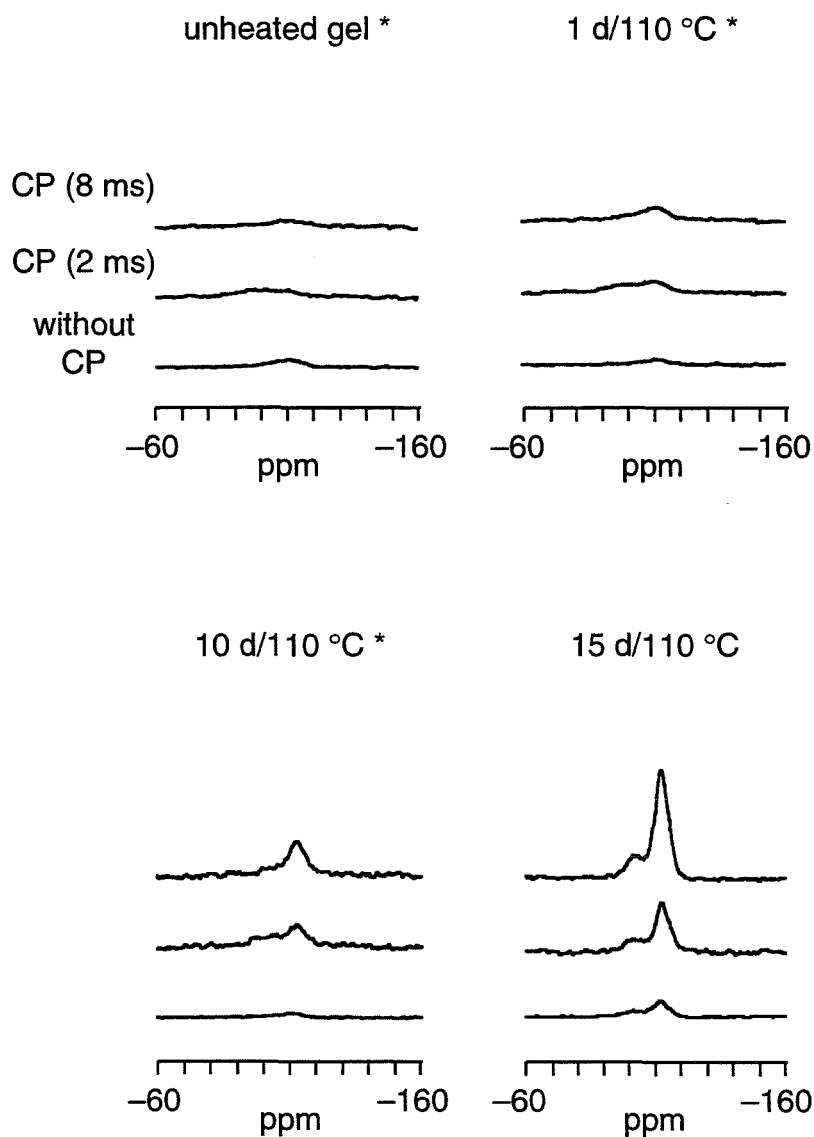


Figure 2.9. ^{29}Si MAS and ^1H - ^{29}Si CP MAS NMR spectra of the freeze-dried samples collected during the TPA-mediated, sodium-free synthesis of Si-ZSM-5 using Cab-O-Sil (CP contact times as indicated; * indicates an expanded intensity scale (x5)).

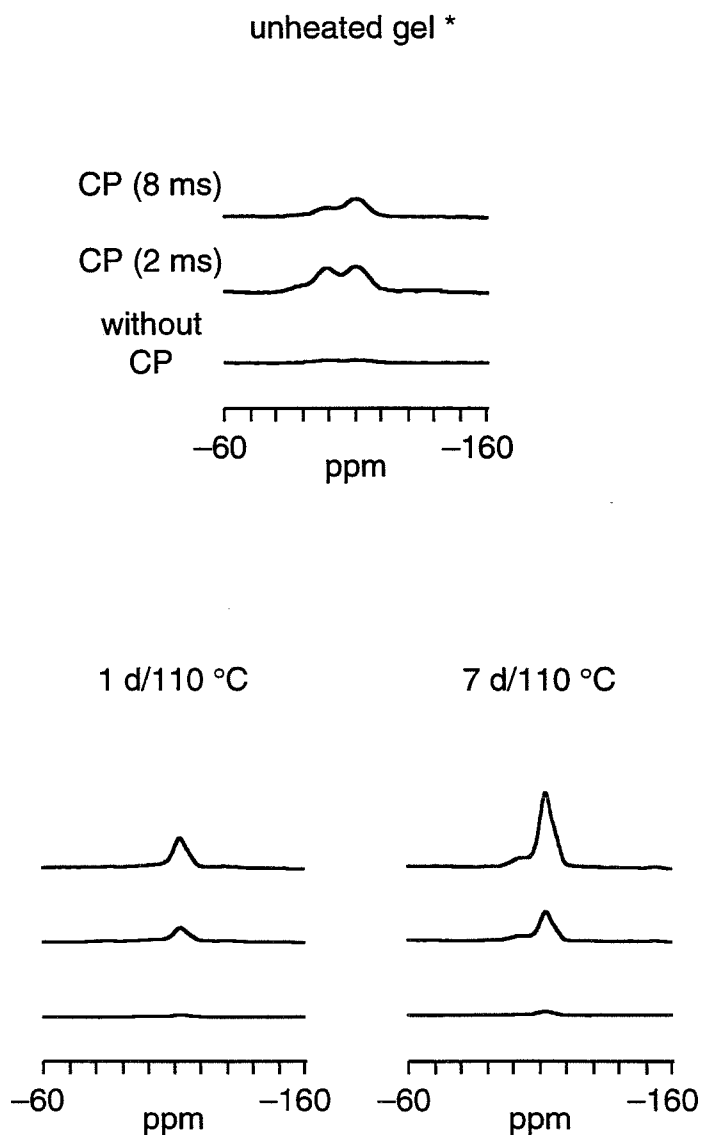


Figure 2.10. ^{29}Si MAS and ^1H - ^{29}Si CP MAS NMR spectra of the freeze-dried samples collected during the TPA-mediated, sodium-free synthesis of Si-ZSM-5 using TEOS (CP contact times as indicated; * indicates an expanded intensity scale (x/5)).

the transformation from amorphous silica to crystalline Si-ZSM-5. The upfield shift has been correlated with the larger Si-O-Si bond angles present in Si-ZSM-5 versus amorphous silica.³¹ The spectra show that the relative positions of the TPA protons and the structural silicon atoms change during the course of the synthesis.

For the sodium-containing system prepared with Cab-O-Sil (Figure 2.8), polarization transfer does not occur in the unheated gel because the TPA molecules cannot interact with the bulk silica; they are only in contact with the surface of the undissolved silica particles. After heating for one day, cross polarization between TPA protons and the silicon atoms is observed although the solid is amorphous by XRD and IR. Even at the shortest contact time measured (2 ms), the intensity of the CP spectrum is greater than that obtained without CP, suggesting that polarization transfer is efficient; for non-deuterated zeolite systems, the intensity of the spectrum obtained with CP is generally weaker than that obtained without CP²² since the presence of mobile H₂O provides an additional pathway for proton relaxation. At the shortest contact time, Q³ species are polarized more rapidly than Q⁴ species, perhaps because the Q³ species are in closer proximity to the organic protons due to a weak coulombic attraction; non-protonated Q³ sites (Si(OSi)₃(O⁻)) apparently provide the charge-balancing anions for TPA cations occluded in crystalline Si-ZSM-5 (Figure 2.11). At the longer contact times, more distant Q⁴ sites are more strongly enhanced. For the partially- and completely-crystalline samples obtained at heating times of two to ten days, the CP profiles follow the same trend with a substantial overall increase in signal intensity of all of the CP spectra. The spectra obtained without CP provide no additional mechanistic information. However, these spectra

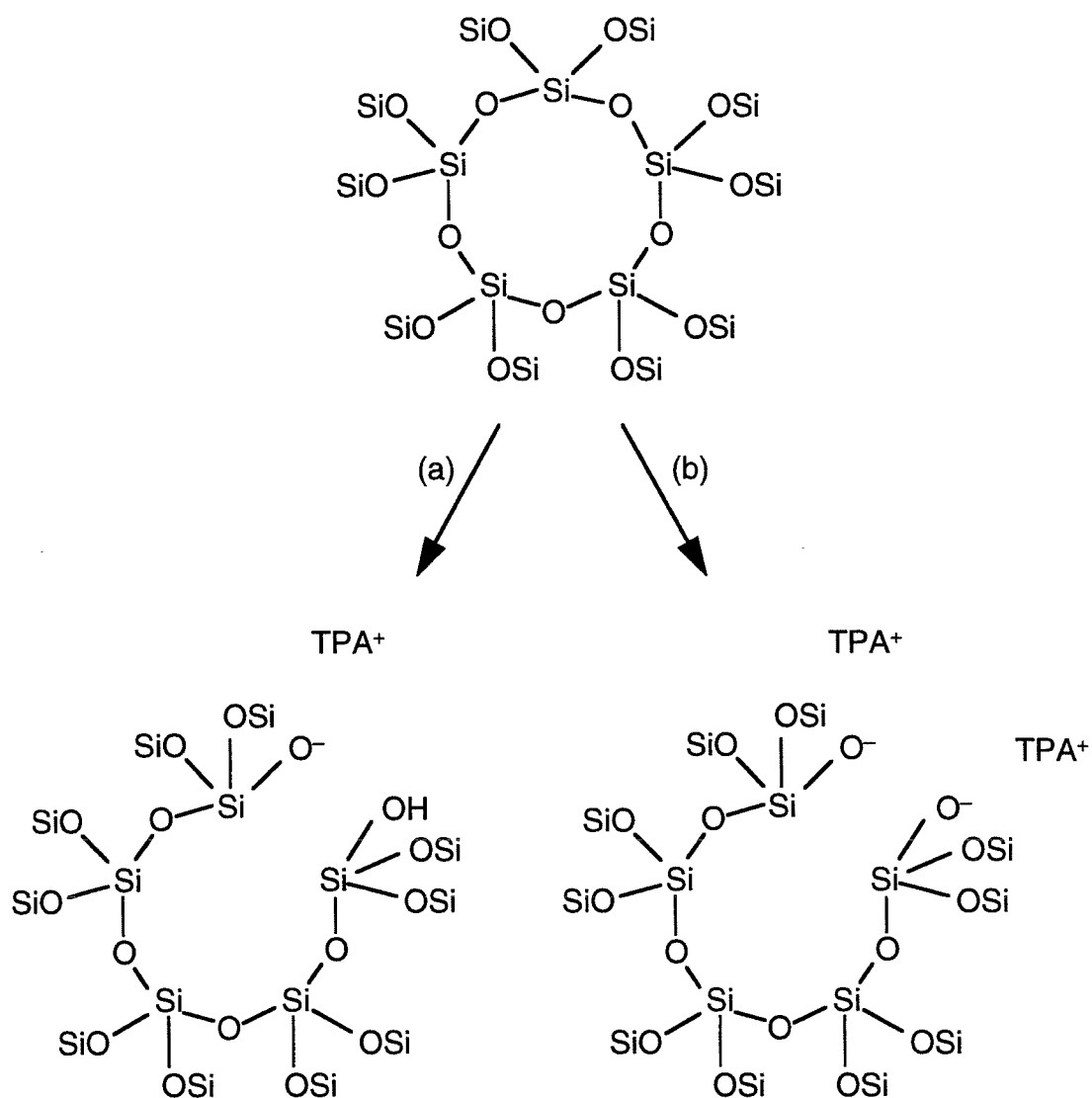


Figure 2.11. Origin of Q³ defect sites in as-synthesized, pure-silica zeolites. Cleavage of one Q⁴-Q⁴ linkage generates two Q³ sites. The resulting pair of silanol groups (one protonated, one non-protonated) can balance the charge of a nearby TPA cation (a). Alternatively, if the silanol groups are appropriately positioned to point into adjacent channel intersections, one pair of silanol groups (both non-protonated) can balance the charge of two TPA cations (b).³²

indicate that 20–25% of the Si atoms in the as-synthesized, crystalline Si-ZSM-5 samples are Q^3 sites, although a content of only 4% non-protonated Q^3 is required for charge balance of the occluded TPA cations. An understanding of the origin and nature of the additional Q^3 sites in these samples remains a topic for future investigation.

The corresponding ^1H – ^{29}Si CP MAS NMR profile of the sodium-free sample prepared with Cab-O-Sil is shown in Figure 2.9. No ^1H – ^{29}Si CP is observed for the unheated gel. After heating the sample for one day, the CP profile resembles that for the case in which sodium is present, even though the appearance of crystalline product occurs more slowly than in the sodium-containing synthesis. After crystal growth has begun, similar correlations between the efficiency of CP and the amount of crystalline material present by XRD are observed for the syntheses in the presence and absence of sodium.

By contrast, when a monomeric silica source is used, polarization transfer is observed not only in the heated, partially- or fully-crystalline samples but also in the unheated synthesis mixture (Figure 2.10). The observed CP is not due to the presence of protons from non-hydrolyzed TEOS or from ethanol produced by hydrolysis since these species are removed by freeze-drying (*vide infra*).

In Figure 2.12, the spectra of a synthesis gel containing TMA in lieu of TPA are shown in order to demonstrate whether there is any influence on the CP profile by an organic species which does not serve as a structure-directing agent and does not yield a crystalline product. Similar to those from the syntheses using TPA and Cab-O-Sil, the spectra of the unheated TMA-containing gel show no transfer of polarization from the TMA protons to the silicate species. After ten days of heating, the gel appears

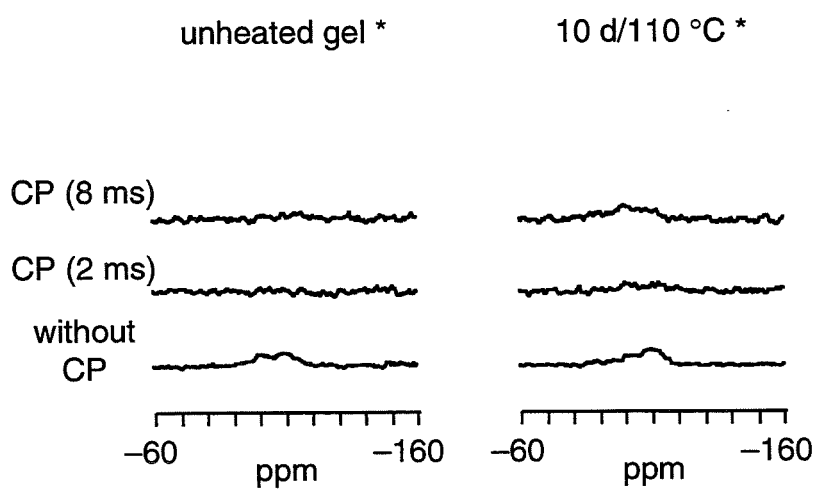


Figure 2.12. ^{29}Si MAS and ^1H - ^{29}Si CP MAS NMR spectra of the freeze-dried samples of the synthesis gel containing TMA in lieu of TPA (CP contact times as indicated; * indicates an expanded intensity scale (x5) relative to Figure 2.8, 10 d sample).

amorphous by XRD and IR (as is expected since Si-ZSM-5 has never been synthesized using TMA³). A small amount of polarization transfer is observed in the ¹H-²⁹Si CP MAS NMR spectra but CP is not nearly as efficient as in the TPA-containing samples after one day of heating.

The ¹H-¹³C CP MAS NMR spectra of solid TPABr, TPA occluded into Si-ZSM-5, and TPA-*d*₂₈ occluded in Si-ZSM-5 are shown in Figure 2.13. When the TPA cation is located in the channel intersections of Si-ZSM-5, its spectrum is markedly changed from that of TPABr.^{33,34} The former is characterized by a downfield shift and broadening of the resonance of the methylene carbon adjacent to the nitrogen group (60.0 ppm for TPABr; 62.6 ppm for occluded TPA) and an upfield shift and splitting of the methyl carbon resonance (12.6 ppm for TPABr; 10.1 and 11.3 ppm for occluded TPA), while the resonance of the second methylene carbon remains essentially unchanged (16.0 ppm for TPABr; 16.3 ppm for occluded TPA). The spectral signature of occluded TPA reflects the change in conformation and the changes in intramolecular and intermolecular van der Waals interactions that are imposed on TPA upon occlusion into the channel intersections of Si-ZSM-5.³³⁻³⁵ TPA in TPABr has an *S*₄ axis at the nitrogen center and an all-trans conformation in the alkyl chains,³⁶ while occluded TPA has approximate *C*_s symmetry at the nitrogen center and some gauche interactions in the alkyl chains.⁶ Although the splitting of the methyl carbon resonance of TPA occluded in ZSM-5 has previously been attributed to steric contact between the methyl groups of two adjacent TPA molecules,³⁴ the absence of splitting of the methyl resonance in the ¹³C MAS NMR spectrum of sterically bulkier TPA-*d*₂₈ occluded in Si-ZSM-5 (9.4 ppm; 15.3 ppm; 61.8 ppm) suggests that the splitting does not arise from methyl-methyl interactions. The splitting

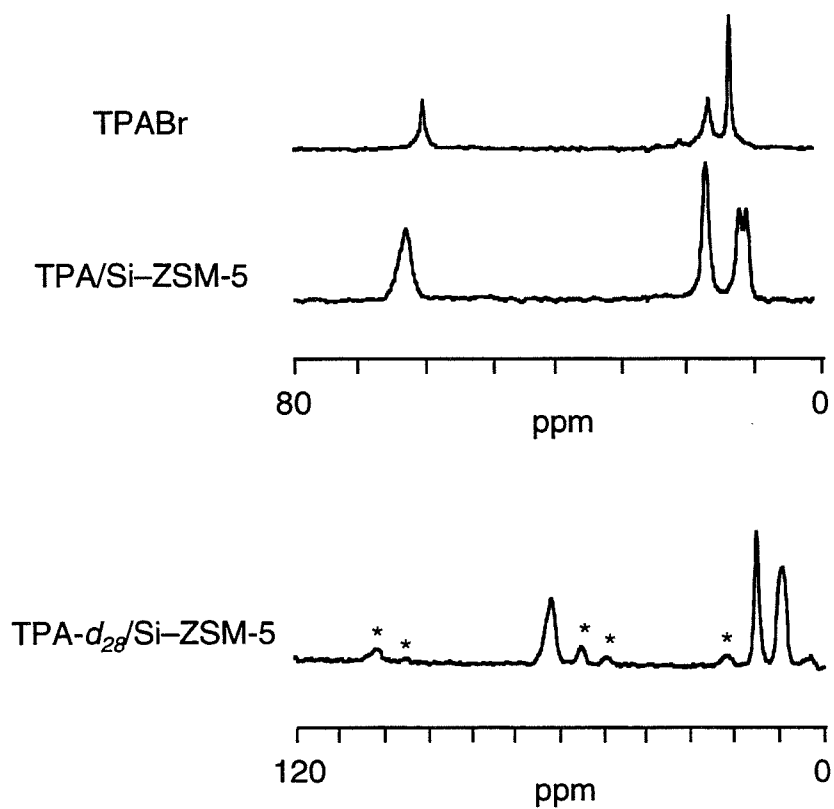


Figure 2.13. ^1H - ^{13}C CP MAS NMR spectra of TPABr, TPA occluded in Si-ZSM-5, and TPA- d_{28} occluded in Si-ZSM-5 (* indicates spinning side bands).

of the methyl carbon resonance is likely due to differences in the van der Waals interactions between the methyl groups and the silicate framework in the straight and sinusoidal channels. Van der Waals interactions between TPA and the silicate structure are also responsible for the upfield shift of the methyl carbon resonance relative to that of TPABr.

Occluded and free TPA molecules are observed in the ^1H - ^{13}C CP MAS NMR spectra of the unwashed, freeze-dried, sodium-containing samples collected at various time intervals during the synthesis, and the spectra are shown in Figure 2.14. It should be noted that 2.4 times the maximum amount of TPA that can be occluded into the final product is present in the synthesis mixture; thus in a fully-crystalline, unwashed, freeze-dried sample there will be at least 1.4 times as much free TPA remaining as occluded TPA. In the unheated gel sample, only free TPA is observed (12.6 ppm, 15.9 ppm, and 60.0 ppm). Although it is difficult to discern whether any TPA is occluded into the sample after one day of heating, it becomes apparent after two days of heating that TPA molecules are present in the channels of Si-ZSM-5 (new peak at 10.1 ppm); this is consistent with the XRD and IR results that indicate that there is some crystalline Si-ZSM-5 present at this time during the synthesis. The relative amount of occluded TPA increases with longer heating times (increased intensity of the peaks at 10.4 ppm, 11.3 ppm, and 62.6 ppm). In the freeze-dried sample obtained after ten days of heating, the spectra of the two species are well resolved (10.2 ppm, 11.3 ppm, 16.3 ppm, and 62.6 ppm for occluded TPA; 12.6 ppm, 16.0 ppm, and 60.0 ppm for TPABr).

The ^1H - ^{13}C CP MAS NMR spectra of the D_2O -washed, sodium-containing samples, i.e., after removal of free TPA, of the freeze-dried gel and the sample collected after one day of heating are shown in Figure 2.15.

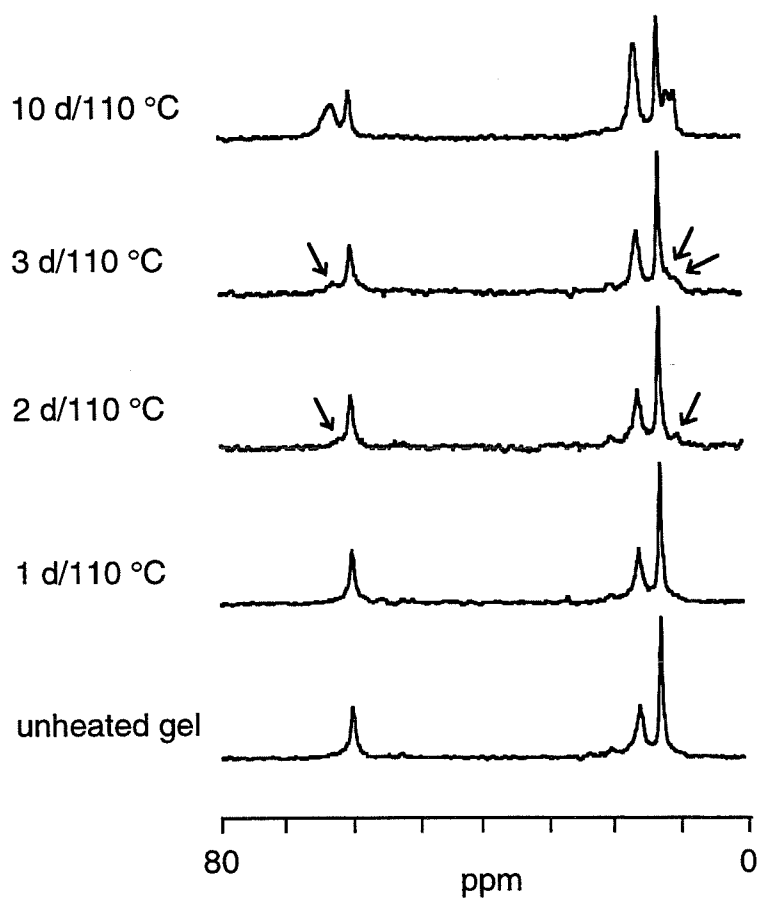


Figure 2.14. ^1H - ^{13}C CP MAS NMR spectra of the freeze-dried samples collected during the TPA-mediated, sodium-containing synthesis of Si-ZSM-5.

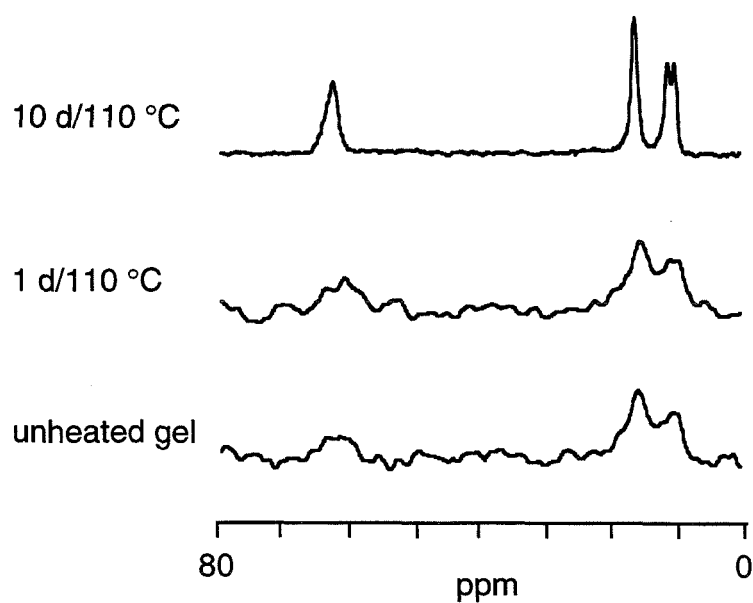


Figure 2.15. ^1H - ^{13}C CP MAS NMR spectra of the D_2O -washed, freeze-dried samples collected during the TPA-mediated, sodium-containing synthesis of Si-ZSM-5.

In spite of the low signal-to-noise ratio of these signals due to the low organic content (the small amount of TPA in these samples is difficult to detect by TGA) and the low resolution due to the large exponential line broadening thus required, it is apparent that the methyl carbon resonance is shifted upfield (9.6 ppm) and that the resonance of the methylene carbon bonded to the nitrogen is shifted downfield (61.0 ppm), indicating some similarity to TPA occluded in Si-ZSM-5. The resonance of the middle methylene group appears at 15.5 ppm.

For the ^1H - ^{13}C CP MAS NMR spectra of the washed, freeze-dried samples collected during the sodium-free synthesis Si-ZSM-5 using Cab-O-Sil as the silica source, similar resonances are observed. Some TPA is evident in the X-ray amorphous material (9.5, 15.5, 60.4 ppm) (Figure 2.16). However, the channel intersections of Si-ZSM-5 are apparently not fully formed, as suggested by the position of the resonance of the methylene carbon adjacent to nitrogen (unshifted relative to that of TPABr). Upon further heating and the appearance of crystalline Si-ZSM-5 in the XRD pattern, the characteristic ^1H - ^{13}C CP MAS NMR spectrum of TPA occluded in Si-ZSM-5 is observed.

For the ^1H - ^{13}C CP MAS NMR spectrum of the unheated, TEOS-containing synthesis mixture, a substantial amount of TPA is present in the washed, freeze-dried sample (Figure 2.17). Residual, non-hydrolyzed TEOS and ethanol produced from the hydrolysis of TEOS are not observed in the spectrum of the unwashed sample because they are removed by freeze-drying. The chemical shifts of the two methylene resonances of TPA in the washed samples (15.7 and 60.0 ppm) are similar to those observed for free TPA, but the upfield shift of the methyl resonance (11.1 ppm) indicates that there is an interaction between TPA and other

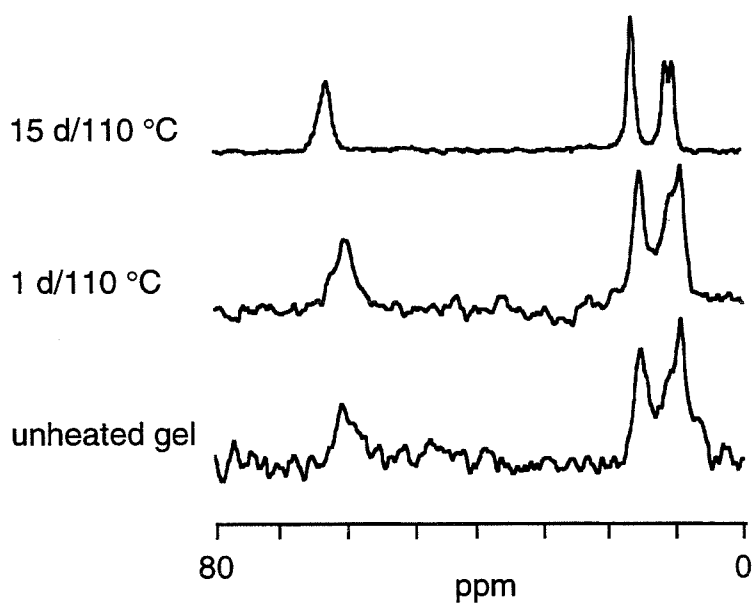


Figure 2.16. ^1H - ^{13}C CP MAS NMR spectra of the D_2O -washed, freeze-dried samples collected during the TPA-mediated, sodium-free synthesis of Si-ZSM-5 using Cab-O-Sil.

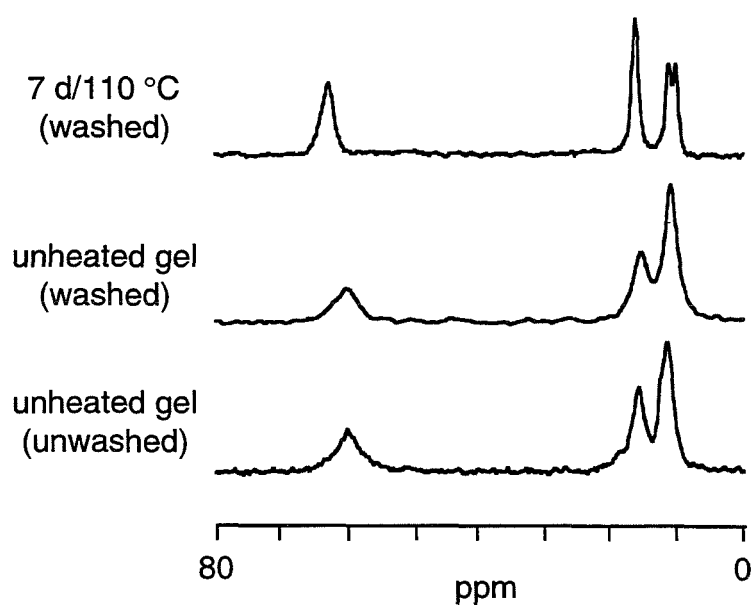


Figure 2.17. ^1H - ^{13}C CP MAS NMR spectra of the unwashed and D_2O -washed, freeze-dried samples collected during the TPA-mediated, sodium-free synthesis of Si-ZSM-5 using TEOS.

species in the synthesis mixture. Upon heating of the synthesis gel and the appearance of crystalline Si-ZSM-5 by XRD, the characteristic resonances of TPA occluded in Si-ZSM-5 are observed.

^1H -decoupled ^{13}C MAS NMR spectra were obtained for the unheated gel containing TMA in lieu of TPA and for this sample after heating for ten days (not shown). In each spectrum, a single resonance was observed (56.1 ppm and 55.8 ppm, respectively) at a shift corresponding to that of TMA in aqueous solution (55.3–56.4 ppm).^{37,38} A downfield shift indicative of TMA occluded into the more constrained (due to van der Waals interactions) environment of a zeolite cage (56.7–58.9 ppm)³⁷⁻³⁹ was not observed. Upon washing the heated sample with D_2O , a single weak ^{13}C resonance was detected (55.7 ppm; not shown), indicating that a small amount of TMA (difficult to detect by TGA) is adsorbed into the silicate solid phase but is not contained within zeolite-like void spaces.

Silylation

The sample collected by silylation of the unheated, TEOS-containing synthesis mixture is amorphous by XRD (not shown). However, the IR spectrum contains the vibrational signature of Si-ZSM-5 at 561 cm^{-1} in addition to the Si-O bending mode at 458 cm^{-1} (Figure 2.18). The bands at 847 and 1254 cm^{-1} correspond to Si- CH_3 modes of the trimethylsilyl groups.⁴⁰ The ^{29}Si MAS and ^1H - ^{29}Si CP MAS NMR spectra each contain four peaks (Figure 2.19). The resonances at -92 , -101 , and -112 ppm are assigned to Q^2 , Q^3 , and Q^4 species, respectively. The resonance at 13 ppm corresponds to the trimethylsilyl groups. The observed enhancement of the resonances of the non-silylated as well as the silylated species by CP suggests that the silicon-containing species are in close contact with

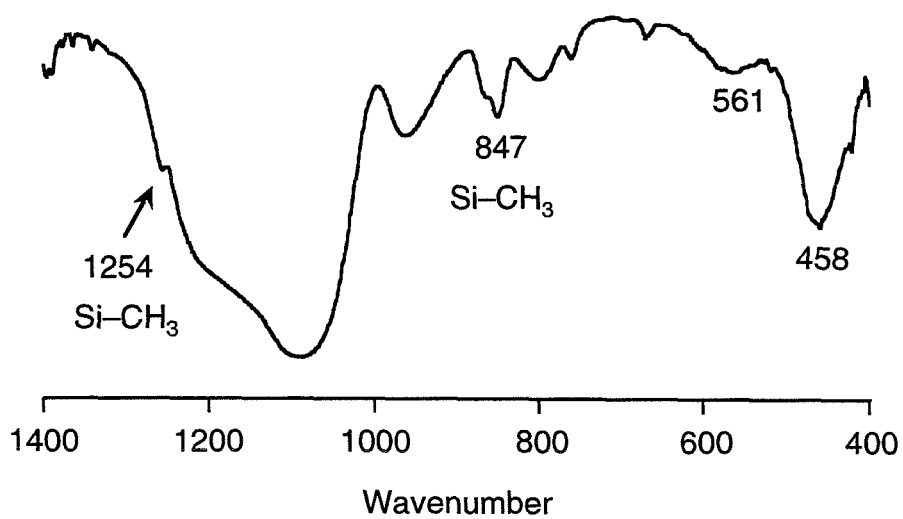


Figure 2.18. IR spectrum of the sample collected by trimethylsilylation of the unheated, TEOS-containing synthesis mixture.

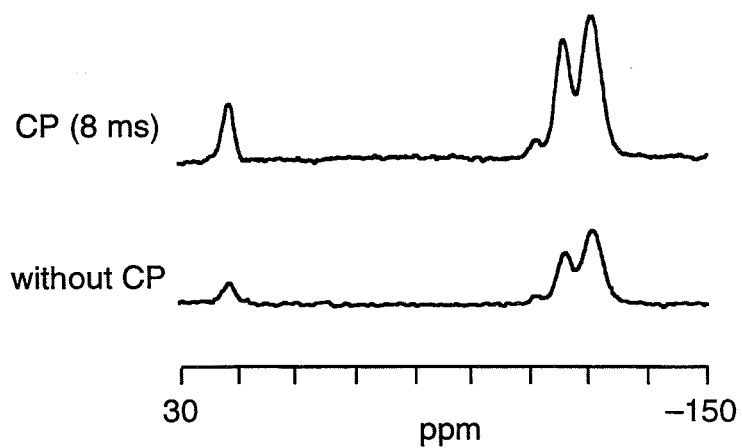


Figure 2.19. ^{29}Si MAS and ^1H - ^{29}Si CP MAS NMR spectra of the sample collected by trimethylsilylation of the unheated, TEOS-containing synthesis mixture (CP contact time as indicated).

organic protons, similar to the case observed at early stages during the TPA-mediated synthesis of Si-ZSM-5 as well as for crystalline, TPA-containing Si-ZSM-5.

The ^1H -decoupled ^{13}C MAS and ^1H - ^{13}C CP MAS NMR spectra of the silylated product indicate the presence of several organic species (Figure 2.20). The resonance at 1.3 ppm corresponds to the trimethylsilyl groups. The resonances at 32.2, 35.7, and 37.6 ppm (methyl groups) and at 165.6 ppm (carbonyl) indicate the presence of residual DMF solvent from the silylation procedure. The ^1H - ^{13}C CP MAS NMR spectrum of DMF adsorbed on fumed silica (not shown) exhibits two methyl resonances (32.2, 37.6 ppm) due to the inequivalence of the two methyl groups in the solid state; the third peak (35.7 ppm) in the spectrum of the silylated sample is assigned to more mobile DMF molecules in which the two methyl groups are chemically equivalent (35.2 ppm for DMF in solution). Finally, the resonances at 10.8, 15.6, and 59.9 ppm correspond to TPA. The chemical shift of the methyl resonance indicates that TPA does not experience the geometric constraints and van der Waals interactions that would be present if the channel intersections of Si-ZSM-5 were fully formed. However, the upfield shift of the TPA methyl resonance for this sample relative to that of free TPA suggests that there are van der Waals interactions between TPA and other species in the silylated sample.

In the TGA of the silylated sample, the rate of weight loss is fairly constant (25 wt % total) during heating to 600 °C, and it is difficult to distinguish different stages of desorption and combustion of the various components. Elemental analysis of the sample indicates a molar composition of approximately 9.7 mol % C; 38.3 mol % H; 1.8 mol % N; 13.5 mol % Si; 36.7 mol % O. Considering the approximate compositions

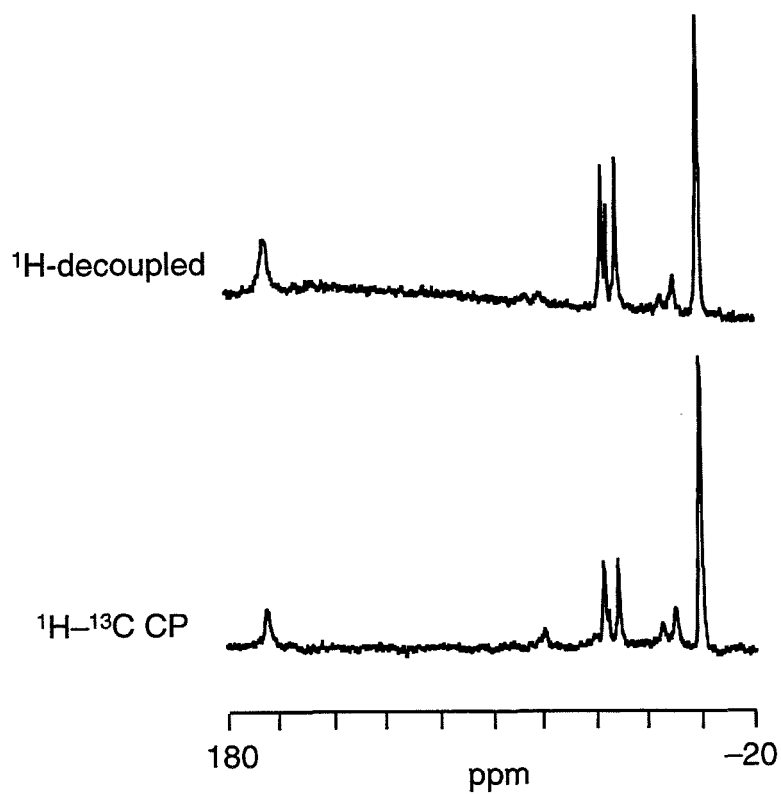


Figure 2.20. ^1H -decoupled ^{13}C MAS and ^1H - ^{13}C CP MAS NMR spectra of the sample collected by trimethylsilylation of the unheated, TEOS-containing synthesis mixture.

indicated by ^{29}Si MAS NMR (11.2 mol % trimethylsilyl; 4.9 mol % Q²; 31.0 mol % Q³; 52.9 mol % Q⁴ relative to the total Si content) and by ^{13}C MAS NMR (4 mol % TPA; 42 mol % trimethylsilyl; 54 mol % DMF relative to the total C content), one estimate of the composition of the precipitate obtained from the silylation procedure is 1 TPA: 76 SiO₂: 9.6 TMS: 6.8 DMF: 25 H₂O. This is a tentative approximation because the various techniques for assessing the product composition do not give mutually-consistent results. Nevertheless, this estimate is valuable because in combination with spectroscopic data it suggests that the silylated precipitate is a complex mixture of species, including amorphous silica and silicon-containing species that are in close contact with organic molecules.

Attempts to isolate the individual components of the silylated product were slightly successful. ^1H NMR of the species that are soluble in organic solvents such as chloroform-*d*, methylene-*d*₂ chloride, benzene-*d*₆, or dimethylsulfoxide-*d*₆ suggested the presence of TPA (0.9 ppm (t), 1.6 ppm (m), 3.1 ppm (m)), DMF (2.9 ppm (s), 3.0 ppm (s), 8.05 ppm (s)), and trimethylsilyl groups (0.1–0.2 ppm (s)) in addition to other, unidentified species. However, these spectra did not provide any additional information. Solution phase ^{13}C and ^{29}Si NMR were also not informative due to the low sensitivities of these nuclei and the low concentration of soluble species. Mass spectrometry of the chloroform-soluble species confirmed the presence of TPA but did not clearly indicate the presence of volatile, ionizable, high molecular-weight components such as the proposed inorganic–organic composite species.

Discussion

The samples collected prior to the appearance of Si-ZSM-5 by XRD and IR are of primary interest because they may aid in the elucidation of some of the molecular reorganization and molecular recognition processes that are involved in the self-assembly processes in zeolite synthesis. ^1H - ^{29}Si CP MAS NMR of the unheated, Cab-O-Sil-containing gels shows no signal, which suggests that polarization transfer does not occur because the TPA molecules and the silicate species are not in close proximity; the TPA molecules can only interact with the surface of the particles of condensed silica, and thus a sufficient number of intermolecular contacts for CP to be observed are not established. However, at this stage of the synthesis, there is a small amount of TPA associated with the solid silicate phase as demonstrated by ^1H - ^{13}C CP MAS NMR of the washed, freeze-dried sample.

Upon heating, the structure of the synthesis mixture undergoes dramatic transformations. Cross polarization between the TPA protons and the silicate species is observed in the Cab-O-Sil-containing samples collected after one day of heating. The solids do not exhibit long-range, crystalline order as indicated by the amorphous XRD patterns and the absence of a distinct $550\text{--}560\text{ cm}^{-1}$ band in the IR spectra. However, the molecular ordering at this stage is different relative to that of the unheated gel. This is suggested in part by a decrease in the Q^3 peak relative to Q^4 in the ^{29}Si MAS NMR spectra. A more significant change is that some silicon atoms (both Q^3 and Q^4) in the sample that was heated are in sufficiently close contact (on the time scale of several milliseconds) with TPA protons, allowing intermolecular polarization transfer to occur

(Figure 2.21). The silica depolymerizes upon heating of the synthesis mixture, and reorganization of the silicate oligomers occurs such that contacts are established between the silicate species and TPA molecules. The work of Mentzen and coworkers suggests that the H...Si interatomic distance necessary for efficient CP is approximately that of a van der Waals interaction ($\approx 3.3 \text{ \AA}$).²⁵ Although the rates of nucleation and crystallization are slowed in the absence of sodium when a condensed silica source (Cab-O-Sil) is used, the presence or absence of small amounts of sodium do not appear to influence the nature of the interactions between the organic and inorganic components since the ^1H - ^{29}Si CP MAS NMR profiles are qualitatively similar.

With further heating, crystalline Si-ZSM-5 is identified by XRD and IR spectroscopy. Tight enclathration of TPA molecules within the fully-formed channel intersections of Si-ZSM-5 significantly enhances the efficiency of ^1H - ^{29}Si cross polarization. The increase in signal intensity with increasing contact time (particularly for the Q^4 peak) confirms that the molecules are held rigidly and that proton magnetization is transferred to more distant silicon atoms ($>3.3 \text{ \AA}$) during longer contact times. In the samples that contain both crystalline and X-ray amorphous material as well as in the final product, washing the freeze-dried material to remove free TPA does not diminish the efficiency of intermolecular ^1H - ^{29}Si polarization transfer. This result suggests that cross polarization occurs only from the protons of occluded TPA molecules and not from those of free TPA. Similarly, the observed ^1H - ^{29}Si polarization transfer is not due to the presence of H_2O as an impurity that may have been introduced into the sample during sample preparation; samples prepared using H_2O rather than D_2O demonstrate markedly less efficient cross

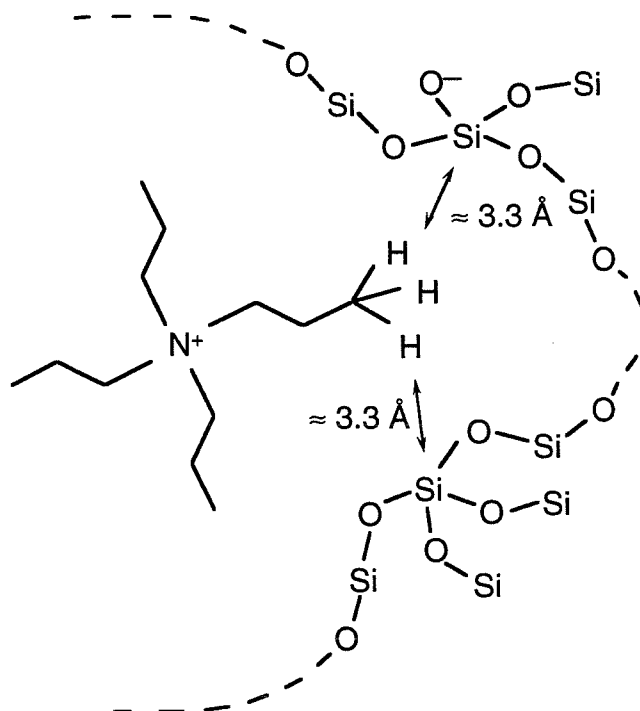


Figure 2.21. Proposed mode of interaction of silicate and TPA within inorganic–organic composite species. The proximity of the organic protons to silicon allows ^1H – ^{29}Si cross polarization to occur.

polarization. Thus, it appears that the observed ^1H - ^{29}Si polarization transfer arises only from TPA molecules that are intimately incorporated into the solid silicate material.

When a readily-hydrolyzed, monomeric silica source such as TEOS is used, association of silicate species with the organic structure-directing agent is possible in the unheated synthesis mixture. This is suggested by the occurrence of efficient ^1H - ^{29}Si CP in the freeze-dried sample of the unheated, TEOS-containing synthesis mixture. The observed signal cannot be due to polarization transfer from the protons of TEOS or the ethanol that is produced by hydrolysis of TEOS because TEOS and ethanol are removed during the process of freeze-drying and are not apparent in the ^1H - ^{13}C CP MAS NMR spectrum. The ^1H - ^{13}C CP MAS NMR spectrum also indicates that TPA is present in the solid silicate phase, even after washing with D_2O . The presence of a distinct vibrational band at 560 cm^{-1} indicates that the silicate ordering in some way resembles that found in crystalline Si-ZSM-5,^{27,28} although no long-range order is apparent by XRD; the $550\text{--}560\text{ cm}^{-1}$ band is absent from the IR spectrum of neat TEOS or of a freeze-dried sample of TEOS hydrolyzed in the presence of an inorganic base. Thus, inorganic-organic composite species are apparently formed as soon as there is a sufficient amount of soluble silicate present in the synthesis mixture.

The ^1H - ^{29}Si CP MAS NMR results suggest that the inorganic-organic interactions established upon molecular restructuring of the sample during the first day of heating (Cab-O-Sil silica source) or in the unheated, TEOS-containing gel are important and unique to structure direction in the synthesis of Si-ZSM-5. If TMA is present in the synthesis mixture rather than TPA (no crystalline product is expected), the relative

amounts of Q^3 and Q^4 in the amorphous, TMA-containing sample after ten days of heating are similar to those observed for the amorphous, TPA-containing sample after one day of heating. This suggests that silicate dissolution and condensation have occurred in both systems. However, the important difference is that there is very little transfer of polarization between TMA and the silicate species during the ^1H - ^{29}Si CP MAS NMR experiment. The substantial reduction in cross polarization efficiency cannot be accounted for simply by the smaller number of protons present. It also cannot be attributed to a substantial difference in the organic content of the silicate solid phase since in both cases the ^{13}C NMR spectra of the washed solids indicate the presence of some adsorbed organic cations. The contrast between the two cross polarization profiles must be due to differences between TPA and TMA in the proximity, mobility, and resulting strengths of their interactions with the silicate species. This difference may be related to the presence or absence of a structure-directing role for the organic species.

The striking efficiency of polarization transfer observed in the Cab-O-Sil-containing samples collected after one day of heating or the unheated, TEOS-containing gel suggests that there is a significant degree of interaction between the TPA molecules and the silicate species in the synthesis mixture at early stages of structure formation. This observation is consistent with the proposed mechanism of structure direction by TPA in the synthesis of Si-ZSM-5; that is, the TPA molecules interact with the silicate species and organize them into inorganic-organic composite structures that are ultimately incorporated into the channel intersections of the zeolite product.^{4,7,8} The propyl chains of TPA may interact preferentially with the hydrophobic silicate species at an appropriate van

der Waals contact distance rather than with bulk water;¹⁵ this may not be the case for TMA. Also, there may be a weak electrostatic attraction between the organic cation and the Q³ sites, as evidenced by the more rapid polarization of the Q³ sites relative to Q⁴ sites at short CP contact times. It thus appears that the TPA molecules are enclathrated into extended silicate structures prior to the appearance of long-range, crystalline order. This process may be related to the formation of cage-like water structures around tetraalkylammonium cations such as TPA due to hydrophobic hydration.⁴¹⁻⁴³ Favorable van der Waals interactions between organic species and hydrophobic silica Q⁴ sites have been suggested as the primary thermodynamic driving force for the organic-mediated self-assembly of pure-silica zeolites.^{15,44}

Additional information regarding the conformation of the TPA molecules during the synthesis of Si-ZSM-5 was sought via ¹H-¹³C CP MAS NMR spectroscopy. The observed upfield shift and splitting of the methyl resonance relative to that of TPABr are characteristic of TPA located at the channel intersections of Si-ZSM-5. Upon washing to remove free TPA, the samples collected from the unheated, TEOS-containing synthesis gel and from the Cab-O-Sil-based syntheses after one day of heating (amorphous by XRD and IR spectroscopy) contain TPA. In all cases, the environment experienced by the TPA molecules within these samples does not exactly resemble that of the channel intersections in crystalline Si-ZSM-5, as suggested by ¹H-¹³C CP MAS NMR. The upfield shift of the methyl resonance of TPA relative to its position in the spectrum of TPABr suggests that TPA molecules in these amorphous samples experience additional van der Waals interactions, most likely with silicate species. However, the chemical shift of the methylene carbon adjacent to

the nitrogen is unchanged relative to that of free TPA. Thus, the self-assembled structures that appear to be involved in the synthesis of Si-ZSM-5 are composed of TPA and silicate; they are related to but do not have the same rigid geometry as the channel intersections of the product. The final structure is apparently determined as the composite species assemble into Si-ZSM-5. The involvement of extended structures in the TPA-mediated synthesis of Si-ZSM-5 is also suggested by small-angle neutron scattering.¹³

The difference in the conformations of TPABr and TPA occluded in ZSM-5 has been also characterized by Raman spectroscopy and correlated to crystallographic data.⁴⁵ In TPABr, the propyl chains adopt an all-trans configuration; for TPA in aqueous solution, the all-gauche conformation is favored.^{43,45} In order to fit in the channel intersections of ZSM-5, TPA must adopt a different conformation in which there are some gauche interactions within the propyl chains; this is the lowest-energy conformation for TPA in ZSM-5. The Raman signature of this new conformation includes decreased intensities of the CH₂ rocking mode at 1160–1166 cm⁻¹ and the CH₂ wagging mode at 1319–1324 cm⁻¹, and the appearance of a new CH₂ rocking mode at 1168–1177 cm⁻¹ and a new CH₂ wagging mode at 1336–1343 cm⁻¹. Although in the present study these vibrational features appear in the Raman spectrum of the Si-ZSM-5 product, they are difficult to observe at early times in the synthesis due to the inherently weak Raman scattering ability of TPA and to the low concentration of occluded TPA molecules in the sample collected after one day of heating. Thus, characterization of the inorganic–organic composite species using Raman spectroscopy is not informative.

Although isolation of well-defined inorganic–organic composite

species from the unheated, TEOS-based synthesis mixture via the silylation technique was not achieved, characterization of the product thus obtained provided observations that are consistent with previous conclusions regarding the nature of the composite species. Enhancement of all of the Si resonances by ^1H - ^{29}Si polarization transfer (despite the presence of H_2O , which can decrease the efficiency of CP) suggests that the organic and inorganic components are in close proximity. ^{13}C MAS NMR indicates that TPA is present in the solid and that the methyl groups experience a constrained environment (van der Waals interactions). However, the environment does not exactly resemble that of the channel intersections in Si-ZSM-5. The organization of silicate units bears some resemblance to that found in Si-ZSM-5, as suggested by the presence of the characteristic vibrational band at 560 cm^{-1} , although the material does not exhibit any long-range order by XRD. The estimated molar composition of the solid phase suggests that even if the composite species have the idealized ratio of silicon to TPA that would be expected from the composition of as-synthesized, crystalline Si-ZSM-5 (Si/TPA=24), amorphous silica must also be present in the solid sample collected by silylation. Thus, the results of the silylation studies are consistent with previous conclusions regarding the presence of inorganic-organic composite species in the synthesis of Si-ZSM-5.

Proposed Mechanism

Gies and Marler have proposed that in the synthesis of silicon-rich zeolites, the structure-directing effect of an organic species involves an

optimization of van der Waals interactions between the alkyl groups of the organic molecule and the hydrophobic silicate species in the synthesis mixture.¹⁵ Additionally, Mentzen and coworkers suggest that efficient intermolecular cross polarization requires interatomic distances on the order of the van der Waals contact distance.²⁵ The results presented here appear to support the model proposed by Gies and Marler by indicating that weak, non-covalent intermolecular interactions such as van der Waals interactions between organic molecules and silicate species are involved in an organic-mediated zeolite synthesis. In essence, the hydrophobic hydration sphere that is formed around TPA in aqueous solution is partially or completely replaced by silica^{1,46,47} when a sufficient amount of soluble silicate species is available. Favorable van der Waals contacts between the alkyl chains of the organic species and the hydrophobic silicate species likely provide the enthalpic driving force for this process, perhaps with an entropic contribution arising from the release of the ordered water molecules from the hydrophobic hydration sphere into bulk water.⁴⁴ ¹H–²⁹Si CP MAS NMR provides evidence of close interactions between the TPA cations and the silicate species that are established during heating of the synthesis gel but prior to the development of long-range, crystalline order. These interactions are indicative of locally-ordered, inorganic–organic composite structures and they do not arise simply upon adsorption of the organic species into the inorganic solid phase. The presence of sodium in small amounts may increase the rate at which the depolymerization of silica occurs, thus accelerating the formation of inorganic–organic composite species. By contrast, at high sodium concentrations the structure-directing influence of sodium is predominant: the formation of layered silicates with a large proportion of

anionic Q^3 sites is favored^{44,48} and the structure-directing tendency of the organic species is no longer observed. Low concentrations of sodium do not appear to affect the nature of the silicate-TPA interactions or, by extension, the mechanism by which structure direction occurs. The extent to which the TPA molecules are surrounded by silicate within these composite structures cannot be ascertained.

These observations are consistent with a mechanism of structure direction in which the TPA molecules organize the silicate into inorganic-organic composite structures that are precursors to the zeolite channel intersections of Si-ZSM-5.^{4,7,8} However, assembly of the zeolite structure by the aggregation route proposed by Chang and Bell⁸ (Figure 2.1) may not be entirely plausible, since it cannot account for the layer-by-layer growth that is evident in the structure of ZSM-5/ZSM-11 intergrowths.⁴⁹ Alternatively, inorganic-organic composite species may provide the fundamental units for nucleation and crystal growth (Figure 2.22). Aggregation of the preformed inorganic-organic composite species is likely responsible for nucleation; this process may occur in solution or on the surface of silica particles¹³ or the walls of the reaction vessel (heterogeneous nucleation). The availability of soluble silicate influences the rate at which composite species are formed; the use of a monomeric silica source such as TEOS or the presence of sodium in the synthesis mixture to facilitate dissolution of a condensed silica precursor leads to an enhanced rate of nucleation since there may be a threshold concentration or size of the inorganic-organic composite species that must be formed in order for nucleation to occur. Subsequent crystal growth can occur in a layer-by-layer fashion via the diffusion of these species to the surface of the growing crystallites. Some free TPA molecules (or other added organic species) and silicate species

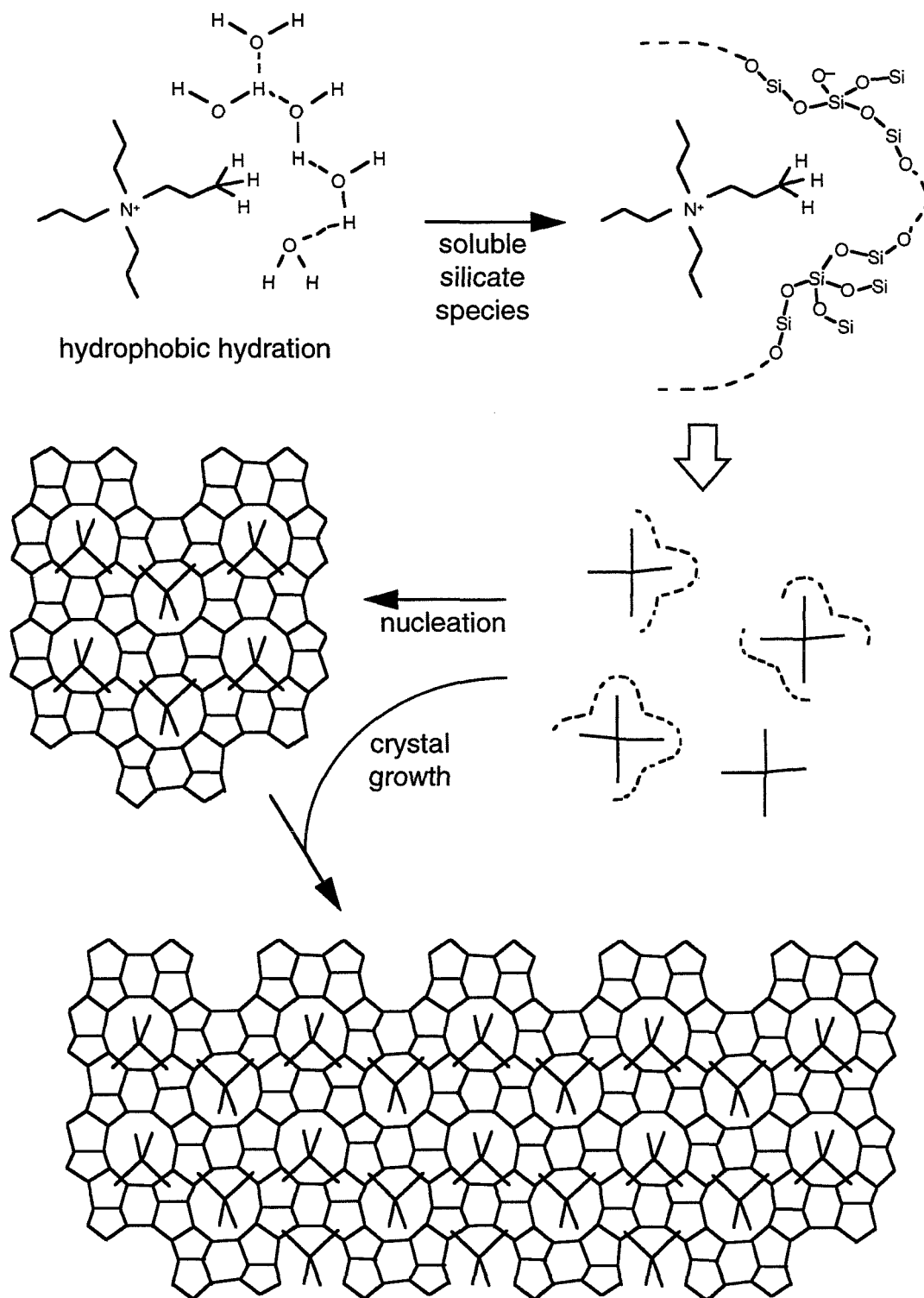


Figure 2.22. Proposed mechanism of structure direction and crystal growth involving inorganic–organic composite species in the TPA-mediated synthesis of Si-ZSM-5.⁵⁰

may also diffuse to the surface of the growing zeolite crystal and be incorporated into the crystalline structure, as suggested by the observation that TMA or tetraethylammonium (TEA) can be occluded into crystalline aluminosilicate ZSM-5 if the gel contains a sufficient amount of TPA to induce nucleation and sustain crystal growth ($\text{Si/TPA}=35$; $\text{TPA/TMA}>1$ or $\text{TPA/TEA}>1$).⁵¹ Nevertheless, formation of the inorganic–organic composite species appears to be the key factor in the synthesis. This proposal for the mechanism of structure direction may be more generally applicable to zeolite synthesis since layer-by-layer crystal growth is also implied by the intergrowth structures of zeolite beta⁵² and SSZ-26/SSZ-33/CIT-1⁵³⁻⁵⁵ (in the latter case, the relative amount of the two structural polymorphs that compose these three materials can be systematically controlled through the use of mixtures of two organic structure-directing agents,⁵⁵ which further supports a layer-by-layer growth mechanism; a similar result has also been demonstrated for the synthesis of FAU/EMT intergrowths⁵⁶).

The results described in the present chapter provides the first direct evidence of specific, intermolecular interactions within preorganized inorganic–organic composite structures during the synthesis of Si–ZSM-5.⁵⁰ It is through these van der Waals interactions that the geometric correspondence between the structure-directing agent and the zeolite pore architecture that is the hallmark of structure direction may arise.¹⁵ Thus, the detection of interactions between the organic structure-directing agent and silicate species has broad implications for the design and synthesis of new molecular sieve materials. It suggests that structure direction in zeolite synthesis can be approached in terms of hydrophobic hydration and weak, non-covalent intermolecular interactions. The

structural features of the product can perhaps be controlled through the judicious choice of an organic species that can interact with the silicate species in a specific manner as determined by an optimization of van der Waals interactions. The technique of intermolecular cross polarization can be used to further probe these structure-directing interactions.

References

- (1) Davis, M. E.; Lobo, R. F. *Chem. Mater.* **1992**, *4*, 756.
- (2) Lok, B. M.; Cannan, T. R.; Messina, C. A. *Zeolites* **1983**, *3*, 282.
- (3) Szostak, R. *Handbook of Molecular Sieves*; Van Nostrand Reinhold: New York, 1992, pp 584.
- (4) Flanigen, E. M.; Bennett, J. M.; Grose, R. W.; Cohen, J. P.; Patton, R. L.; Kirchner, R. M.; Smith, J. V. *Nature* **1978**, *271*, 512.
- (5) Chao, K. J.; Lin, J. C.; Wang, Y.; Lee, G. H. *Zeolites* **1986**, *6*, 35.
- (6) van Koningsveld, H.; van Bekkum, H.; Jansen, J. C. *Acta Crystallogr., Sect. B* **1987**, *43*, 127.
- (7) Bodart, P.; Nagy, J. B.; Gabelica, Z.; Derouane, E. G. *J. Chim. Phys.* **1986**, *83*, 777.
- (8) Chang, C. D.; Bell, A. T. *Catal. Lett.* **1991**, *8*, 305.
- (9) Lawton, S. L.; Rohrbaugh, W. J. *Science* **1990**, *247*, 1319.
- (10) Iton, L. E.; Trouw, F.; Brun, T. O.; Epperson, J. E.; White, J. W.; Henderson, S. J. *Langmuir* **1992**, *8*, 1045.
- (11) Regev, O.; Cohen, Y.; Kehat, E.; Talmon, Y. *J. Phys. IV (Orsay, Fr.)* **1993**, *C8*, 397.
- (12) Regev, O.; Cohen, Y.; Kehat, E.; Talmon, Y. *Zeolites* **1994**, *14*, 314.
- (13) Dokter, W. H.; Beelen, T. P. M.; van Garderen, H. F.; Rummens, C. P. J.; van Santen, R. A.; Ramsay, J. D. F. *Colloids Surfaces A* **1994**, *85*, 89.
- (14) Wijnen, P. W. J. G.; Beelen, T. P. M.; van Santen, R. A. In *Expanded Clays and Other Microporous Solids*; M. L. Occelli and H. E. Robson, Eds.; Van Nostrand Reinhold: New York, 1992; pp 341.
- (15) Gies, H.; Marler, B. *Zeolites* **1992**, *12*, 42.
- (16) Hartmann, S. R.; Hahn, E. L. *Phys. Rev.* **1962**, *128*, 2042.

- (17) Pines, A.; Gibby, M. G.; Waugh, J. S. *J. Chem. Phys.* **1973**, *59*, 569.
- (18) Gobbi, G. C.; Silvestri, R.; Russell, T. P.; Lyster, J. R.; Fleming, W. W. *J. Polym. Sci., Polym. Lett.* **1987**, *25*, 61.
- (19) Parmer, J. F.; Dickinson, L. C.; Chien, J. C. W.; Porter, R. S. *Macromolecules* **1987**, *20*, 2308.
- (20) Voelkel, R. *Angew. Chem. Int. Ed. Engl.* **1988**, *27*, 1468.
- (21) Engelhardt, G.; Lohse, U.; Samoson, A.; Mägi, M.; Tarmak, M.; Lippmaa, E. *Zeolites* **1982**, *2*, 59.
- (22) Nagy, J. B.; Gabelica, Z.; Derouane, E. G. *Chem. Lett.* **1982**, 1105.
- (23) Meinhold, R. H.; Bibby, D. M. *Zeolites* **1990**, *10*, 74.
- (24) Challoner, R.; Harris, R. K.; Packer, K. J.; Taylor, M. J. *Zeolites* **1990**, *10*, 539.
- (25) Lefebvre, F.; Sacerdote-Peronnet, M.; Mentzen, B. F. *C. R. Acad. Sci. Paris, Ser. 2* **1993**, *316*, 1549.
- (26) Agaskar, P. A. *Inorg. Chem.* **1990**, *29*, 1603.
- (27) Jacobs, P. A.; Derouane, E. G.; Weitkamp, J. *J. Chem. Soc., Chem. Commun.* **1981**, 591.
- (28) Coudurier, G.; Naccache, C.; Vedrine, J. C. *J. Chem. Soc., Chem. Commun.* **1982**, 1413.
- (29) Flanigen, E. M.; Khatami, H.; Szymanski, H. A. In *Molecular Sieve Zeolites*; E. M. Flanigen and L. B. Sand, Eds.; American Chemical Society: Washington, DC, 1971; pp 201.
- (30) Pinnavaia, T. J.; Tzou, M. S.; Landau, S. D.; Raythatha, R. H. *J. Mol. Catal.* **1984**, *27*, 195.
- (31) Engelhardt, G.; Michel, D. *High-Resolution Solid-State NMR of Silicates and Zeolites*; John Wiley & Sons: Chichester, 1987.

- (32) Lobo, R. F.; Zones, S. I.; Davis, M. E. In *Inclusion Chemistry with Zeolites: Nanoscale Materials by Design*; N. Herron and D. Corbin, Eds.; in press.
- (33) Boxhoorn, G.; van Santen, R. A.; van Erp, W. A.; Hays, G. R.; Huis, R.; Clague, D. *J. Chem. Soc., Chem. Commun.* **1982**, 264.
- (34) Nagy, J. B.; Gabelica, Z.; Derouane, E. G. *Zeolites* **1983**, 3, 43.
- (35) Gabelica, Z.; Nagy, J. B.; Bodart, P.; Dewaele, N.; Nastro, A. *Zeolites* **1987**, 7, 67.
- (36) Zalkin, A. *Acta. Crystallogr.* **1957**, 10, 557.
- (37) Jarman, R. H.; Melchior, M. T. *J. Chem. Soc., Chem. Commun.* **1984**, 414.
- (38) Hasha, D.; Sierra de Saldarriaga, L.; Saldarriaga, C.; Hathaway, P. E.; Cox, D. F.; Davis, M. E. *J. Am. Chem. Soc.* **1988**, 110, 2127.
- (39) Hayashi, S.; Suzuki, K.; Shin, S.; Hayamizu, K.; Yamamoto, O. *Chem. Phys. Lett.* **1985**, 113, 368.
- (40) Anderson, R. C.; Muller, R. S.; Tobias, C. W. *J. Electrochem. Soc.* **1993**, 140, 1393.
- (41) Nakayama, H.; Kuwata, H.; Yamamoto, N.; Akagi, Y.; Matsui, H. *Bull. Chem. Soc. Jpn.* **1989**, 62, 985.
- (42) Shimizu, A.; Taniguchi, Y. *Bull. Chem. Soc. Jpn.* **1990**, 63, 3255.
- (43) Harmon, K. M.; Budrys, N. M. *J. Mol. Struct.* **1991**, 249, 149.
- (44) Helmkamp, M. M.; Davis, M. E. *Ann. Rev. Mater. Sci.*
- (45) Dutta, P. K.; Puri, M. *J. Phys. Chem.* **1987**, 91, 4329.
- (46) Wiebcke, M. *J. Chem. Soc., Chem. Commun.* **1991**, 1507.
- (47) Twomey, T. A. M.; Mackay, M.; Kuipers, H. P. C. E.; Thompson, R. W. *Zeolites* **1994**, 14, 162.
- (48) Zones, S. I. *Microporous Mater.* **1994**, 2, 281.

- (49) Millward, G. R.; Ramdas, S.; Thomas, J. M. *J. Chem. Soc., Faraday Trans. 2* **1983**, *79*, 1075.
- (50) Burkett, S. L.; Davis, M. E. *J. Phys. Chem.* **1994**, *98*, 4647.
- (51) Rossin, J. A.; Davis, M. E. *Ind. J. Tech.* **1987**, *25*, 621.
- (52) Treacy, M. M. J.; Newsam, J. M. *Nature* **1988**, *332*, 249.
- (53) Lobo, R. F.; Pan, M.; Chan, I.; Li, H. -X.; Medrud, R. C.; Zones, S. I.; Crozier, P. A.; Davis, M. E. *Science* **1993**, *262*, 1543.
- (54) Lobo, R. F.; Davis, M. E. (California Institute of Technology). U.S. Patent appl., 1993.
- (55) Lobo, R. F.; Zones, S. I.; Davis, M. E. In *Zeolites and Related Microporous Materials: State of the Art 1994*; J. Weitkamp, H. G. Karge, H. Pfeifer and W. Hölderich, Eds.; Elsevier: Amsterdam, 1994; pp 461.
- (56) Arhancet, J. P.; Davis, M. E. *Chem. Mater.* **1991**, *3*, 567.

Chapter Three

Hydrophobic Hydration and the Origin of Structural Specificity in the Synthesis of Pure-Silica Zeolites

Abstract

The origin of structural specificity in the synthesis of zeolites in the presence of organic structure-directing agents is investigated via the intermolecular ^1H - ^{29}Si CP MAS NMR technique developed in a previous study of structure direction in zeolite synthesis. The nature and extent of the structure-directing, inorganic-organic interactions in the tetrapropylammonium- and 1,6-hexanediamine-mediated syntheses of pure-silica ZSM-5 (Si-ZSM-5) are compared; these results are contrasted to those from the 1,6-hexanediamine-mediated synthesis of pure-silica ZSM-48 (Si-ZSM-48), in which the diamine serves as a space-filling agent. Synthesis gels containing tetramethylammonium, tetraethylammonium, tetrabutylammonium, tetrapentylammonium, and tetraethanolammonium in lieu of tetrapropylammonium are also evaluated by ^1H - ^{29}Si CP MAS NMR in order to identify the significance of hydrophobic hydration behavior in the synthesis of pure-silica zeolites. Finally, the effects of sodium, the silica source, and the substitution of D_2O for H_2O on the kinetics of Si-ZSM-5 and Si-ZSM-48 nucleation and crystallization are discussed for their mechanistic implications. A modified mechanism of structure direction is proposed in which the formation of inorganic-organic composite structures is initiated by overlap of the hydrophobic hydration spheres of the inorganic and organic components, followed by the release of ordered water and the establishment of favorable intermolecular van der Waals interactions.

Introduction

In the previous chapter, a mechanism of structure direction in the tetrapropylammonium-mediated synthesis of the pure-silica analogue of zeolite ZSM-5 (Si-ZSM-5) was proposed based on the results of ^1H - ^{29}Si cross polarization, magic angle spinning (CP MAS) NMR. The NMR data suggest that upon heating of the synthesis gel, close contact is established between the protons of tetrapropylammonium (TPA) and the silicon atoms of the inorganic phase, i.e., on the order of van der Waals interactions,¹ prior to the formation of the long-range order of the crystalline zeolite structure. It was proposed that silicate is closely associated with the TPA molecules, thus forming inorganic-organic composite species that are the key components in the nucleation and crystal growth processes for the self-assembly of Si-ZSM-5.² This description of inorganic-organic interactions in structure direction leads to questions regarding the nature of these interactions and how an understanding thereof can be applied to the design and synthesis of zeolite pore architectures. One of the primary issues is how these intermolecular interactions give rise to a particular zeolite structure, i.e., the origin of structural specificity. Additionally, the extent to which the occurrence of the cross polarization phenomenon in a sample that appears amorphous by X-ray powder diffraction can be correlated with the occurrence of a structure-directing effect remains to be clarified.

A comparison of the cross polarization profiles from syntheses using two different structure-directing agents that produce the same zeolite structure should provide relevant information regarding the features of the organic species and their interactions with the inorganic

components that are essential to the phenomenon of structure direction. Similarly, a comparison of the cross polarization profiles from the syntheses of two different pure-silica zeolites that are formed using the same organic species at different synthesis temperatures should provide insight into the characteristics of the intermolecular interactions that give rise to structural specificity. Appropriate systems in which to examine such influences are the synthesis of Si-ZSM-5 (a structure composed of intersecting straight and sinusoidal 10-ring channels) in the presence of tetrapropylammonium (TPA) and 1,6-hexanediamine (HXN) and the hexanediamine-mediated synthesis of pure-silica ZSM-48 (Si-ZSM-48) (a linear 10-ring channel system) at a higher temperature.³

The first step in the mechanism proposed for structure direction and self-assembly in the synthesis of Si-ZSM-5 involves the formation of an ordered, hydrophobic hydration sphere around the TPA cation.² The phenomenon of hydrophobic hydration has been invoked to account for the excess molar heat capacities of aqueous solutions of tetraalkylammonium species and other soluble, hydrophobic organic species relative to that of pure water (on the order of $0.1 \text{ kcal deg}^{-1} \text{ mol}^{-1}$);⁴ at the molecular level, hydrophobic hydration is described as the reorientation or restructuring of water molecules in the vicinity of the hydrophobic solute in order to accommodate the species while maintaining a fully hydrogen bonded network of water.^{5,6} This is in contrast to the hydrophilic hydration of alkali metal ions, for example, in which ion-dipole interactions provide the primary stabilizing interactions and compensate for the hydrogen bonds that are broken due to the spherically-symmetric orientation of water molecules.⁷ In the proposed mechanism of zeolite synthesis, replacement of the water molecules in the hydrophobic hydration sphere of the

structure-directing agent by silicate species generates the inorganic-organic composite species that serve as the key components in nucleation and crystal growth. These species apparently provide the means by which the geometry of the organic structure-directing agent is translated into the zeolite pore architecture. The question thus arises regarding the relationship between the ability of the organic species to form a hydrophobic hydration sphere and the occurrence of structure direction. Is the formation of a hydrophobic hydration sphere an essential step in the mechanism of structure direction? Alternatively, are the same molecular characteristics that lead to hydrophobic hydration also responsible for favorable interactions between the organic species and the resulting pure-silica zeolite framework, without the hydrophobic hydration sphere being directly involved in the structure forming process? In an examination of these issues, the series of symmetric, short-chain tetraalkylammonium ions (tetramethylammonium (TMA), tetraethylammonium (TEA), TPA, tetrabutylammonium (TBA), and tetrapentylammonium (TPenA)) represents a suitable system for study because of the well-documented hydration behavior of these cations^{4,8-11} and their utility in numerous zeolite syntheses.¹² Tetraethanolammonium (TEOA) is also included in the series to be studied because it is approximately the same size as TPA but does not form a hydrophobic hydration sphere (no excess molar heat capacity is observed for aqueous solutions of TEOA) because the alcohol moieties participate in the hydrogen bonding network of water.⁴

In adapting the syntheses of Si-ZSM-5 and Si-ZSM-48 for investigation by the ¹H-²⁹Si CP MAS NMR technique, it was observed that the replacement of H₂O by D₂O in the synthesis mixture necessitated longer synthesis times. An isotope effect of D₂O on zeolite crystallization

kinetics has only been reported once previously and was attributed to the slowed rates of O–D (versus O–H) bond cleavage and bond formation in the silicate condensation polymerization in the synthesis of zeolite A.¹³ In the present investigation of the role of hydrophobic hydration in structure direction, an understanding of the isotope effect may provide additional mechanistic insight. Because zeolite synthesis is a kinetically-controlled phenomenon,¹⁴ the mechanism proposed for this process must be consistent with the observed kinetics. Thus, in the present chapter, additional factors that influence the kinetics of zeolite formation such as the presence of alkali metal ions¹⁵ and the use of different silica sources are investigated for their mechanistic implications.

Experimental

Synthesis

The sodium-free synthesis procedure for Si–ZSM-5 in which the only sources of protons are the organic structure-directing agent and its hydroxide counterion was performed as described in the previous chapter. The gel composition for the synthesis of Si–ZSM-5 using fumed SiO₂ (Cab-O-Sil, Grade M-5) was 0.5 TPA₂O: 10 SiO₂: 380 D₂O. The fluid gel was heated statically at 110 °C and autogenous pressure in Teflon-lined, stainless steel reactors for 15 d. Samples were collected from the unheated gel, and after 1, 10, and 15 days of heating. The samples were freeze-dried according to the procedure described in the previous chapter. The freeze-dried samples were handled in a N₂ or Ar atmosphere. Spectral analyses were performed on freeze-dried samples both before and after

washing with D₂O to remove non-occluded organic species and soluble silicate species.

For the hexanediamine-mediated syntheses of Si-ZSM-5 and Si-ZSM-48, the gel composition was 5 HXN: 2 SiO₂: 10 D₂O.³ In a typical synthesis, a gel containing 9.68 g 1,6-hexanediamine (Aldrich), 2.0 g fumed SiO₂ (Cab-O-Sil, Grade M-5), and 30.0 g D₂O (Cambridge Isotope Laboratories, 99.9 atom % D) was aged for 5 min. The fluid synthesis gel was heated statically at 120 °C and autogenous pressure for 60 d to form Si-ZSM-5 or at 150 °C for 15 d to form Si-ZSM-48; when H₂O was used, the synthesis times were 40 d and 10 d, respectively. The synthesis temperature of Si-ZSM-5 must be carefully controlled: at 110 °C, no crystalline material is apparent after 60 days of heating, whereas at 125 °C, some Si-ZSM-48 is crystallized. Samples were collected at prescribed time intervals by freeze-drying.

For the experiments involving other tetraalkylammonium (TAA) ions, solutions of approximately 0.5 M TAAOH in D₂O were prepared using Amberlite IRA-400 (OH) anion exchange resin (Aldrich) and TMACl (Aldrich), TEABr (Aldrich), TBABr (Aldrich), or TPenABr (Aldrich) in D₂O; the exact concentrations of TAAOH were determined by titration with 0.096 N HCl (Aldrich). TEOAOH (98%) was used as received from Pfaltz & Bauer. Gels of composition 0.5 TAA₂O: 10 SiO₂: 380 D₂O were prepared in a manner analogous to the synthesis of Si-ZSM-5 using TPAOH. The gels were heated at 110 °C for up to 30 d; a portion of the unheated gel and a sample after 10 days of heating were collected by freeze-drying, whereas the sample at 30 d was collected by cooling to room temperature, filtering, and washing with H₂O. These synthesis gels did not yield any crystalline products after 30 d at 110 °C.

Gels of composition 0.5 TAA₂O: 10 SiO₂: 380 H₂O were also prepared using TEOA or mixtures of TEOA and TPA (0.29 TEOA₂O: 0.21 TPA₂O or 0.45 TEOA₂O: 0.05 TPA₂O). These gels were heated at 150 or 175 °C for 7 d. Products were collected by cooling to room temperature, filtering, and washing with H₂O.

For studies of the effect of sodium on the kinetics of Si-ZSM-5 synthesis, gels were prepared with a composition of 0.5 TPA₂O: 3 Na₂O: 10 SiO₂: 380 H₂O (or D₂O) using NaNO₃ (Aldrich) as the sodium source. Investigations of the effect of the silica source used involved gels that were prepared with a composition of 0.5 TPA₂O: 10 SiO₂: 380 H₂O (or D₂O) using tetraethylorthosilicate (TEOS) as the silica source. For studies of the kinetic effect of deuterated TPA (TPA-*d*₂₈) on the TPA-mediated synthesis of Si-ZSM-5, gels were prepared with a composition of 0.5 (TPA-*d*₂₈)₂O: 10 SiO₂: 380 H₂O (or D₂O) using TEOS as the silica source. (TPA-*d*₂₈)Br was purchased from Isotec (custom synthesis) and converted to the hydroxide form using Amberlite IRA-400 (OH) anion exchange resin, as described above. Samples were collected at intervals by cooling to room temperature and drying the entire synthesis mixture under ambient conditions, followed by washing with H₂O and filtering to isolate the solid product.

For kinetic studies of the effect of sodium on the hexanediamine-mediated syntheses of Si-ZSM-5 and Si-ZSM-48, gels were prepared with a composition of 5 HXN: 0.6 Na₂O: 2 SiO₂: 10 H₂O (or D₂O) using NaNO₃ as the sodium source. For seeded syntheses, 5 wt % of the starting silica was replaced by HXN/Si-ZSM-5 (≈85 wt % SiO₂) or HXN/Si-ZSM-48 (≈90 wt % SiO₂), as appropriate. Samples were collected at intervals using the room-temperature filtration technique described above. HXN/Si-ZSM-5

could not be synthesized using TEOS as the silica source. Some amorphous material was present in the HXN/Si-ZSM-48 sample synthesized using TEOS (20 days of heating at 150 °C).

Analysis

Solid state ^{29}Si MAS, ^1H - ^{29}Si CP MAS, and ^1H - ^{13}C CP MAS NMR studies were performed on a Bruker AM 300 spectrometer, as described in the previous chapter. Solution-phase ^{13}C (75.47 MHz) NMR spectroscopy was performed using a General Electric QE 300 spectrometer, as described previously.

X-ray powder diffraction (XRD) data were collected on a Scintag XDS-2000 diffractometer using $\text{CuK}\alpha$ radiation. As a qualitative assessment of the amount of crystalline material present, the percent crystallinity of each sample was determined from the ratio of height of the most intense reflection in the XRD pattern ($23.19^\circ 2\theta$ (501) for Si-ZSM-5; $21.3^\circ 2\theta$ for Si-ZSM-48) to the height of the corresponding reflection of the Si-ZSM-5 or Si-ZSM-48 samples prepared using Cab-O-Sil, sodium, and D_2O . Because the choice of reference sample (assigned as 100% crystallinity) is somewhat arbitrary, it is possible that a product may have a percent crystallinity value greater than 100%. For amorphous samples, the percent crystallinity is zero.

IR spectroscopy was performed on a Nicolet System 800 FTIR Instrument. IR samples were prepared as KBr pellets. Thermogravimetric analyses (TGA) were performed on a DuPont 951 Thermogravimetric Analyzer. Approximately 10 mg of sample were heated at a rate of 5°C min^{-1} to 600 °C.

Results

Structural Specificity

The XRD, IR, TGA, and ^1H - ^{29}Si CP MAS NMR data for the crystallization of TPA/Si-ZSM-5 are described in the previous chapter. In summary, crystalline Si-ZSM-5 is apparent after 5–10 days of heating at 110 °C, and crystallization is complete in 15 days. By TGA, the product has a unit cell composition of 4.6 TPA: 96 SiO₂: 1.5 D₂O. With four channel intersections per unit cell, this equates to approximately one TPA molecule per channel intersection (Figure 3.1). Efficient cross polarization between the TPA protons and the silicate species is possible after one day of heating² even though the material does not exhibit long-range order observable by XRD or IR spectroscopy.^{16,17} The efficiency of polarization transfer in the ^1H - ^{29}Si CP MAS NMR spectrum increases as crystalline TPA/Si-ZSM-5 is formed.

The XRD patterns for the washed, freeze-dried samples collected at intervals during the synthesis of HXN/Si-ZSM-5 are shown in Figure 3.2. Crystalline order observable by XRD (approximately 4–5 unit cells)¹⁶ is present after approximately 30–40 days of heating at 120 °C, and crystallization is complete after 60 days. The IR spectra show that silica ordering that is characteristic of the Si-ZSM-5 structure (band at 550–560 cm⁻¹)^{16,17} is present after 20 days of heating (Figure 3.3). TGA of HXN/Si-ZSM-5 indicates two stages of weight loss: the first, from 25 °C to 305 °C corresponds to desorption of water, and the second, from 305 °C to 600 °C, corresponds to combustion of hexanediamine. The observed losses of D₂O (2.1 wt %) and hexanediamine (13.6 wt %) indicate a unit cell composition of 8.0 HXN: 96 SiO₂: 7.2 D₂O. HXN/Si-ZSM-5 thus contains two

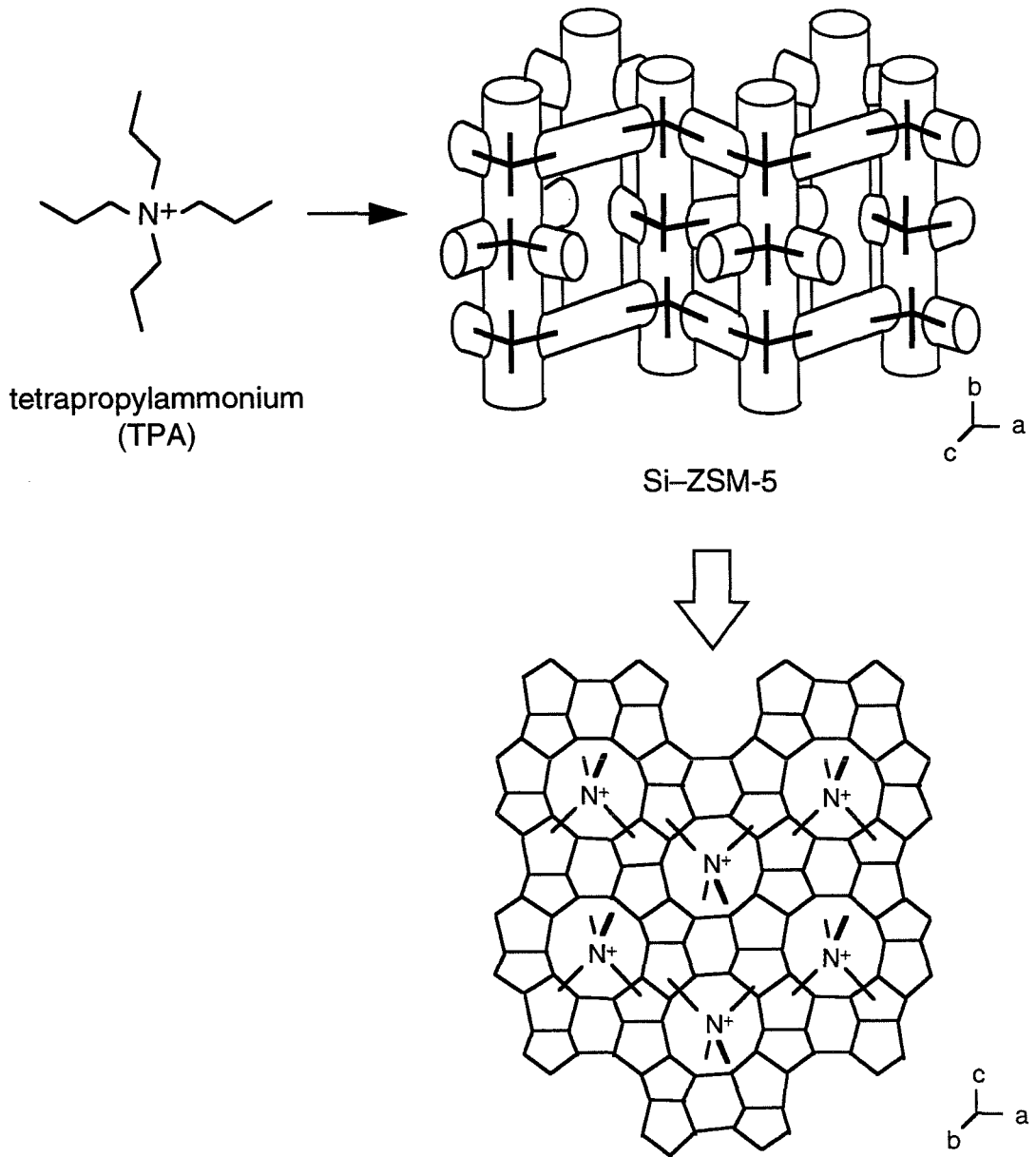


Figure 3.1. Location of TPA occluded in Si-ZSM-5.

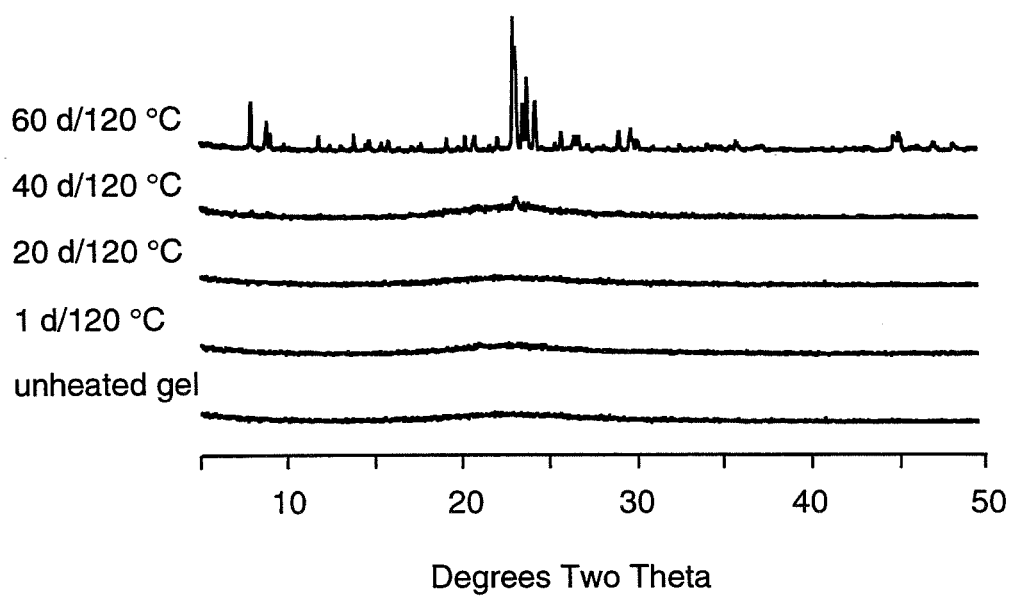


Figure 3.2. X-ray diffraction patterns of the D₂O-washed, freeze-dried samples collected during the hexanediamine-mediated synthesis of Si-ZSM-5.

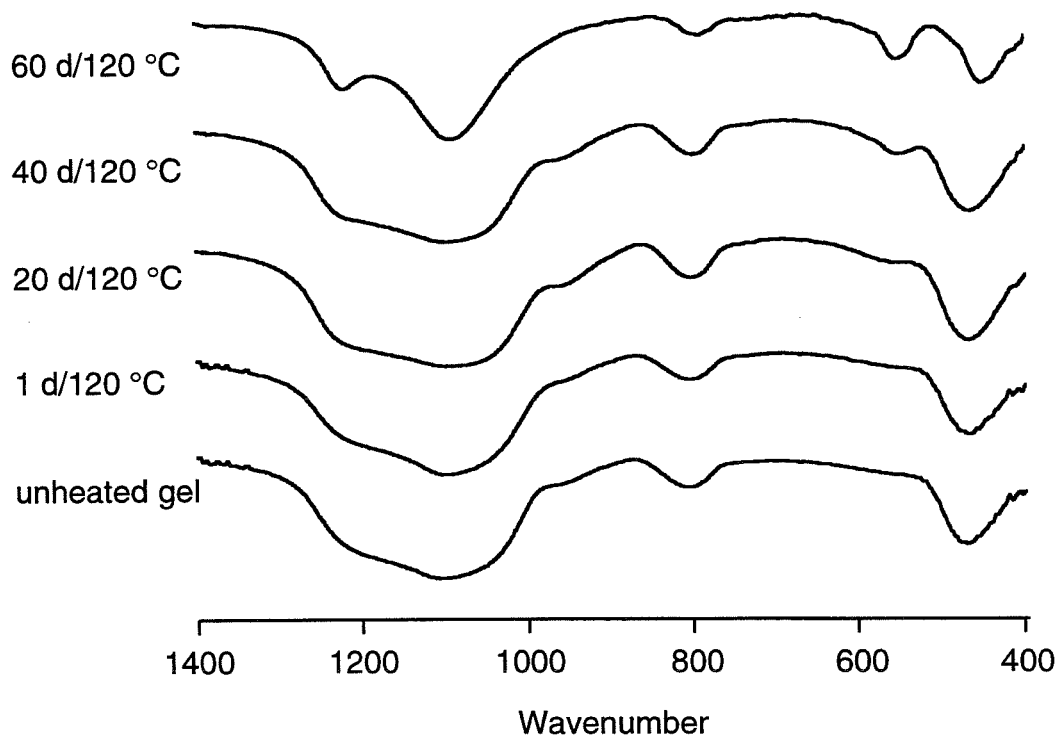


Figure 3.3. IR spectra of the D₂O-washed, freeze-dried samples collected during the hexanediamine-mediated synthesis of Si-ZSM-5.

hexanediamine molecules per channel intersection, and the hexanediamine completely fills the available void space of the ZSM-5 structure (Figure 3.4).

The X-ray powder diffraction data for the washed, freeze-dried samples collected at intervals during the synthesis of HXN/Si-ZSM-48 are shown in Figure 3.5. Some crystalline material is present after 5 days of heating at 150 °C, with crystallization being complete in 15 days. The IR spectra exhibit the same trend in the crystallization profile (Figure 3.6). TGA of the product shows similar stages of weight loss as HXN/Si-ZSM-5. The observed losses of D₂O (1.8 wt %) and hexanediamine (6.1 wt %) indicate a composition of 3.3 HXN: 96 SiO₂: 5.6 D₂O (two unit cells).¹⁸ The TGA results indicate that HXN/Si-ZSM-48 has approximately half the organic content of HXN/Si-ZSM-5. However, the void volume of Si-ZSM-48 is also nearly half that of Si-ZSM-5¹⁹, which implies that hexanediamine completely fills the void space of Si-ZSM-48 (Figure 3.4).

The ²⁹Si MAS and ¹H-²⁹Si CP MAS NMR spectra for the solids collected from the hexanediamine-mediated synthesis of Si-ZSM-5 are shown in Figure 3.7. As in the spectra for the solids obtained from the TPA-mediated synthesis of Si-ZSM-5, two resonances are observed that correspond to Q³ (downfield resonance) and Q⁴ (upfield resonance) species (Qⁿ represents Si(OSi)_n(OD)_{4-n}). During the course of the synthesis, the overall intensities of the spectra obtained without CP remain constant but show an increase in the number of Q⁴ sites relative to Q³. The positions of the Q³ and Q⁴ signals shift from -100 to -102 ppm and from -110 to -112 ppm, respectively, during the transformation from amorphous silica to crystalline Si-ZSM-5; the upfield shift has been correlated with the larger Si-O-Si bond angles present in Si-ZSM-5 versus amorphous silica.²⁰

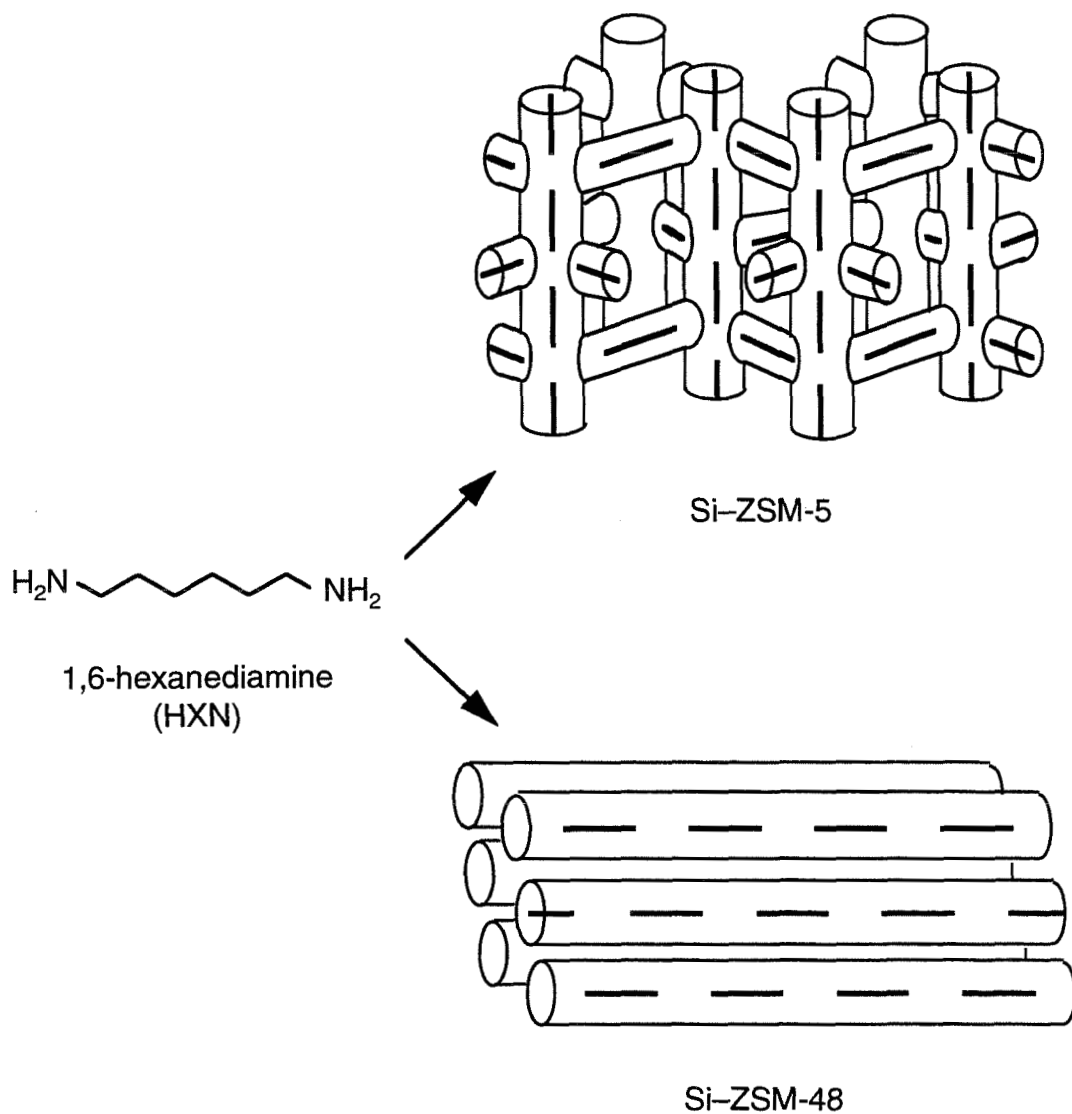


Figure 3.4. Proposed location of hexanediamine occluded in Si-ZSM-5 and Si-ZSM-48.

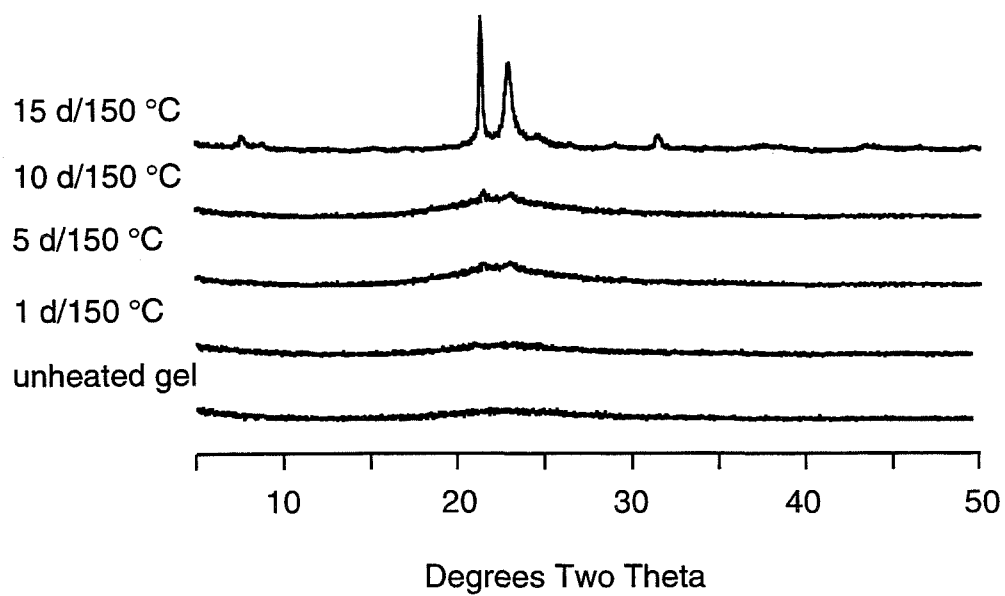


Figure 3.5. X-ray diffraction patterns of the D₂O-washed, freeze-dried samples collected during the hexanediamine-mediated synthesis of Si-ZSM-48.

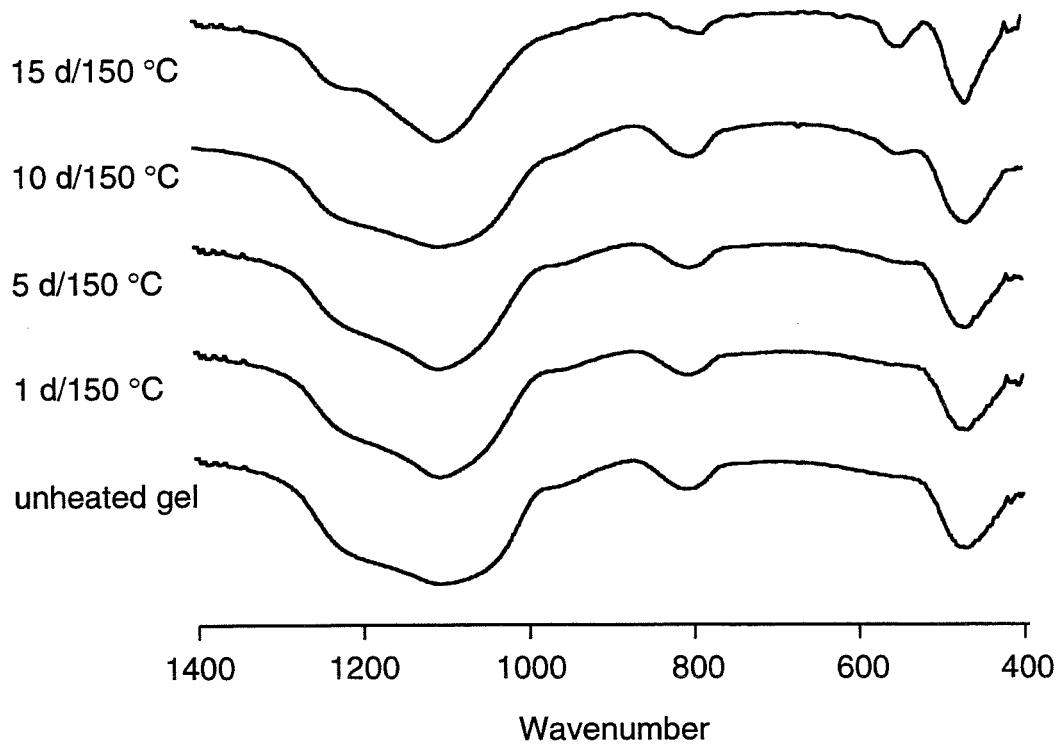


Figure 3.6. IR spectra of the D₂O-washed, freeze-dried samples collected during the hexanediamine-mediated synthesis of Si-ZSM-48.

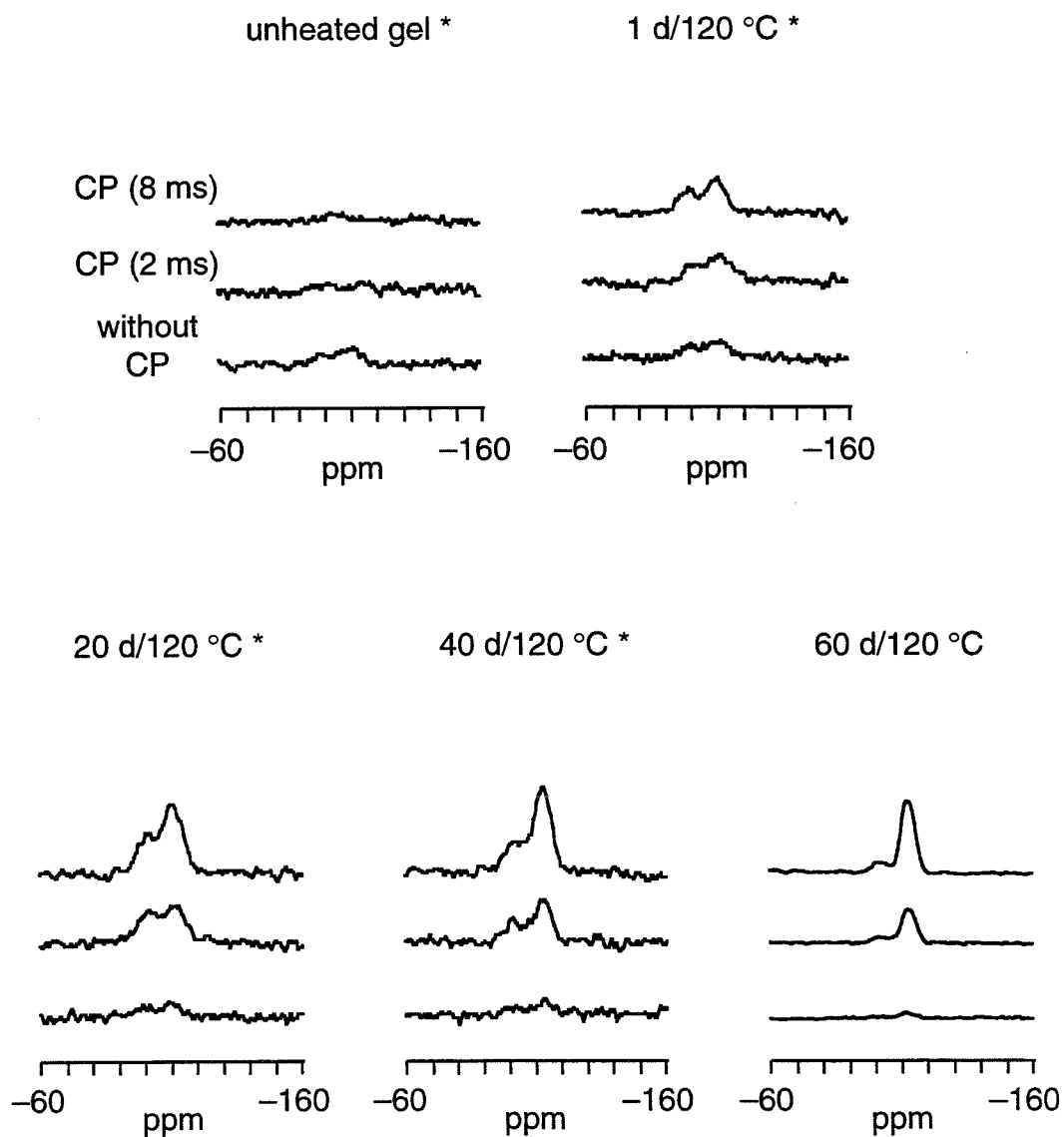


Figure 3.7. ^{29}Si MAS and ^1H - ^{29}Si CP MAS NMR spectra of the freeze-dried samples collected during the hexanediamine-mediated synthesis of Si-ZSM-5 (CP contact times as indicated; * indicates an expanded intensity scale (x5)).

Polarization transfer between the protons of hexanediamine and the silicate species does not occur in the unheated gel sample. After the sample has been heated at 120 °C for 1 day, CP between the organic and inorganic components is observed. The intensities of the CP spectra are greater than the intensity of the spectrum obtained without CP, which suggests that efficient polarization transfer is occurring. More efficient polarization transfer is observed in the sample obtained after heating for 20 days even though the solid still does not have long-range order detectable by XRD. Further increases in the intensities of the CP spectra are observed for the partially- and completely-crystalline samples obtained after 40–60 days of heating. The trend in the efficiency of CP relative to the degree of crystalline order observed by XRD is similar to that observed for the TPA-mediated synthesis of Si–ZSM-5.

The ^{29}Si MAS and ^1H – ^{29}Si CP MAS NMR spectra shown in Figure 3.8 for the solids collected from the hexanediamine-mediated synthesis of Si–ZSM-48 reveal a different trend. As is expected, no polarization transfer is observed in the unheated gel. However, unlike the NMR results from the TPA- and hexanediamine-mediated syntheses of Si–ZSM-5, efficient CP between the hexanediamine protons and the silicate species is not observed until long-range order is also detected by XRD and IR; the onset of CP does not precede the emergence of crystallinity. The intensities of the peaks with CP then rise as the amount of crystalline material in the sample increases.

IR spectroscopic characterization of the HXN/Si–ZSM-5 and HXN/Si–ZSM-48 samples synthesized from a H_2O -containing gel suggests that hexanediamine is occluded as the neutral diamine rather than in the mono- or diprotonated form. In the spectrum of HXN/Si–ZSM-5

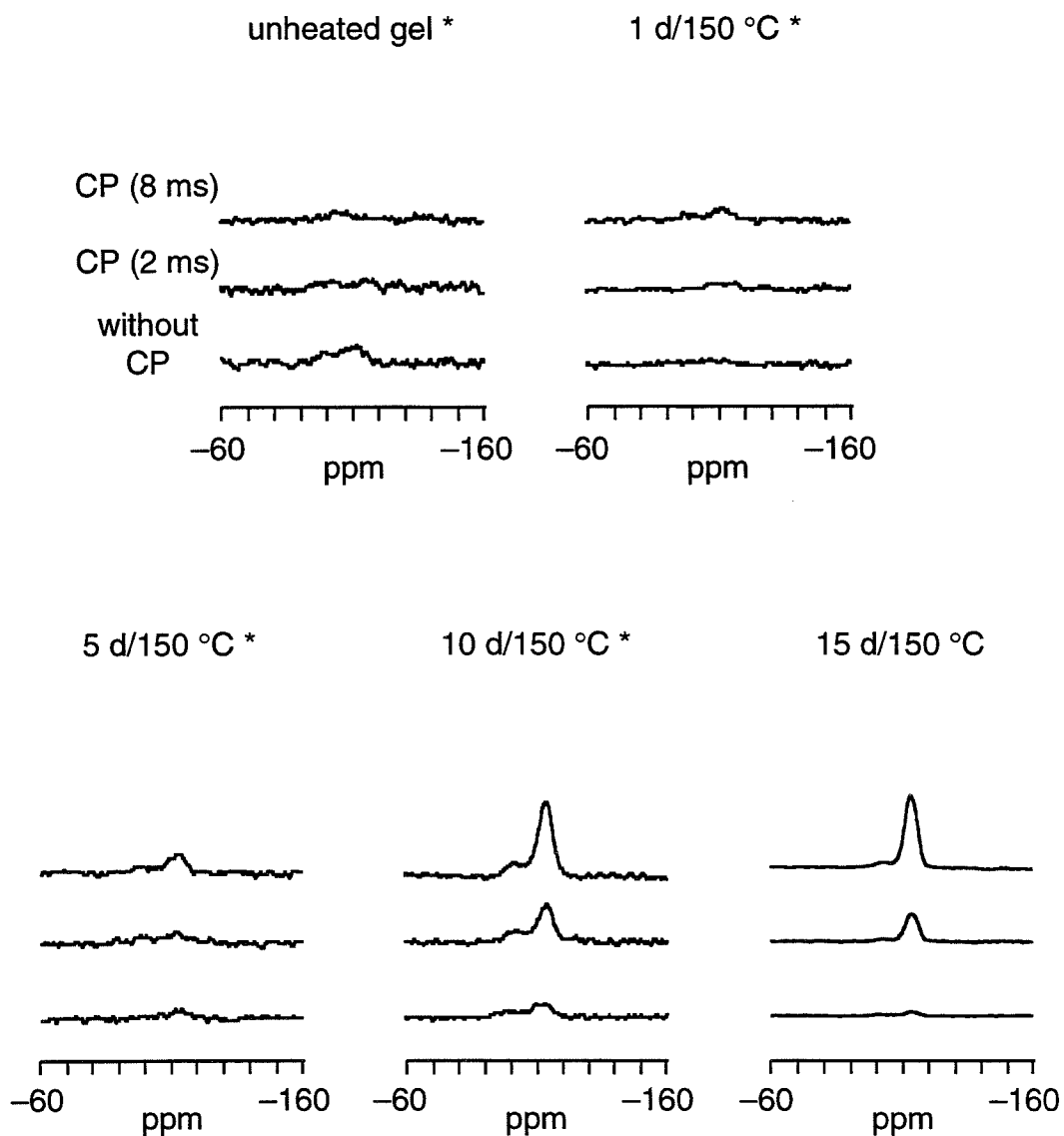


Figure 3.8. ^{29}Si MAS and ^1H - ^{29}Si CP MAS NMR spectra of the freeze-dried samples collected during the hexanediamine-mediated synthesis of Si-ZSM-48 (CP contact times as indicated; * indicates an expanded intensity scale (x5)).

(Figure 3.9), the vibrational bands at 3380 and 3312 cm^{-1} correspond to NH stretches of the free amine, and the band at 1601 cm^{-1} is the NH_2 deformation mode;²¹ the NH_3^+ stretching mode (2725 cm^{-1}) and NH_3^+ deformation modes (1564, 1505 cm^{-1}) expected for protonated hexanediamine are not observed.²¹ It is reasonable that hexanediamine is also occluded as the neutral diamine in Si-ZSM-48,²² although due to the low organic content the vibrations are too weak to be assigned definitively. The ^1H - ^{13}C CP MAS NMR spectra of these products (not shown) are inconclusive regarding the protonation state of the organic species due to the broad linewidths of the resonances, but they are not inconsistent with the presence of the neutral diamine. When Si-ZSM-5 and Si-ZSM-48 are synthesized from a D_2O -containing gel, the characteristic IR vibrational modes of the diamine or its protonated forms are not observed. One possible explanation is that protonation and deprotonation of the amine groups during the synthesis ($\text{pK}_{\text{a}(1)}=9.8$; $\text{pK}_{\text{a}(2)}=10.9$;²³ synthesis gel $\text{pH}>12$) results in H/D exchange, and that the mixture of NH_2 , NHD , and ND_2 groups present in the occluded species results in multiple vibrational modes that are too low in intensity to be observed. However, only neutral hexanediamine is observed by liquid-phase ^{13}C NMR of the synthesis mixture (neutral diamine: 26.9, 32.7, 41.4 ppm; diprotonated form: 25.5, 26.9, 40.0 ppm; synthesis gel: 27.0, 32.8, 41.5 ppm), which suggests that mono- or diprotonated hexanediamine is a minor (but potentially important) component of the synthesis mixture that produces Si-ZSM-5 and Si-ZSM-48.

Hydrophobic Hydration

The ^{29}Si MAS and ^1H - ^{29}Si CP MAS NMR spectra of the unheated

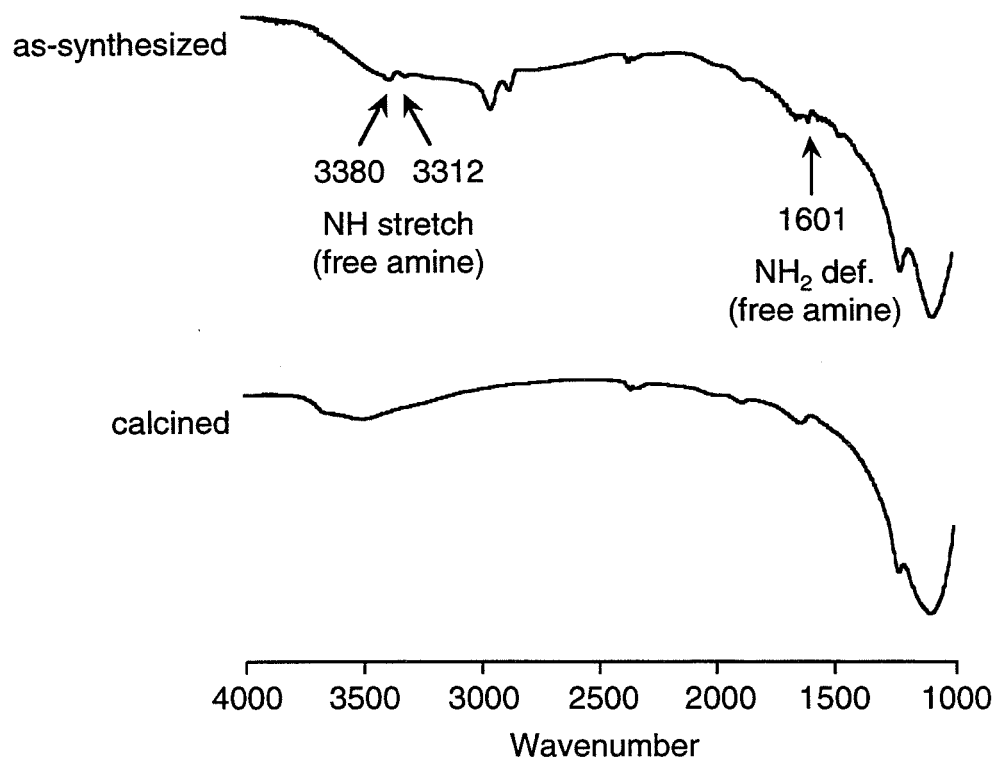


Figure 3.9. IR spectra of Si-ZSM-5 synthesized in the presence of hexanediamine and H₂O.

and heated (10 d at 110 °C) gels prepared with TMA, TEA, TPA, TBA, TPenA, and TEOA are shown in Figures 3.10–3.12; the spectra of unheated fumed silica (Cab-O-Sil) is also shown in Figure 3.10. In each of the ^{29}Si MAS NMR spectra, two resonances are observed, corresponding to Q^3 (–100 ppm) and Q^4 (–110 ppm) species. Efficient CP from the organic protons to silica does not occur in the unheated gels (note the expanded intensity scale relative to that in Figures 3.7 and 3.8); the CP spectra resemble that of Cab-O-Sil silica in which there is some intramolecular polarization transfer from surface hydroxyl (Q^3) groups. The additional resonances in the spectra of the unheated TMA- and TEA-containing gels are assigned to the cubic octamer ($\text{Si}_8\text{O}_{20}^{8-}$) at –99 ppm (for TMA and TEA) and the prismatic hexamer ($\text{Si}_6\text{O}_{15}^{6-}$) at –89 ppm (for TMA only);²⁰ these species form readily in aqueous solutions of TMAOH or TEAOH, but are not abundant in the presence of other tetraalkylammonium species.²⁴ ^1H – ^{29}Si cross polarization to the double-ring silicate species is efficient due to the proximity of the charge-balancing TMA or TEA cations.²⁵

After heating for 10 days at 110 °C, all of the TAA-containing samples except for the TPA-containing synthesis mixture are amorphous by XRD and IR (not shown). Changes in the distributions of Q^3 and Q^4 species shown by the ^{29}Si MAS NMR spectra suggest that depolymerization and recondensation of the silica have occurred. Double-ring silicate species are no longer present in the TMA- or TEA-containing systems. Only a small amount of polarization transfer is observed in these spectra (except for those of TPA and perhaps TBA (*vide infra*)). For the TPA-containing sample, efficient CP is observed because some crystalline TPA/Si–ZSM-5 is present after 10 days of heating; the TPA-containing, X-ray amorphous sample after 1 day of heating provides a closer

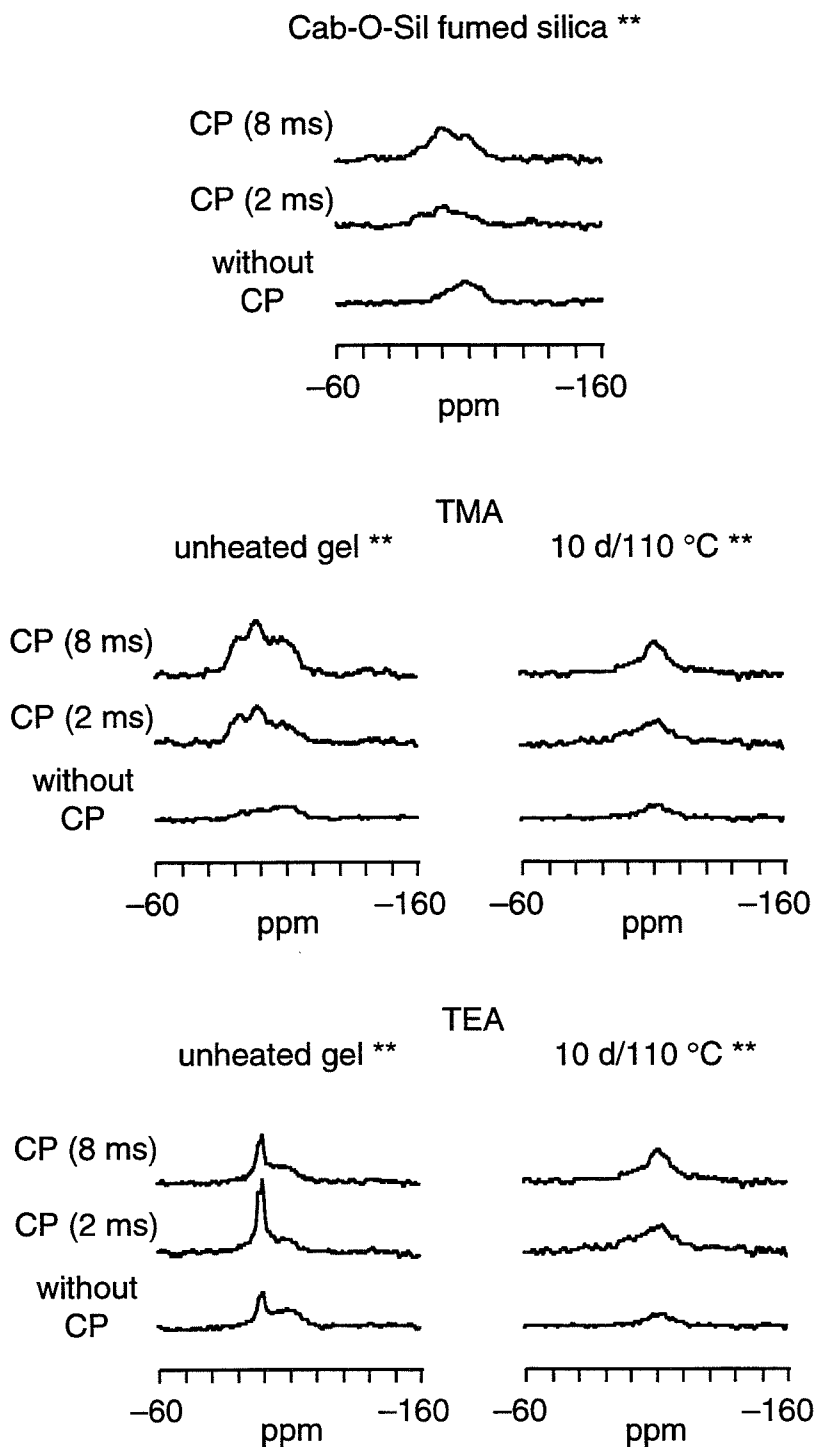


Figure 3.10. ^{29}Si MAS and ^1H - ^{29}Si CP MAS NMR spectra of Cab-O-Sil and of the freeze-dried samples collected from synthesis gels containing TMA and TEA (CP contact times as indicated; ** indicates an expanded intensity scale (x25) relative to Figure 3.7, 60 d sample).

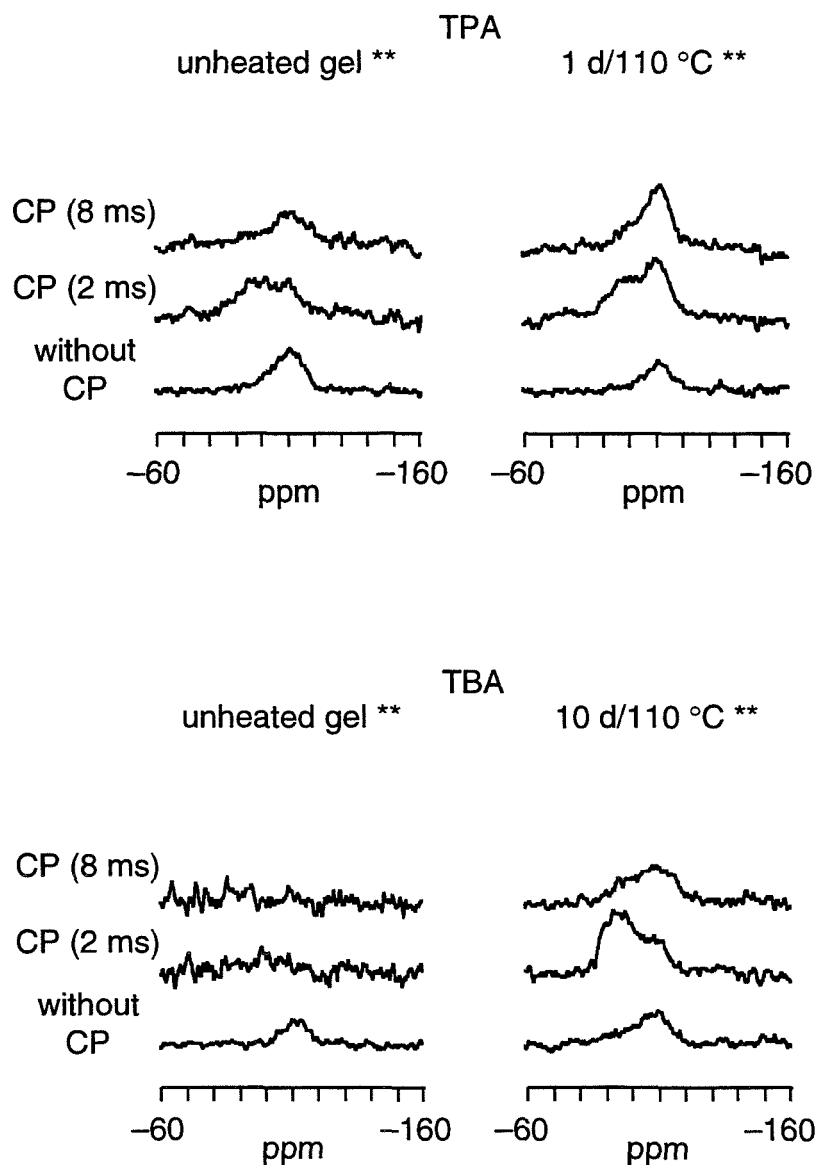


Figure 3.11. ^{29}Si MAS and ^1H - ^{29}Si CP MAS NMR spectra of the freeze-dried samples collected from synthesis gels containing TPA and TBA (CP contact times as indicated; ** indicates an expanded intensity scale (x25) relative to Figure 3.7, 60 d sample).

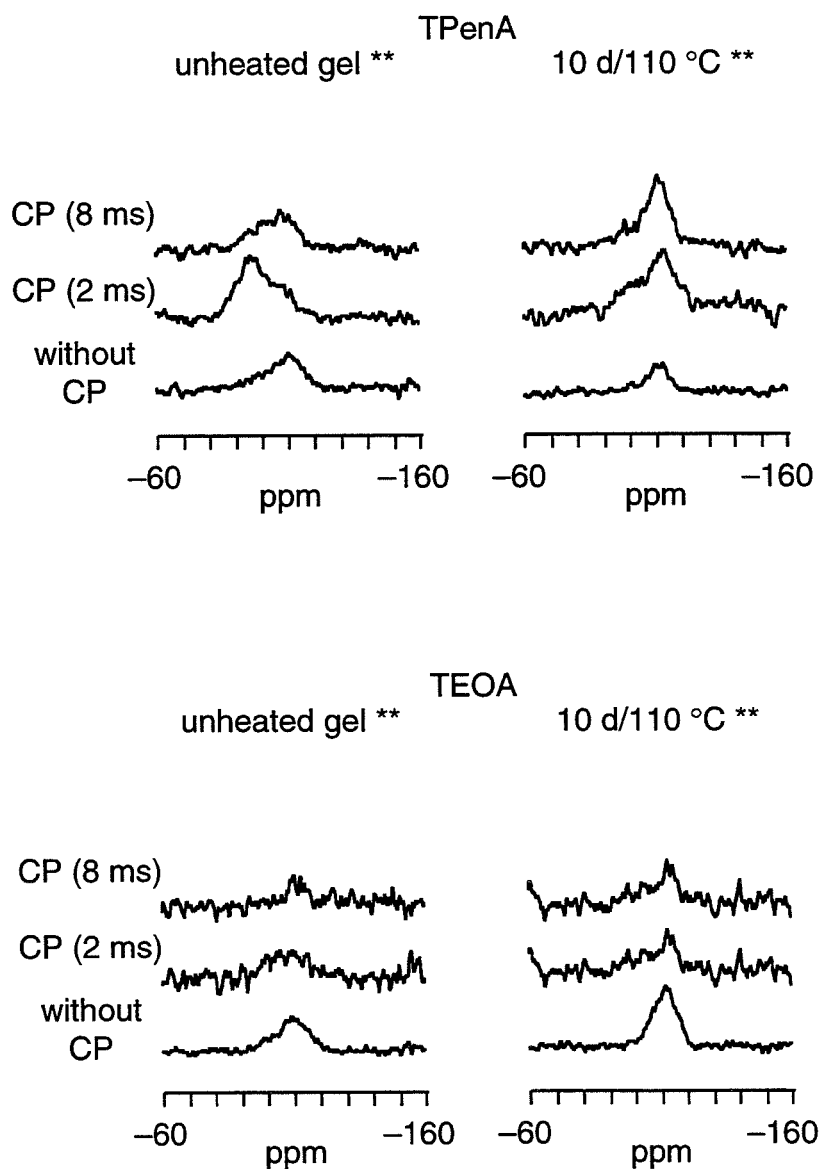


Figure 3.12. ^{29}Si MAS and ^1H - ^{29}Si CP MAS NMR spectra of the freeze-dried samples collected from synthesis gels containing TPenA and TEOA (CP contact times as indicated; ** indicates an expanded intensity scale (x25) relative to Figure 3.7, 60 d sample).

comparison to the other tetraalkylammonium-containing samples, although CP is still more efficient in the TPA-containing sample.

No crystalline products were formed from synthesis gels containing TEOA, even at higher synthesis temperatures. Using mixtures of TEOA and TPA, Si-ZSM-5 was formed in 4 days at 175 °C only when a sufficient amount of TPA was present in the gel to completely fill the void space of the zeolite product (TPA/Si=1/24; gel composition 0.21 TPA₂O: 0.29 TEOA₂O: 10 SiO₂: 380 H₂O). However, no TEOA was detected by ¹H-¹³C CP MAS NMR in the TPA-containing product formed under these conditions (not shown). When a lower TPA content was used (TPA/Si=1/96; gel composition 0.05 TPA₂O: 0.45 TEOA₂O: 10 SiO₂: 380 H₂O), no crystalline material was obtained under the same conditions of heating time and temperature.

Crystallization Kinetics

The crystallization profiles of TPA/Si-ZSM-5, TPA-*d*₂₈/Si-ZSM-5, HXN/Si-ZSM-5, and HXN/Si-ZSM-48 are presented in Figures 3.13–3.16, respectively. In all cases, the presence of sodium appears to increase the rates of nucleation and crystal growth. Similarly, the use of TEOS rather than fumed silica as the silica source enhances the rates of nucleation and crystallization for the synthesis of TPA/Si-ZSM-5. TEOS cannot be used for the hexanediamine-mediated syntheses of Si-ZSM-5 because the ethanol produced from the hydrolysis of TEOS apparently interferes with the gel chemistry or with an essential step in structure direction. Similarly, crystalline HXN/Si-ZSM-5 is not formed at 120 °C when 8 equivalents of ethanol are added to a Cab-O-Sil-based synthesis gel. At 150 °C, however, HXN/Si-ZSM-48 is formed in 20 days using TEOS (some amorphous

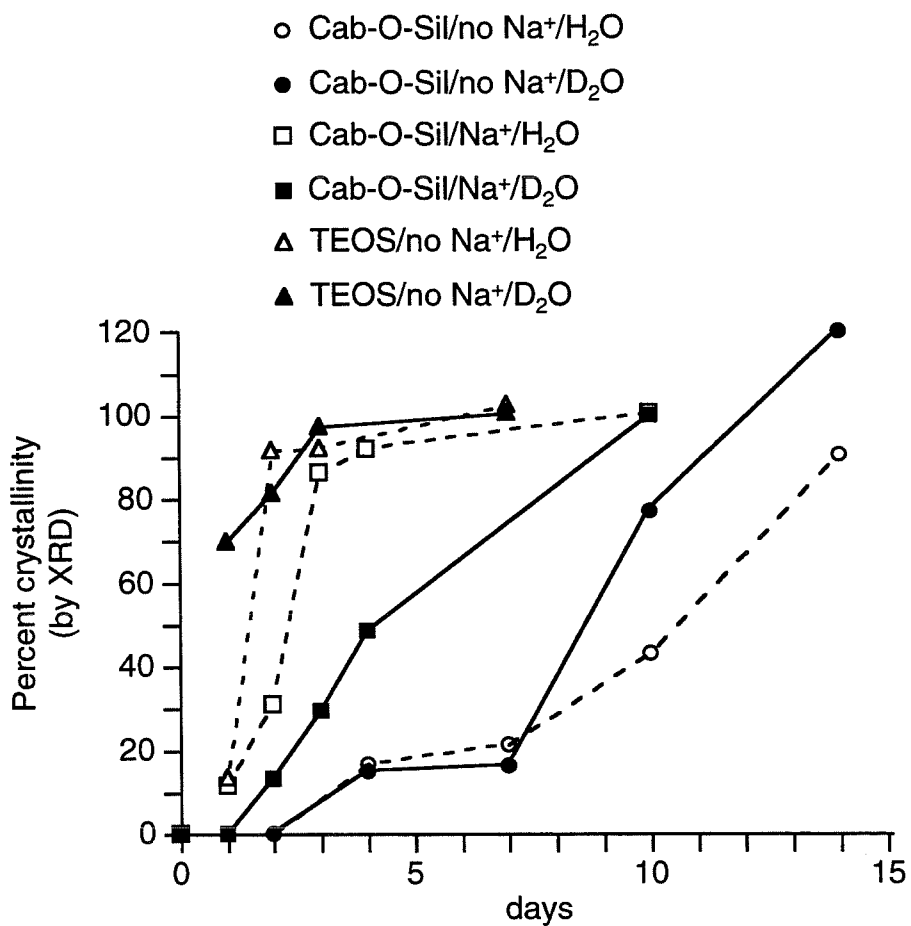


Figure 3.13. Crystallization profiles of TPA-mediated syntheses of Si-ZSM-5.

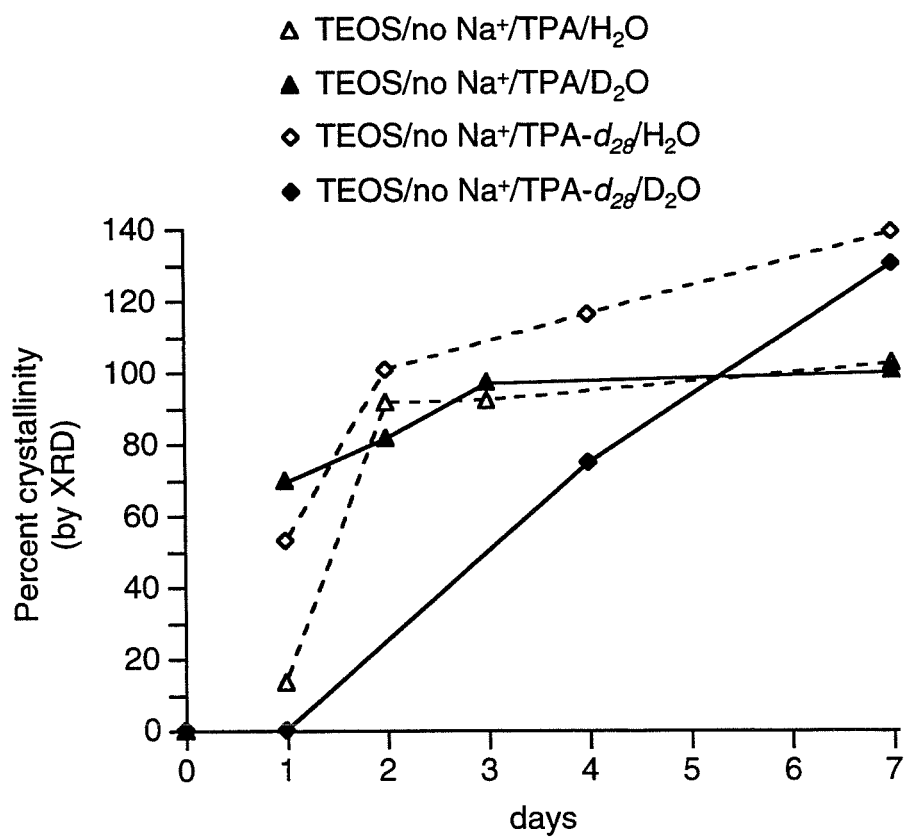


Figure 3.14. Crystallization profiles of TPA-*d*₂₈-mediated syntheses of Si-ZSM-5.

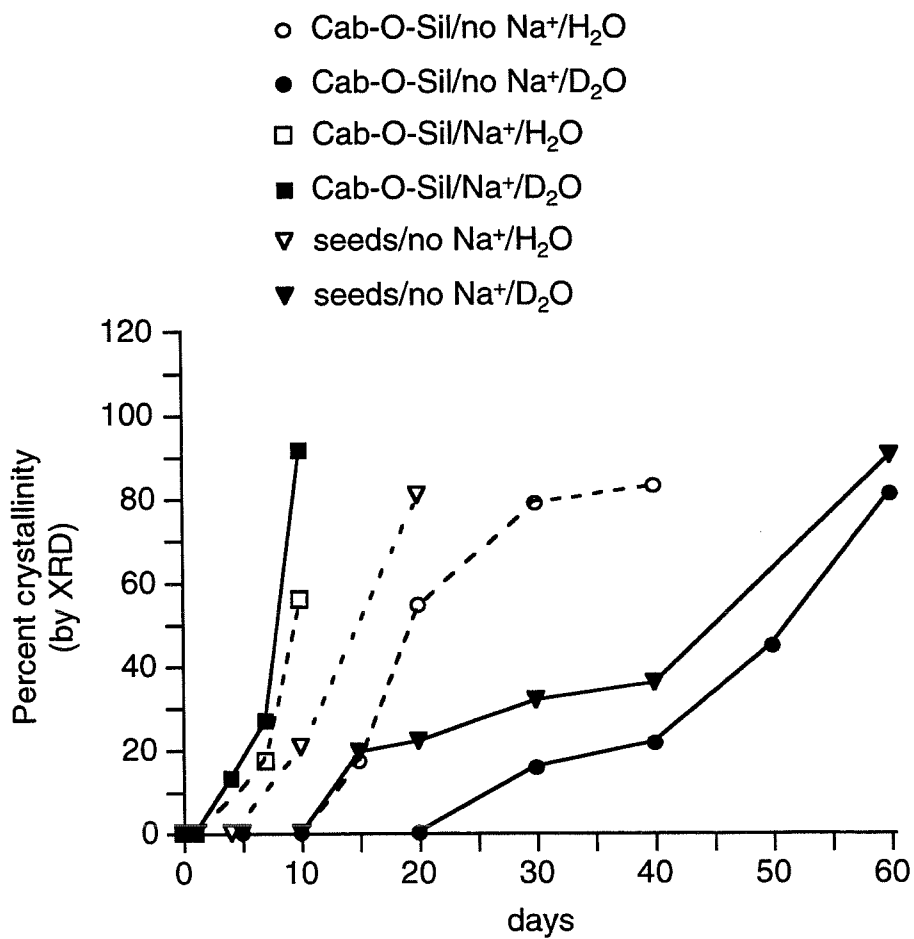


Figure 3.15. Crystallization profiles of hexanediamine-mediated syntheses of Si-ZSM-5.

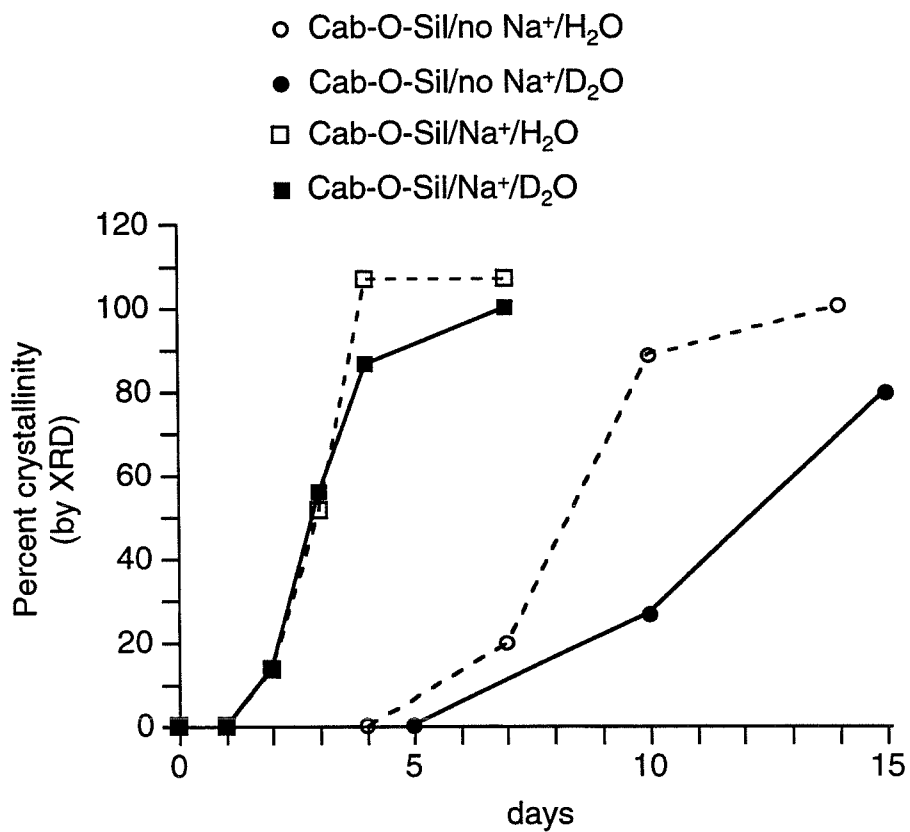


Figure 3.16. Crystallization profiles of hexanediamine-mediated syntheses of Si-ZSM-48.

material is also present in the product collected) or using Cab-O-Sil and added ethanol; the slower rates of product formation are likely due to an effect of dilution by ethanol. Seeding of the synthesis of HXN/Si-ZSM-5 accelerates the rate of nucleation when fumed silica is used as the silica source.

In the absence of sodium or when a condensed silica source is used, a difference in the time of appearance of crystalline material in the growth curves is observed for syntheses performed in H₂O and D₂O solutions. The use of D₂O results in markedly delayed nucleation for the syntheses of TPA/Si-ZSM-5, HXN/Si-ZSM-5, and HXN/Si-ZSM-48. However, the rate of nucleation of Si-ZSM-5 is not affected when TPA-*d*₂₈ is used in lieu of TPA.

Discussion

In the TPA-mediated synthesis of Si-ZSM-5, it has been proposed that a key step in structure direction is the replacement of water molecules in the hydration sphere of TPA by silicate species to form inorganic-organic composite species.² Favorable overlap of the hydrophobic hydration sphere formed around TPA with the domains of hydrophobic hydration that are present at the siloxane bridges between two Q⁴ groups in silica²⁶ may be responsible for bringing the organic and inorganic components into proximity. By contrast, Q³ groups are hydrophilically hydrated and thus their hydration spheres may be incompatible with that of TPA in spite of the electrostatic attraction.^{4,7,26,27} The release of water molecules from the ordered hydrophobic hydration spheres into the bulk and the subsequent establishment of favorable van der Waals contacts

between the alkyl chains of TPA and the hydrophobic silica may provide the entropic and enthalpic driving forces for the formation of the composite inorganic–organic species (Figure 3.17). Efficient ^1H – ^{29}Si CP in the X-ray amorphous, heated synthesis mixture provides evidence for the existence of close inorganic–organic contacts (without intervening water (D_2O) molecules) at an early stage during synthesis, which is consistent with the presence of these composite species in the synthesis of TPA/Si–ZSM-5. The intensities of the signals in the CP spectra increase as crystalline material is formed because the rigidity of the zeolite framework and the occluded organic molecules leads to stronger intermolecular $\text{H}\cdots\text{Si}$ dipolar interactions and thus to more efficient polarization transfer.^{2,28} A mechanism for the TPA-mediated synthesis of Si–ZSM-5 that incorporates all of these considerations is proposed in Figure 3.18.

In the hexanediamine-mediated synthesis of Si–ZSM-5, a similar correlation between the XRD and CP profiles is observed. Although no crystalline material is detected until after 30–40 days of heating, polarization transfer between the organic protons and the silicate species occurs in the X-ray amorphous, heated samples. Again, the observation of efficient intermolecular CP at an early stage in zeolite synthesis suggests that the organic and inorganic components are in close contact. Although the hydration behavior of hexanediamine has not been described in the literature, it is possible that hydrophobic hydration occurs in the vicinity of the alkyl backbone of the diamine molecule, with subsequent replacement of the water molecules by silicate species to form inorganic–organic composites. A small number of the amine groups may be protonated and hydrophilically hydrated and thus may interact favorably with the soluble, anionic silicate species. However, hexanediamine is occluded in the final

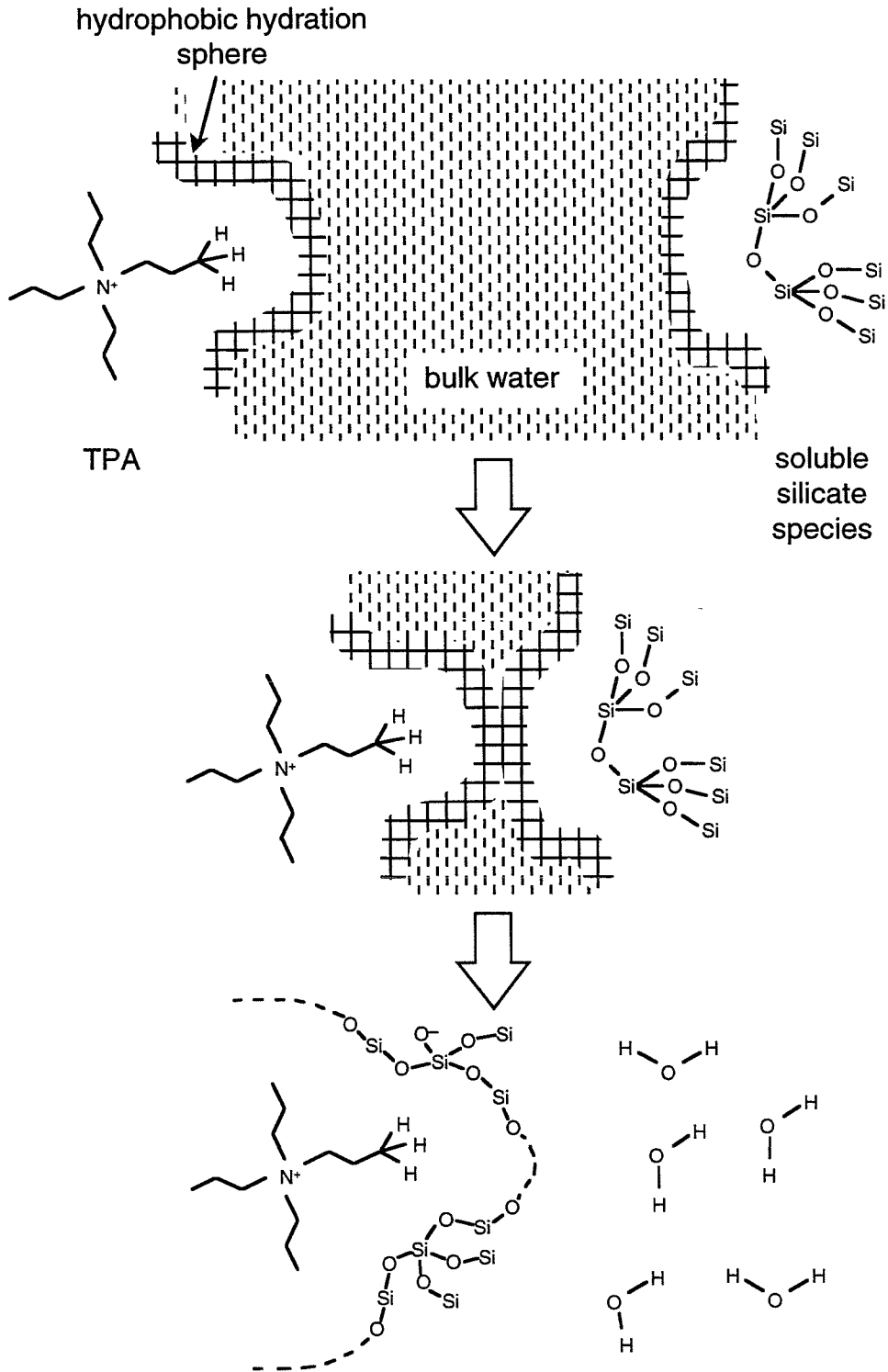


Figure 3.17. Proposed mechanism of formation of inorganic–organic composite species from hydrophobically hydrated TPA and silicate species.

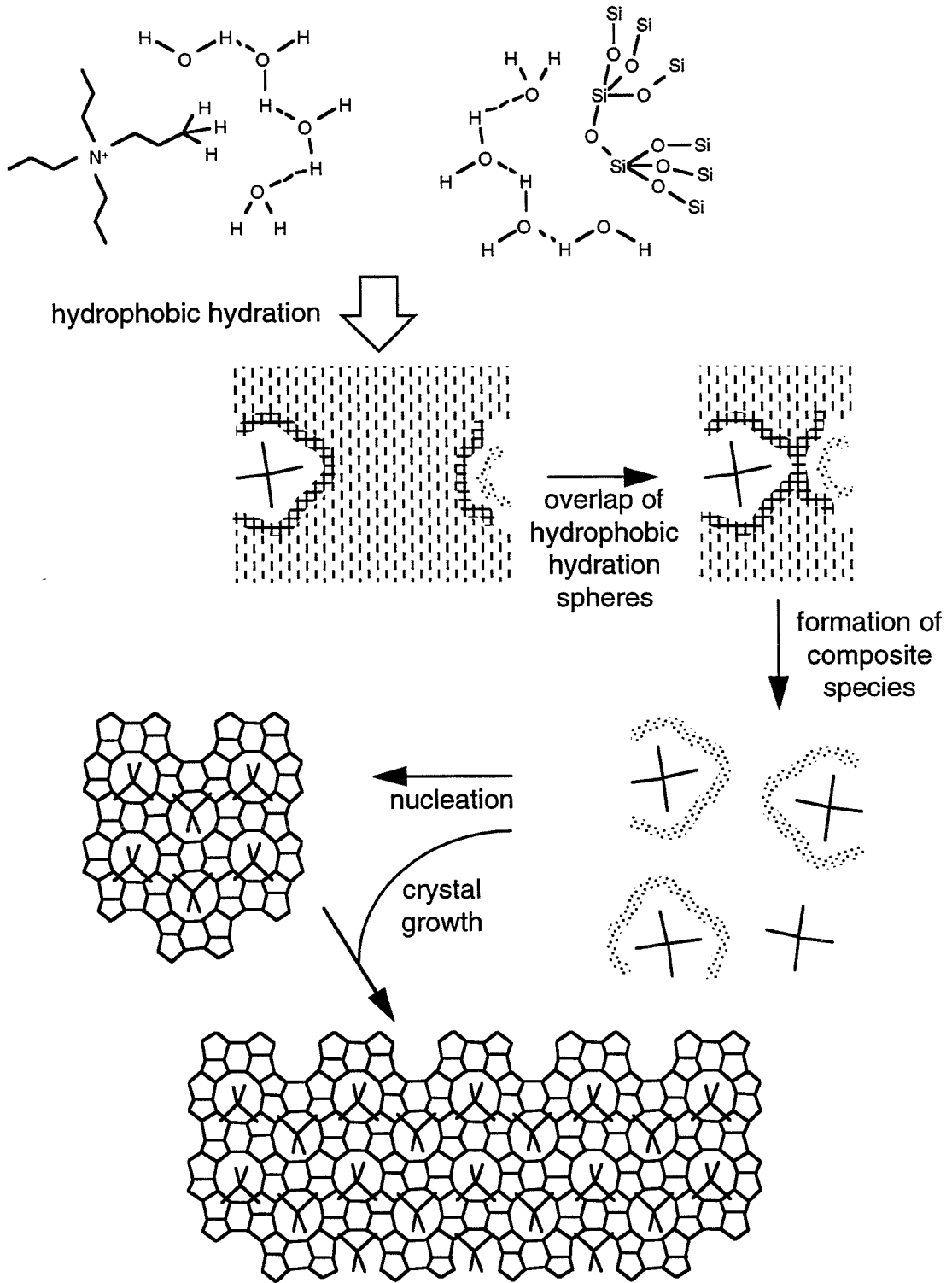


Figure 3.18. Proposed mechanism of structure direction in the TPA-mediated synthesis of Si-ZSM-5.

product as the neutral diamine and protons apparently balance the charge of the anionic Q^3 sites present. Alternatively, the amine groups may form hydrogen bonds to water or interact with the amine groups of other diamine molecules, thus bringing the diamine molecules or composite species into close proximity and promoting the formation of the channel intersections of the Si-ZSM-5 structure. The presence of ethanol when TEOS is used as the silica source may influence these interactions and thus account for the observation that HXN/Si-ZSM-5 cannot be formed using TEOS. However, it is difficult to probe these effects directly. Nevertheless, a proposed mechanism for structure direction in the hexanediamine-mediated synthesis of Si-ZSM-5 similar to that proposed for the TPA-mediated synthesis is presented in Figure 3.19.

A structure-directing effect is not apparent in the hexanediamine-mediated synthesis of Si-ZSM-48. Intermolecular $^1H-^{29}Si$ polarization transfer is not observed until crystalline Si-ZSM-48 is also evident by XRD. The absence of efficient CP from the X-ray amorphous, heated samples suggests that close contacts between the organic and inorganic components are not established and thus that a significant quantity of inorganic-organic composite species is not formed. The difference in the interactions between the inorganic and organic components relative to those observed in the hexanediamine-mediated synthesis of Si-ZSM-5 may be due to the higher temperature at which Si-ZSM-48 is synthesized. At 150 °C, the hydration behavior of hexanediamine may be sufficiently different from that observed at 120 °C such that the silicate species are not brought into close proximity to the diamine. The silicate condensation chemistry under the conditions of concentration, pH, and temperature present may favor the formation of Si-ZSM-48 and be independent of the

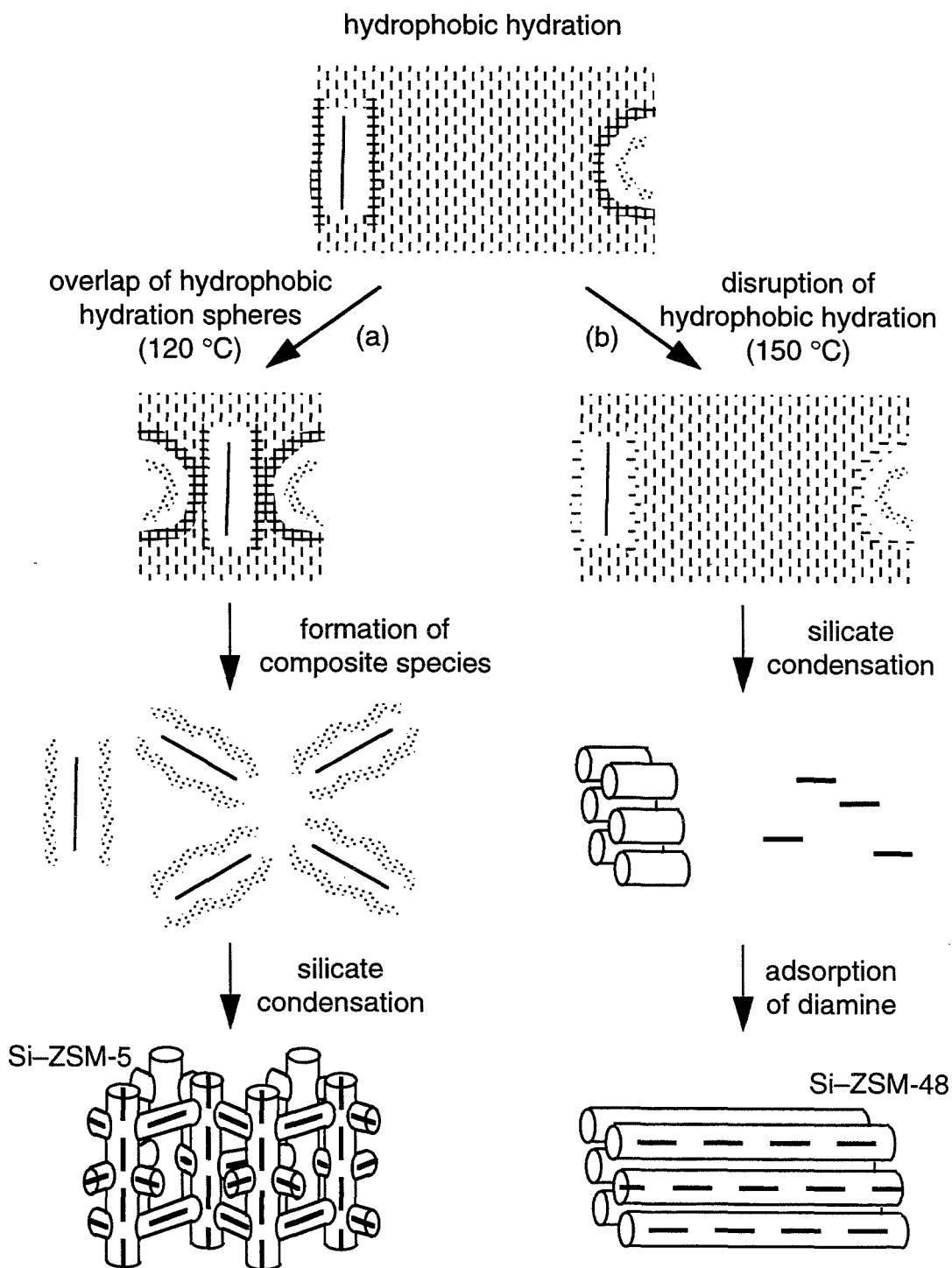


Figure 3.19. Proposed structure-directing (a) and space-filling (b) roles of hexanediamine in the syntheses of Si-ZSM-5 and Si-ZSM-48.

presence of hexanediamine. The observations that Si-ZSM-48 can also be synthesized when ethanol is present in the synthesis mixture and that the synthesis of Si-ZSM-48 is accessible through the use of several different organic bases¹² provide additional support for this explanation. By contrast, Si-ZSM-5 has only been synthesized in the presence of TPA or hexanediamine, although aluminosilicate ZSM-5 can be synthesized using other organic species or in an organic-free system;¹² for the aluminum-containing syntheses, structure formation is most likely controlled by the aluminosilicate gel chemistry alone rather than by the inorganic-organic interactions that are apparently necessary for stabilization of pure-silica, crystalline microporous materials.^{29,30} In the synthesis of Si-ZSM-48, the diamine molecules may be adsorbed into the void space of the zeolite as it crystallizes and stabilize the metastable inorganic material against dissolution in the basic synthesis medium. The occurrence of a specific structure-directing effect is not apparent, and hexanediamine may serve simply as a space-filling agent in the synthesis of Si-ZSM-48.

The effect of temperature in changing the role of an organic species (HXN) from that of a structure-directing agent (Si-ZSM-5 synthesis) to that of a space-filling species (Si-ZSM-48 synthesis) may not be universally applicable. Structure-directing effects from other organic species have been observed at synthesis temperatures above 150 °C.¹² If hydrophobic hydration is implicated in structure direction, then the temperature dependence of this effect will vary depending on the hydrophobicity of the specific species used; in general, the degree of hydrophobic hydration is decreased at higher temperatures and by some estimates may be absent at temperatures above 130–160 °C.⁵ However, the use of lower synthesis temperatures is not necessarily the key factor in achieving structure

direction because silicate dissolution and recondensation are less favorable at lower temperatures.³¹

The significance of hydrophobic hydration is investigated further in the series of synthesis mixtures containing different TAA cations or TEOA. In general, the degree of hydrophobic hydration is greater for species with longer alkyl chains.⁴ TMA and TEA can be considered essentially as large, spherical or elliptical cations³² with the charge located on the α -carbons.³³ TMA and TEA exhibit a somewhat different influence on the water structure than species with longer alkyl chains. Their hydration enthalpies are influenced primarily by electrostatic interactions, whereas those of TAA species with longer alkyl chains have both electrostatic and non-electrostatic (hydrophobic hydration) contributions (Figure 3.20).³² TPA and TBA behave as soluble, hydrophobic species and thus form hydrophobic hydration spheres. However, at high concentrations such as the concentration range used in zeolite synthesis (≈ 0.3 M), TBA may exhibit a reduced hydrophobic hydration effect due to the formation of aggregates.⁴ TPenA is not very soluble⁹ and tends to aggregate and phase separate in aqueous solution rather than existing as isolated, hydrophobically hydrated cations. In contrast, the alcohol moiety of TEOA can participate in the hydrogen bonding network of water and thus does not form a hydrophobic hydration sphere despite the similarity in size to TPA.⁴

Among the TAA species investigated, a crystalline product is formed at the aforementioned synthesis composition and temperature only in the presence of TPA. In this case, intermolecular ^1H - ^{29}Si polarization transfer is observed in the heated synthesis mixture prior to the formation of a crystalline product, which suggests that molecular organization

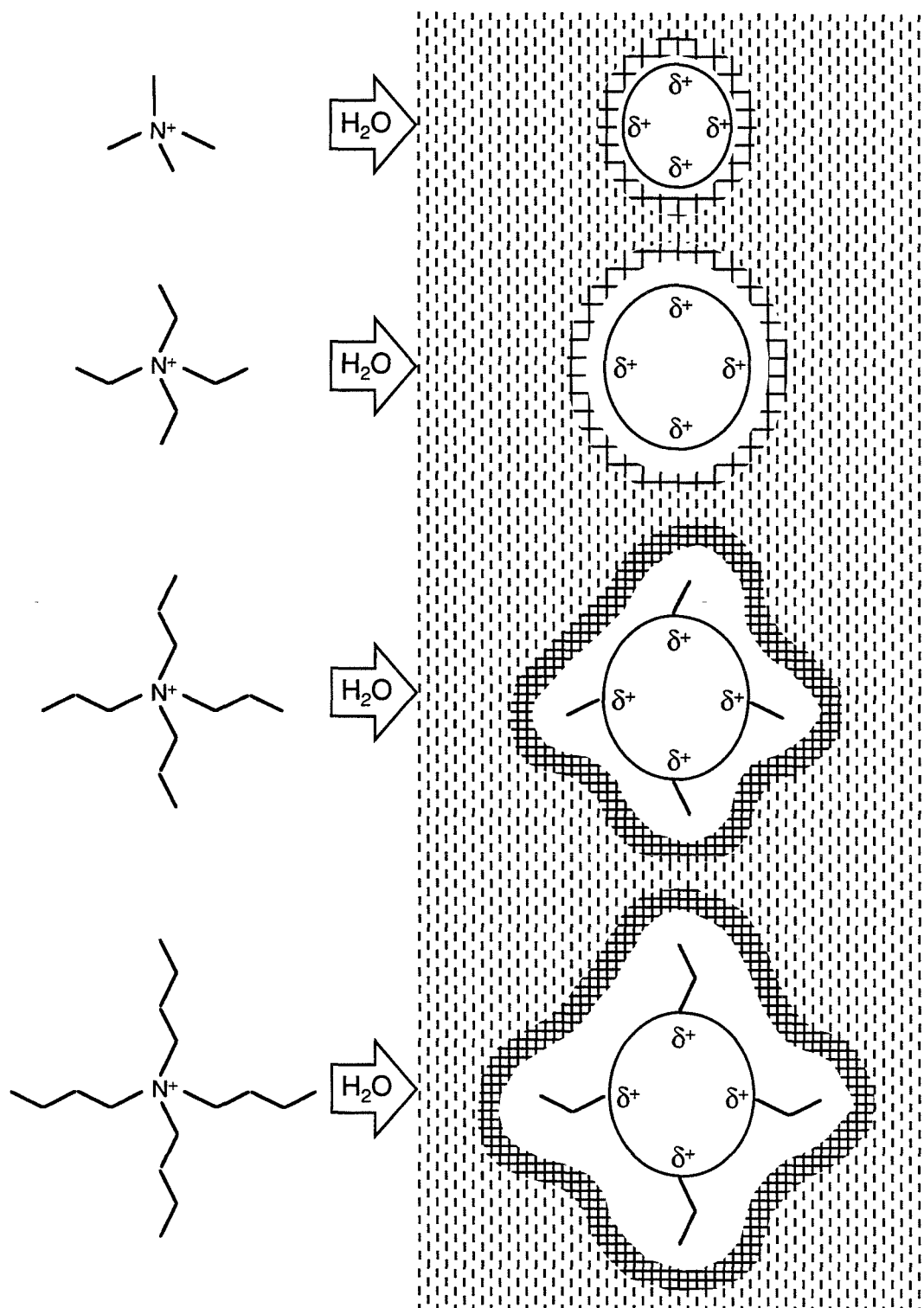


Figure 3.20. Differences in hydration of tetraalkylammonium cations. The hydration of TMA and TEA is dominated by electrostatic interactions, whereas TPA and TBA have a stronger contribution from non-electrostatic interactions (hydrophobic hydration).³²

events relevant to structure direction are occurring. In order for CP to be efficient, the organic and silicate species must be in van der Waals contact, without intervening water molecules. Polarization transfer is not observed to a significant extent in samples prepared using TEOA or TAA species other than TPA, except when anionic double-ring silicate structures are present in the unheated, TMA- or TEA-containing gels. The hydration spheres of TMA and TEA may not be sufficiently hydrophobic to interact favorably with hydrophobically hydrated silica, as is suggested by the observation that short-chain TAA ions do not adsorb onto silica as readily as long-chain species.²⁶ In addition, even if TMA interacts with silica, TMA may be too mobile for intermolecular CP to occur.² On the other hand, TBA and TPenA may form aggregates, thus minimizing the extent of hydrophobic hydration and the potential for interaction with silica; nevertheless, a small amount of CP is observed for samples prepared using TBA. The ability of TBA to serve as a structure-directing agent for the synthesis of Si-ZSM-5 and Si-ZSM-11 at higher synthesis temperatures^{29,34} may be due to the increased solubility of TBA (reduced tendency to aggregate). At temperatures above 110 °C, isolated TBA molecules may exhibit the appropriate hydrophobic hydration for inorganic-organic composite species to subsequently form; the possibility that the necessary interactions between silicate and TBA could be established at higher temperatures is suggested by the observation of some CP in the TBA-containing samples prepared at 110 °C. By contrast, TEOA may interact preferentially with water via hydrogen bonding of the alcohol moiety rather than interacting with silica. Thus, the observation of intermolecular CP in the X-ray amorphous, heated synthesis mixture appears to correlate with the observation of a structure-direction effect;

only when Si-ZSM-5 is eventually formed is efficient CP observed in the heated, X-ray amorphous precursor.

An explanation of the molecular level interactions that are relevant to the presence or absence of a structure-directing effect and are reflected by the ^1H - ^{29}Si CP profiles needs to be clarified in order to move toward the ultimate goal of the a priori design of effective structure-directing agents. In particular, it is of interest whether the ability to form a hydrophobic hydration sphere is a requisite property for a species to serve as a structure-directing agent. Alternatively, the molecular characteristics that induce hydrophobic hydration may also be those that generate the requisite favorable organic-inorganic interactions in the zeolite product, without hydrophobic hydration spheres playing a role in the mechanism of structure direction. It has been shown that although the thermodynamic driving force for the synthesis of TPA⁺F⁻/Si-ZSM-5 from amorphous silica is dominated by the enthalpically favorable, inorganic-organic van der Waals interactions within the product ($\Delta H \approx -1.5 \text{ kcal (mol SiO}_2\text{)}^{-1}$), there is an entropic contribution resulting from the release of ordered water molecules from the hydrophobic hydration sphere of TPA in going from the synthesis solution into the zeolite ($-T\Delta S \approx -0.4 \text{ kcal (mol SiO}_2\text{)}^{-1}$).³⁰ TPA/Si-ZSM-5 likely represents a nearly optimum case for inorganic-organic van der Waals interactions in zeolite synthesis; when the intermolecular interactions are less favorable and the enthalpic contribution to the driving force is thus less strong, it is possible that the entropic factor arising from the release of water from the hydrophobic hydration sphere of the organic species may be a predominant factor in determining whether the formation of inorganic-organic composite species and a crystalline product are thermodynamically favored. The

observation that no crystalline product was obtained using TEOA even when a small amount of TPA (sufficient for nucleation to occur) was present, suggests that the formation of a hydrophobic hydration sphere might be significant to the mechanism of structure direction. However, these results do not provide a clear distinction between the role of enthalpic and entropic considerations, and further investigation is warranted.

All molecules that form hydrophobic hydration spheres may not necessarily exhibit structure-directing effects. It has been suggested that the ability of an organic molecule to serve as a structure-directing agent lies in a delicate balance of hydrophilic properties, which provide solubility in aqueous solution, and hydrophobic character, which generates favorable interactions with the crystalline silica host.^{29,35,36} Although TPA is the only member of the series of homoleptic TAA species that has the proper balance of hydrophobic and hydrophilic properties to serve as structure-directing agent at the synthesis composition and temperature investigated (TBA can be used to synthesize Si-ZSM-5 and Si-ZSM-11 at higher temperatures (*vide supra*)), nonsymmetric quaternary alkylammonium species may be found that exhibit these characteristics. Zones has demonstrated a correlation between the C/N⁺ ratios (an estimate of hydrophobic or hydrophilic character) of various quaternary alkylammonium species and the extent to which these species transfer from aqueous solution to a chloroform phase,³⁶ for molecules with C/N⁺ ratios less than 11, a small degree of transfer (<10%) occurs, whereas for molecules with C/N⁺ ratios greater than 15, a large degree of transfer (>70%) occurs. The observation that many of the species investigated that have intermediate C/N⁺ ratios (11<C/N⁺<15) serve as structure-directing agents in the synthesis of high-silica zeolites supports the suggestion that

a balance of hydrophilic and hydrophobic properties is important for structure-directing ability.³⁶

All of the mechanistic considerations up to this point have been thermodynamic ones. However, zeolites are metastable relative to quartz, and thus zeolite synthesis is a kinetically controlled process.^{14,37} The crystallization profiles demonstrate that several factors in the synthesis mixture can influence the rates of nucleation and crystal growth of Si-ZSM-5 and Si-ZSM-48, even in the presence of a structure-directing agent. The more rapid nucleation that occurs when sodium is present or when a monomeric silica source (TEOS) is used suggests that nucleation in the TPA-mediated synthesis of Si-ZSM-5 and in the hexanediamine-mediated syntheses of Si-ZSM-5 and Si-ZSM-48 may be limited by the rate of dissolution of the highly-condensed silica source (Cab-O-Sil) that is used. Sodium has been shown to enhance the rate of dissolution of quartz,^{38,39} and it is thus consistent that nucleation is dependent on the rate at which soluble silicate species are made available to form inorganic-organic composites. The rate of crystal growth may also be limited by the availability of soluble silicate and thus enhanced by the presence of sodium in low concentrations. At high concentrations of sodium, the structure-directing influence of sodium is predominant over that of the organic species, and layered silicates with a large proportion of anionic Q³ sites are formed for optimum electrostatic interactions.^{30,40} The observation that nucleation of HXN/Si-ZSM-5 from a seeded synthesis mixture is faster than that from the non-seeded preparation but slower than that from a sodium-containing gel suggests that the rate of nucleation is not determined solely by the rate of dissolution of silica; otherwise, similar rates would be expected for the sodium-containing and seeded syntheses.

Sodium may also facilitate the association, orientation, and condensation of the inorganic–organic composite species within aggregates of the appropriate size ($\approx 50\text{--}60$ Å) to form nuclei.^{41,42}

In the absence of the accelerating influences of sodium or TEOS, the slowed rates of nucleation for syntheses using D_2O in lieu of H_2O are noteworthy. The existence of an isotope effect suggests that cleavage of O–H or O–D bonds may figure prominently in rate-determining steps in the nucleation process. However, it is not likely that this effect simply involves the base-catalyzed dissolution of silica since OD^- is a stronger base than OH^- ; the presence of OD^- would be expected to accelerate rather than decelerate the dissolution process.¹³ The hydrogen bonding network of D_2O is more strongly bonded than that of H_2O ,⁴ and thus restructuring of the network to allow the organic and silicate components to come into contact in order for nucleation to occur may be slowed in D_2O . There may also be a decelerating influence of D_2O on the silicate condensation chemistry due to the slower rates of O–D bond formation and cleavage,¹³ which may lead to slower nucleation and crystal growth. However, the similar rates of nucleation in the syntheses comparing TPA and TPA- d_{28} in H_2O demonstrate that direct hydrogen bonds between the organic and inorganic (H_2O or silica) components may not be present; if such bonds were involved, observation of an isotope effect would be expected in the presence of TPA- d_{28} . Thus, the observed kinetics of nucleation are consistent with a mechanism that includes the formation of inorganic–organic composite species via favorable van der Waals interactions as a key step.

Proposed Mechanism

The fundamental aspects of the previously proposed mechanism of structure direction and self-assembly in the TPA-mediated synthesis of Si-ZSM-5 are supported by the present results (Figure 3.18). The key step in this process is the formation of inorganic–organic composite units that then provide the primary species involved in zeolite nucleation and crystal growth. The ability of TPA to form a hydrophobic hydration sphere is an important factor in structure direction because favorable overlap of the hydrophobic hydration sphere formed around the organic species with the hydrophobically hydrated domains of the soluble silicate species may be responsible for bringing the organic and inorganic components into proximity.²⁶ Favorable van der Waals contacts between the alkyl chains of TPA and hydrophobic silica are established upon release of water molecules from the ordered hydration spheres into the bulk;²⁹ this process may be slowed in the presence of D₂O due to the more structured hydration sphere that must be reorganized. The establishment of van der Waals interactions and the release of ordered water molecules provide the thermodynamic driving force for the formation of inorganic–organic composite species.³⁰ Optimization of van der Waals interactions within these species gives rise to the geometric correspondence between the organic molecules and the inorganic architecture that is characteristic of the structure direction phenomenon.

The availability of soluble silicate influences the rate at which these composite species are formed; the use of a monomeric silica source such as TEOS or the presence of sodium in the synthesis mixture to facilitate dissolution of a condensed silica precursor results in an enhanced rate of

nucleation. When a critical concentration of the inorganic–organic composite species is present, aggregation of these species likely leads to nucleation;^{41,43} this process may occur in solution or on the surface of silica particles⁴¹ or the walls of the reaction vessel (heterogeneous nucleation). Subsequent crystal growth can occur via the attachment of composite species to the crystallite surface in a layer-by-layer fashion,² as suggested by the layered structure of ZSM-5/ZSM-11 intergrowths⁴⁴ and other intergrowths of high-silica zeolites.⁴⁵⁻⁴⁷ Free TPA molecules (and additional organic molecules that may have been introduced into the synthesis mixture, such as TMA or TEA)⁴⁸ and silicate species may also be able to diffuse to the surface of the growing zeolite crystal and be incorporated into the crystalline structure.

It is possible that the mechanism can be generalized to other examples of structure direction in the synthesis of known and novel high-silica and pure-silica zeolites. If the organic species exhibits the appropriate balance of hydrophobic and hydrophilic character, a sufficient extent of hydrophobic hydration can occur in solution such that the formation of inorganic–organic composite species is favored. It may be possible to screen potential organic structure-directing agents by observing their interactions with silicate species via the ^1H – ^{29}Si CP MAS NMR technique. The structure-directing effect of the organic species is exhibited primarily via optimized van der Waals interactions with the inorganic species; it is through these interactions in the formation of composite species that the geometry of the organic molecule can be translated into the zeolite pore architecture. A better understanding of the hydrophobic hydration behavior of quaternary alkylammonium species may provide insight into the design of new structure-directing agents. The synthesis of

a novel zeolite material by tailoring of the hydrophobic hydration behavior of an organic structure-directing agent remains to be demonstrated.

References

- (1) Lefebvre, F.; Sacerdote-Peronnet, M.; Mentzen, B. F. *C. R. Acad. Sci. Paris, Ser. 2* **1993**, *316*, 1549.
- (2) Burkett, S. L.; Davis, M. E. *J. Phys. Chem.* **1994**, *98*, 4647.
- (3) Franklin, K. R.; Lowe, B. M. *Zeolites* **1988**, *8*, 495.
- (4) Wen, W. -Y. In *Water and Aqueous Solutions*; R. A. Horne, Ed.; Wiley-Interscience: New York, 1972; pp 613.
- (5) Muller, N. *Acc. Chem. Res.* **1990**, *23*, 23.
- (6) Blokzijl, W.; Engberts, J. B. F. N. *Angew. Chem. Int. Ed. Engl.* **1993**, *32*, 1545.
- (7) Franks, F. *Water*; Royal Society of Chemistry: London, 1983, pp 96.
- (8) Heuvelsland, W. J. M.; de Visser, C.; Somsen, G. *J. Phys. Chem.* **1978**, *82*, 29.
- (9) Nakayama, H.; Kuwata, H.; Yamamoto, N.; Akagi, Y.; Matsui, H. *Bull. Chem. Soc. Jpn.* **1989**, *62*, 985.
- (10) Shimizu, A.; Taniguchi, Y. *Bull. Chem. Soc. Jpn.* **1990**, *63*, 3255.
- (11) Harmon, K. M.; Budrys, N. M. *J. Mol. Struct.* **1991**, *249*, 149.
- (12) Szostak, R. *Handbook of Molecular Sieves*; Van Nostrand Reinhold: New York, 1992, pp 584.
- (13) Dutta, P. K.; Puri, M.; Bowers, C. In *Zeolite Synthesis*; M. L. Ocelli and H. E. Robson, Eds.; American Chemical Society: Washington, DC, 1989; pp 98.
- (14) Davis, M. E.; Lobo, R. F. *Chem. Mater.* **1992**, *4*, 756.
- (15) Goepper, M.; Li, H. -X.; Davis, M. E. *J. Chem. Soc., Chem. Commun.* **1992**, 1665.

- (16) Jacobs, P. A.; Derouane, E. G.; Weitkamp, J. *J. Chem. Soc., Chem. Commun.* **1981**, 591.
- (17) Coudurier, G.; Naccache, C.; Vedrine, J. C. *J. Chem. Soc., Chem. Commun.* **1982**, 1413.
- (18) Schlenker, J. L.; Rohrbaugh, W. J.; Chu, P.; Valyocsik, E. W.; Kokotailo, G. T. *Zeolites* **1985**, *5*, 355.
- (19) Dartt, C. B.; Khouw, C. B.; Li, H. -X.; Davis, M. E. *Microporous Mater.* **1994**, *2*, 425.
- (20) Engelhardt, G.; Michel, D. *High-Resolution Solid-State NMR of Silicates and Zeolites*; John Wiley & Sons: Chichester, 1987.
- (21) Lambert, J. B.; Shurvell, H. F.; Lightner, D. A.; Cooks, R. G. *Introduction to Organic Spectroscopy*; MacMillan: New York, 1987.
- (22) Giordano, G.; Dewale, N.; Gabelica, Z.; Nagy, J. B.; Derouane, E. G. *Appl. Catal.* **1991**, *71*, 79.
- (23) Dean, J. A. *Lange's Handbook of Chemistry*; 14th ed.; McGraw-Hill: New York, 1992.
- (24) Groenen, E. J. J.; Kortbeek, A. G. T. G.; Mackay, M.; Sudmeijer, O. *Zeolites* **1986**, *6*, 403.
- (25) van der Donck, J. C. J.; Stein, H. N. *Langmuir* **1993**, *9*, 2270.
- (26) van der Donck, J. C. J.; Vaessen, G. E. J.; Stein, H. N. *Langmuir* **1993**, *9*, 3553.
- (27) Frank, H. S.; Evans, M. W. *J. Chem. Phys.* **1945**, *13*, 507.
- (28) Pines, A.; Gibby, M. G.; Waugh, J. S. *J. Chem. Phys.* **1973**, *59*, 569.
- (29) Gies, H.; Marler, B. *Zeolites* **1992**, *12*, 42.
- (30) Helmkamp, M. M.; Davis, M. E. *Ann. Rev. Mater. Sci.*, in press.
- (31) Iler, R. K. *The Chemistry of Silica*; John Wiley & Sons: New York, 1979.

- (32) Nagano, Y.; Mizuno, H.; Sakiyama, M.; Fujiwara, T.; Kondo, Y. *J. Phys. Chem.* **1991**, *95*, 2536.
- (33) Jorgensen, W. L.; Gao, J. *J. Phys. Chem.* **1986**, *90*, 2174.
- (34) Li, H. -X.; Cambor, M. A.; Davis, M. E. *Microporous Mater.* **1994**, *3*, 117.
- (35) Burkett, S. L.; Davis, M. E. *Microporous Mater.* **1993**, *1*, 265.
- (36) Lobo, R. F.; Zones, S. I.; Davis, M. E. In *Inclusion Chemistry with Zeolites: Nanoscale Materials by Design*; N. Herron and D. Corbin, Eds.; in press.
- (37) Petrovic, I.; Navrotsky, A.; Davis, M. E.; Zones, S. I. *Chem. Mater.* **1993**, *5*, 1805.
- (38) Brady, P. V.; Walther, J. V. *Chem. Geol.* **1990**, *82*, 253.
- (39) Dove, P. M.; Crerar, D. A. *Geochim. Cosmochim. Acta* **1990**, *54*, 955.
- (40) Zones, S. I. *Microporous Mater.* **1994**, *2*, 281.
- (41) Dokter, W. H.; Beelen, T. P. M.; van Garderen, H. F.; Rummens, C. P. J.; van Santen, R. A.; Ramsay, J. D. F. *Colloids Surfaces A* **1994**, *85*, 89.
- (42) van Santen, R. A., unpublished results.
- (43) Harris, T. V.; Zones, S. I. In *Zeolites and Related Microporous Materials: State of the Art 1994*; J. Weitkamp, H. G. Karge, H. Pfeifer and W. Hölderich, Eds.; Elsevier: Amsterdam, 1994; pp 29.
- (44) Millward, G. R.; Ramdas, S.; Thomas, J. M. *J. Chem. Soc., Faraday Trans. 2* **1983**, *79*, 1075.
- (45) Lobo, R. F.; Pan, M.; Chan, I.; Li, H. -X.; Medrud, R. C.; Zones, S. I.; Crozier, P. A.; Davis, M. E. *Science* **1993**, *262*, 1543.
- (46) Lobo, R. F.; Davis, M. E. (California Institute of Technology). U.S. Patent appl., 1993.

- (47) Lobo, R. F.; Zones, S. I.; Davis, M. E. In *Zeolites and Related Microporous Materials: State of the Art 1994*; J. Weitkamp, H. G. Karge, H. Pfeifer and W. Hölderich, Eds.; Elsevier: Amsterdam, 1994; pp 461.
- (48) Rossin, J. A.; Davis, M. E. *Ind. J. Tech.* **1987**, *25*, 621.

Chapter Four

Mechanism of Structure Direction in the Crown Ether-Mediated Syntheses of FAU and EMT Zeolites

Reprinted with permission from *Microporous Mater.* **1993**, *1*, 265.

Copyright 1993 Elsevier Science B. V.

Abstract

The structure-directing effects of 15-crown-5 and 18-crown-6 in the syntheses of cubic faujasite (FAU) and hexagonal faujasite (EMT), respectively, are investigated. The conformation and distribution of sodium/crown ether complexes during synthesis and in the product materials are characterized by Raman spectroscopy and by solid state ^1H - ^{13}C CP NMR. The balance between the structure-directing influences of alkali metal ions and crown ethers on product formation is investigated. The structural relationships between the two polymorphs of faujasite and the specificity of the crown ether structure-directing agents to these products are discussed in relation to a proposed mechanism of synthesis.

Introduction

Interest in the design and synthesis of new zeolitic materials with specific pore dimensions or structural features has focused on the factors affecting zeolite crystallization, in particular on the role of organic structure-directing agents. Addition of organic species such as alkylammonium compounds, amines, alcohols, or ethers to a synthesis mixture can bring about the production of crystalline, microporous materials from gels that would otherwise give denser products or remain amorphous. Organic additives can also increase the silicon-to-aluminum ratios of zeolite products.^{1,2} However, the mechanism by which the presence of an organic species induces the transformation of an aluminosilicate synthesis gel to a crystalline material is not well understood. Particularly noteworthy is the absence of a one-to-one correlation between the structure-directing agent used and the product obtained.^{2,3} The features of the organic species that are significant to structure direction and the modes of interaction among the organic and inorganic species during structure formation remain to be elucidated.

Structure-directing effects are apparent in the synthesis of faujasite. Two distinct polymorphs of faujasite can be obtained from the same synthesis gel by adding crown ethers as structure-directing agents.⁴⁻⁶ The cubic structure (FAU) can be synthesized by a variety of methods, both with and without organic structure-directing agents, over a wide range of Si/Al ratios (faujasite, zeolite Y, and zeolite X). The hexagonal polymorph of faujasite (EMT) was postulated by Moore and Smith in 1964⁷ and was observed as an intergrowth with FAU in ZSM-3,⁸ ZSM-20,^{9,10} and other materials,^{11,12} but was only recently synthesized in its pure form.^{4-6,13}

Each structure can be considered as a stack of faujasite sheets that are comprised of rings of six sodalite cages connected through hexagonal prisms. An ABCABC stacking of faujasite sheets (zinc blende structure) yields FAU; pairs of sodalite cages in adjoining sheets are related by an inversion center (Figure 4.1). An ABABAB stacking of sheets (wurtzite structure), for which pairs of sodalite cages in adjoining sheets are related by a mirror plane, gives EMT (Figure 4.2).^{10,14-17} In FAU there is one type of spherical supercage (eight per unit cell) which has an internal diameter of 13 Å and is accessed by four 7.4 Å circular apertures. In EMT there are two different supercages (two of each type per unit cell); the larger supercage has an internal diameter of 13 Å by 14 Å, with three 6.9 Å by 7.4 Å elliptical apertures and two 7.4 Å circular apertures, while the smaller elliptical supercage has a maximum diameter of 12 Å, with three 6.9 Å by 7.4 Å elliptical apertures.

FAU and EMT can be synthesized at the same bulk chemical composition (approximately 8 crown ether molecules: Na₄₂Al₄₂Si₁₅₀O₃₈₄: 115 H₂O in one unit cell of FAU or two unit cells of EMT) from an aged gel composed of 1 crown ether: 2.4 Na₂O: Al₂O₃: 10 SiO₂: 140 H₂O. With 1,4,7,10,13-pentaoxacyclopentadecane (15-crown-5), the cubic polymorph is produced, and the material contains one intact crown ether molecule per supercage.⁴⁻⁶ The use of 1,4,7,10,13,16-hexaoxacyclooctadecane (18-crown-6) instead of 15-crown-5 yields EMT with one intact, occluded crown ether molecule in each of the two types of supercages,⁶ or with two molecules in the larger supercage and none in the smaller.⁵ In the absence of crown ether or with different organic species, pure crystalline FAU is obtained only when a higher concentration of sodium hydroxide (3.1 Na₂O total) is employed in the gel.^{5,6}

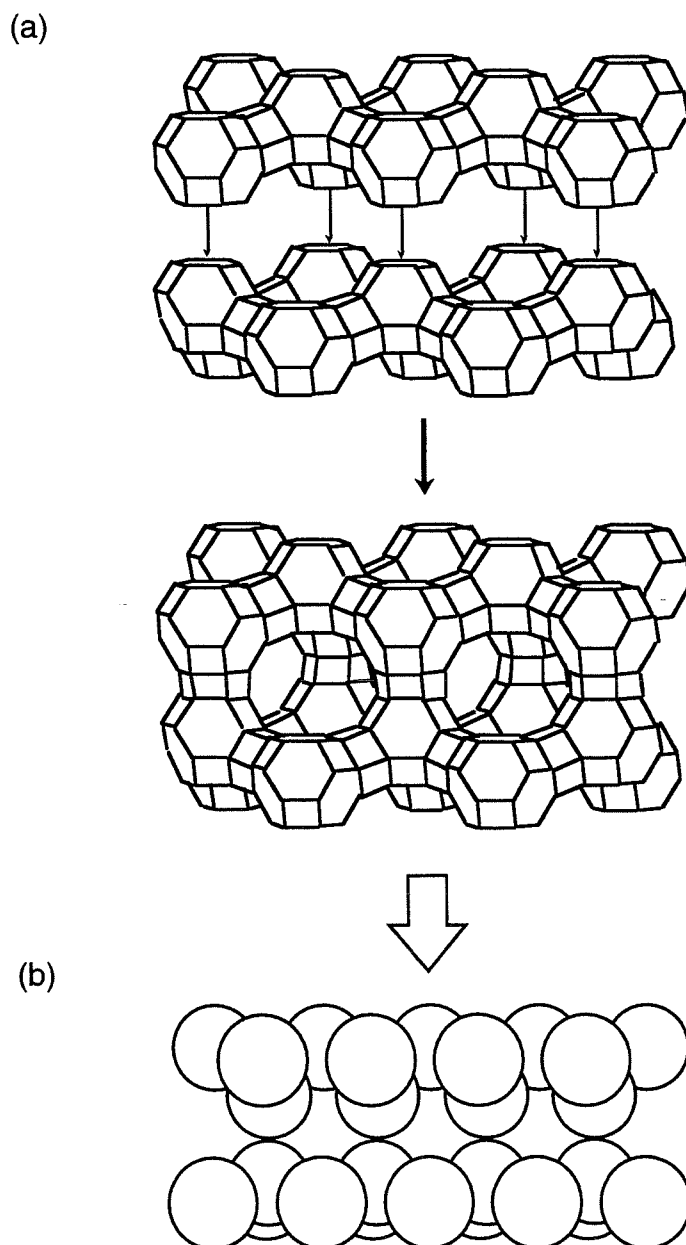


Figure 4.1. Structure of FAU. The sodalite cages in adjoining faujasite sheets are related by an inversion center through the hexagonal prisms which are formed in the sites indicated by an arrow. In this diagram, three equivalent supercages are formed^{10,14} (a). Each supercage of FAU, represented by a sphere, is connected to four other supercages in a tetrahedral arrangement, producing the zinc blende structure (b).

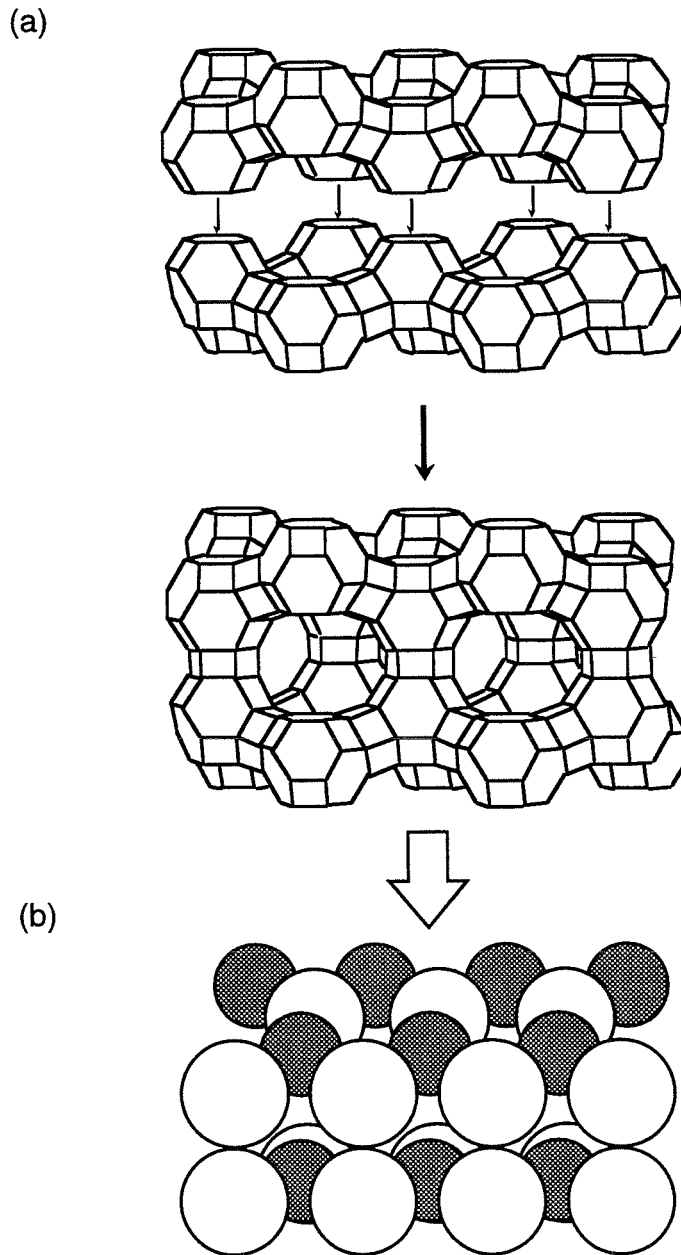


Figure 4.2. Structure of EMT. The sodalite cages in adjoining faujasite sheets are related by a mirror plane through the hexagonal prisms which are formed in the sites indicated by an arrow. In this diagram, three supercages are formed: two larger supercages are on the left and right, and a smaller supercage connects them in the rear.^{10,14} (a).

The connectivity of the larger and smaller supercages of EMT, which are represented by the light and dark spheres, respectively, is illustrated in this diagram. This arrangement produces the wurtzite structure (b).

This chapter presents a multifaceted investigation of the crown ether-mediated syntheses of FAU and EMT. Detailed product characterization and syntheses using modified crown ethers and other macrocycles are described in order to identify the physicochemical properties of 15-crown-5 and 18-crown-6 that are significant to their structure-directing capabilities. The distribution of 18-crown-6 molecules in the supercages of EMT is also addressed. The structure-forming processes (gel aging, nucleation, and crystal growth) during which the crown ethers may be influential are investigated, and the role of inorganic structure-directing agents, e.g., the higher concentration of sodium hydroxide that is necessary for the synthesis of FAU in the absence of crown ethers, is examined. Finally, a possible mechanism of synthesis and structure direction is proposed.

Experimental

Synthesis

The gel composition used for template-mediated faujasite syntheses was R: 2.4 Na₂O: Al₂O₃: 10 SiO₂: 140 H₂O (R=15-crown-5 or 18-crown-6).^{5,6} In a typical synthesis, 3.63 g sodium aluminate (Na₂O · Al₂O₃ · 3 H₂O; EM Scientific), 3.74 g 50 wt % aqueous sodium hydroxide (Fisher), and crown ether (3.67 g 15-crown-5 or 4.40 g 18-crown-6, provided as a gift from Union Carbide) were stirred in 24.22 g distilled water until the solution was clear. To this was added 25.0 g Ludox HS-40 colloidal silica (DuPont), and the gel (pH 12) was stirred for 48 hours. The final reaction mixture was heated statically in Teflon-lined, autoclaves at 110 °C for 8–12 days.

The product was recovered by filtration.

For syntheses at higher alkali concentration, an additional 0.7 M₂O (M=alkali metal) was introduced and the gels heated for 12 days. Organic-free synthesis of FAU was obtained by heating a gel of composition 3.1 Na₂O: Al₂O₃: 10 SiO₂: 140 H₂O at 110 °C for 4 days.^{5,6} The addition of 18-crown-6 to this gel (R/Al₂O₃=1) produced FAU with occluded 18-crown-6 in 8 days. Other organic species used were 1,4,7,10,13,16-hexathiacyclooctadecane (S₆-18-crown-6), 1,4,10,13-tetraoxa-7,16-diazacyclooctadecane (N₂-18-crown-6), 1,4,7,10,13,16-hexaazacyclooctadecane (N₆-18-crown-6), 2,5,8,11,14-pentaoxapentadecane (tetraethylene glycol dimethyl ether; TEGDME), tetraethylene glycol (TEG), pentaethylene glycol (PEG), 4,7,13,16,21,24-hexaoxa-1,10-diazabicyclo[8.8.8]hexacosane (Kryptofix 2.2.2), and 2,3,11,12-dibenzo-1,4,7,10,13,16-hexaoxacyclooctadeca-2,11-diene (dibenzo-18-crown-6), which were used as received from Aldrich; α-cyclodextrin was obtained from Amaizo.

Solid sodium/crown ether complexes were prepared by filtering the product obtained by mixing concentrated aqueous solutions of crown ether and sodium hexafluorophosphate (Aldrich).

In order to ascertain whether crown ethers are able to absorb into calcined FAU and EMT, 1.5 ml 0.4 M aqueous crown ether, 0.96 M sodium chloride, and 25 g calcined zeolite were heated at 110 °C and autogenous pressure for 8 days. The absorption of crown ethers was verified by Raman spectroscopy and thermogravimetric analysis.

Analysis

X-ray powder diffraction (XRD) data were collected on a Scintag XDS-2000 diffractometer using CuKα radiation. Analyses were performed

on the acid form of the zeolites, which were prepared by calcining the as-synthesized samples in air at 550 °C, exchanging with 1 M ammonium nitrate at 100 °C, and calcining again at 450 °C. Evidence suggesting the presence of intergrowth structures of FAU and EMT was obtained from the reflections in the $5^{\circ} \leq 2\theta \leq 7^{\circ}$ region (EMT 100; EMT 002, coincident with FAU 111; EMT 101), and by broadening of the reflection at 11.0° (EMT 103) relative to the reflections at 10.1° (EMT 110/FAU 220) and at 18.7° (EMT 302/FAU 511).^{18,19}

Thermogravimetric analyses were performed on a DuPont 951 Thermogravimetric Analyzer (TGA). Approximately 7 mg of sample were heated at a rate of $5^{\circ}\text{C min}^{-1}$ to 600 °C.

Raman spectroscopy was performed on a Nicolet System 800 with a Fourier-Transform (FT) Raman Accessory (Nd-YAG laser; $\lambda=1064$ nm; 600 mW).

Solid state NMR studies were performed on a Bruker AM 300 spectrometer equipped with a Bruker dual channel MAS probe, a Bruker solid state CP MAS accessory, and high-power proton and X-channel amplifiers. ^{13}C spectra (75.47 MHz) were obtained using ^1H - ^{13}C CP with ^1H decoupling or using high-power ^1H decoupling only, and were referenced to an adamantane external standard (downfield resonance at 38.4 ppm). ^{29}Si spectra (59.63 MHz) were collected using MAS and were referenced to a tetrakis(trimethylsilyl)silane external standard (downfield resonance at -10.05 ppm). Product Si/Al ratios were calculated from ^{29}Si NMR spectra, using Bruker LINESIM spectral fitting software. Samples were packed into ZrO_2 rotors and spun at 3–5 kHz for MAS studies. For static spectra, bearing gas (350 mbar N_2) was passed over the rotor to prevent artifacts due to sample heating. Dehydrated zeolite

samples were prepared by heating at 100 °C and 0.05 Torr for 12 hours. Dehydrated samples were handled and sealed in NMR rotors under a dry N₂ atmosphere. Samples were allowed to equilibrate for 20 minutes during variable-temperature studies.

Modeling of zeolite-occluded crown ethers was performed using Cerius software from Molecular Simulations on a Silicon Graphics Personal Iris system.

Results and Discussion

Chemical Composition of FAU and EMT

The chemical compositions of FAU and EMT were obtained from ²⁹Si NMR and TGA results. The ²⁹Si NMR spectra of FAU and EMT were each fit to four Gaussian peaks (−89.3 ppm (Si(3Al)), −94.8 ppm (Si(2Al)), −100.6 ppm (Si(1Al)), −106.3 ppm (Si(0Al))), yielding a Si/Al ratio of 3.6 for each material. The Si/Al ratio of FAU synthesized in the absence of crown ether structure-directing agent is higher than in the synthesis in which a high concentration of sodium hydroxide produces FAU (Si/Al=3.0) (*vide infra*).⁶ Product yields were 85–90% (based on Al₂O₃) for all syntheses.

TGA of FAU and EMT revealed two stages of weight loss: the first, from 25 °C to 210 °C (FAU) or 260 °C (EMT), corresponds to desorption of water, and the second, to 600 °C, corresponds to combustion of occluded crown ether. (It has been demonstrated previously by ¹H–¹³C CP MAS NMR⁴⁻⁶ as well as in this study by Raman spectroscopy and ¹H–¹³C CP NMR (*vide infra*) that crown ether molecules are intact within the supercages of FAU and EMT). The observed losses of water (12.3 wt %) and

15-crown-5 (12.7 wt %) indicate a unit cell composition of 9.6 15-crown-5: Na₄₂Al₄₂Si₁₅₀O₃₈₄: 113.4 H₂O for FAU (sodium content is calculated from charge-balance considerations), equating to approximately one crown ether molecule per supercage; FAU has been synthesized previously at unit cell compositions of 9.0 15-crown-5: Na₃₇Al₃₇Si₁₅₅O₃₈₄: 118.8 H₂O⁵ and 8.6 15-crown-5: Na₄₃Al₄₃Si₁₄₉O₃₈₄: 120.6 H₂O.⁶ Similarly, losses of water (11.0 wt %) and 18-crown-6 (14.7 wt %) indicate a composition of 4.7 18-crown-6: Na₂₁Al₂₁Si₇₅O₁₉₂: 51.2 H₂O for EMT; previously reported unit cell compositions are 4.1 18-crown-6: Na_{18.5}Al_{18.5}Si_{77.5}O₁₉₂: 60.2 H₂O⁵ and 3.5 18-crown-6: Na₂₂Al₂₂Si₇₄O₁₉₂: 57.5 H₂O.⁶ Because there are two types of supercage in EMT, the observed weight fraction of 18-crown-6 corresponds to either one crown ether molecule in each large and small supercage,⁶ or to double occupation of the larger supercages with the smaller supercages remaining organic-free.⁵ Resolution of this issue should provide important information regarding the structure-directing activity of crown ethers since the presence of two 18-crown-6 molecules into one supercage, or the siting of crown ether molecules in two different supercage environments should have different implications for the relationship between the inorganic structure and the organic species during synthesis.

Raman Spectroscopy

Raman spectroscopy is used to characterize zeolite structures and occluded organic species. The Raman spectra of as-synthesized EMT and FAU are shown in Figures 4.3 and 4.4. Although the vibrations of individual oxide rings within the framework cannot be distinguished, the frequency of the Raman structural vibration (300–600 cm⁻¹) has been

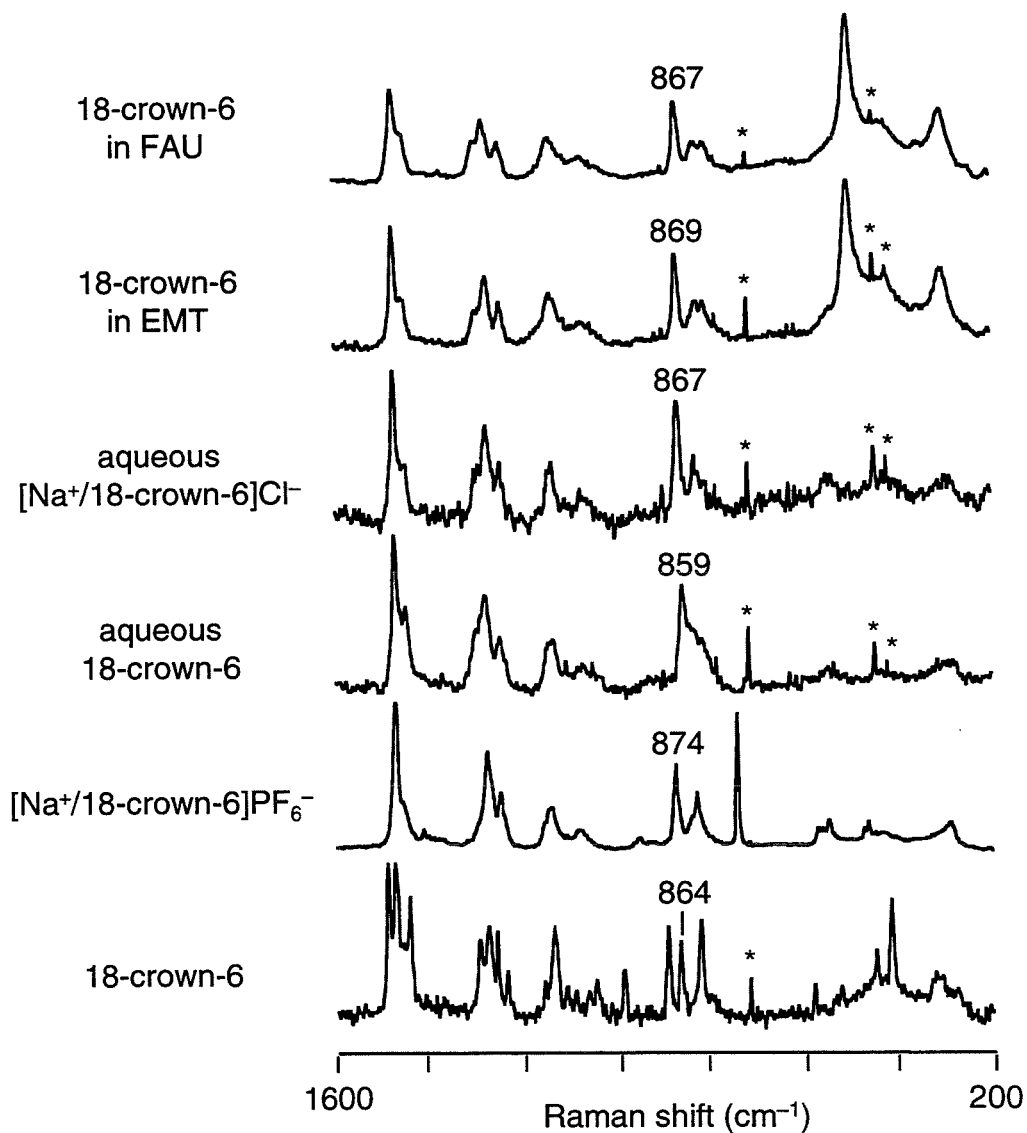


Figure 4.3. Raman spectra of 18-crown-6 in various environments. The structurally-indicative ring-breathing mode is labeled in each spectrum (* indicates Raman laser lines).

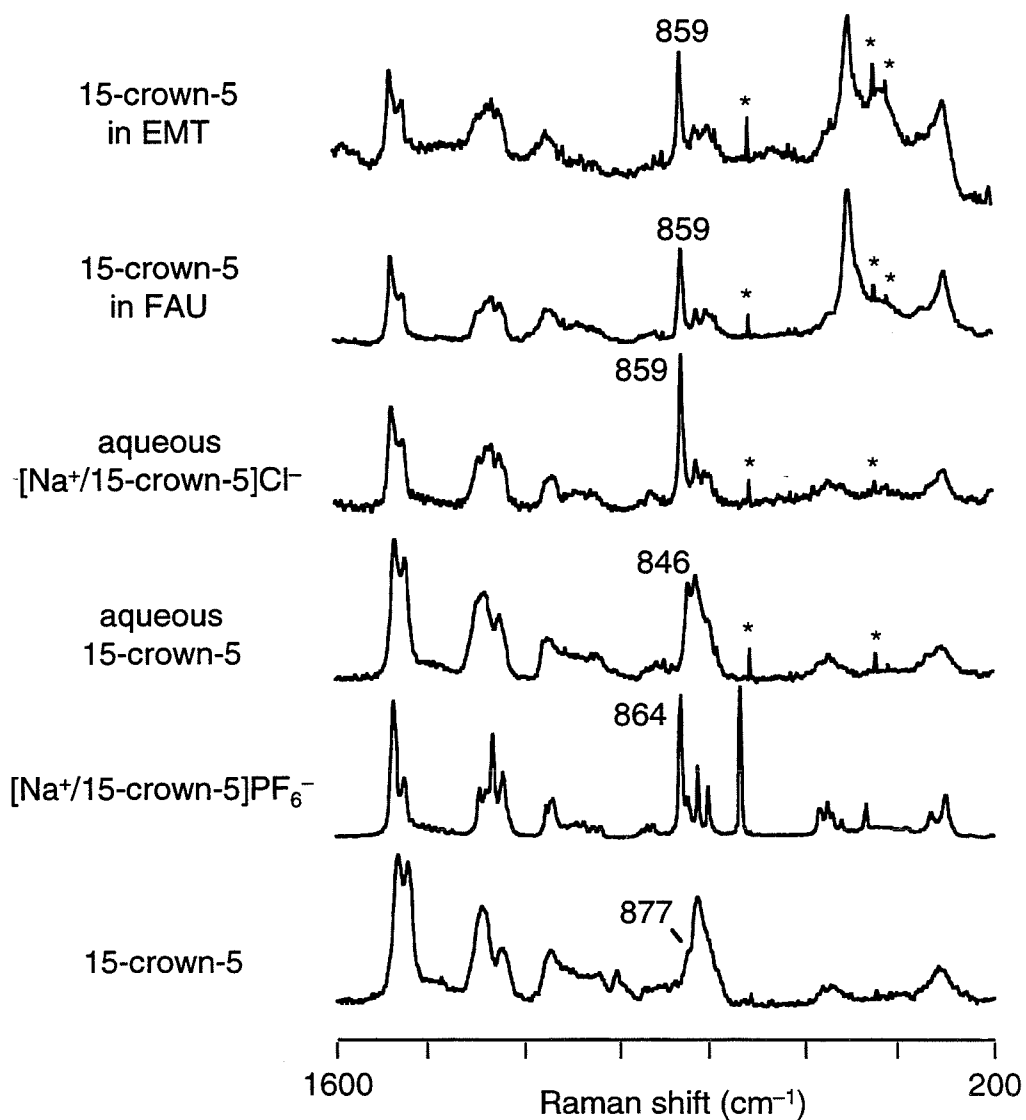


Figure 4.4. Raman spectra of 15-crown-5 in various environments. The structurally-indicative ring-breathing mode is labeled in each spectrum (* indicates Raman laser lines).

shown to correlate with the size of the smallest ring in the zeolite structure.^{20,21} The structural bands for FAU and EMT (500–503 cm^{-1}) correspond well to a minimum four T-atom (T=Si or Al) oxide ring, and indicate structural similarity between the two polymorphs, as is expected. The additional bands (800–1500 cm^{-1} and 3100–3200 cm^{-1}) in the as-made materials (which disappear upon calcination of the products) are vibrations from the occluded crown ethers.

15-Crown-5, 18-crown-6, and their alkali metal ion complexes exhibit characteristic vibrations in five regions: coupled CCO deformation and COC bending at 500–600 cm^{-1} ;²² coupled CO stretching and CH_2 rocking at 800–900 cm^{-1} ;²²⁻²⁴ CH_2 deformation and twisting in the 1200–1300 cm^{-1} region;^{22,25} the CH_2 scissor mode at 1400–1500 cm^{-1} ;^{22,25} and CH_2 stretching vibrations at 2800–3000 cm^{-1} .²⁶ A comparison of Raman spectroscopic data and crystal structural data has been used to assess the conformational flexibility of crown ethers,²²⁻³² although single crystal analyses do not indicate the exact conformations of molecules in solution. The most structurally-indicative Raman vibrations are the A_1 or A_{1g} ring-breathing mode at 840–900 cm^{-1} ;^{23,24} and the CH_2 scissor modes. The 1450 cm^{-1} band of the latter decreases in intensity relative to the 1477 cm^{-1} band when the crown ether forms complexes. The Raman shift of the ring-breathing frequency is sensitive to changes in conformation, and is considered to be a structural marker.

The Raman spectrum of 18-crown-6 in EMT is compared with the spectra of neat 18-crown-6, the solid sodium/crown ether complex ($[\text{Na}^+/\text{18-crown-6}] \text{PF}_6^-$), a 50 wt % aqueous solution of 18-crown-6 (crown ethers complex to water molecules in a manner similar to alkali cation binding),^{27,28} and a 50 wt % aqueous solution of the sodium/crown ether

complex ($[\text{Na}^+/\text{18-crown-6}] \text{Cl}^-$) (Figure 4.3). The spectrum of the aqueous sodium/crown ether complex most closely reproduces that of 18-crown-6 in EMT, particularly in the position of the $867\text{--}869 \text{ cm}^{-1}$ ring-breathing mode. Because EMT supercages contain a high concentration of water, this assignment appears reasonable. In addition, molecular mechanics calculations demonstrate a stabilizing effect of water molecules on the sodium/18-crown-6 complex.³³ The spectrum of 18-crown-6 occluded in FAU suggests that the conformation of 18-crown-6 is not sensitive to the supercage environment, and that the predominant influence on conformation is the immediate coordination sphere.

The Raman spectra of 15-crown-5 exhibit trends similar to those observed for 18-crown-6 (Figure 4.4). The $1446\text{--}1454 \text{ cm}^{-1}$ CH_2 scissor vibration decreases in intensity relative to the $1472\text{--}1477 \text{ cm}^{-1}$ vibration as the molecules form complexes, although alkali metal ion and water complexation are not as strong for 15-crown-5 as for 18-crown-6.^{27,34} The ring-breathing vibration occurs at 859 cm^{-1} for the aqueous sodium/crown ether complex, for 15-crown-5 in FAU, and for 15-crown-5 absorbed into EMT. Thus, for both 15-crown-5 and 18-crown-6, the organic species contained in the hydrated supercages is a cationic complex, analogous to alkylammonium compounds used in many zeolite syntheses.

The sodium binding constants for 15-crown-5 and 18-crown-6 in aqueous solution are 5.0 M^{-1} and 6.3 M^{-1} , respectively.³⁴ Estimating the void volume of a FAU supercage to be the volume of a 13 \AA diameter sphere (1150 \AA^3), and assuming that 20 sodium ions per unit cell are found in supercage sites,³⁵ the percentages of the sodium/15-crown-5 complex and free 15-crown-5 in as-synthesized FAU are calculated to be 10.8 wt % and 0.8 wt %, respectively. Therefore, at least 92% of the crown ether molecules

are most likely complexed to sodium. If it assumed that the total supercage void volume of two unit cells of EMT approximately equals the supercage void volume in one unit cell of FAU,⁶ and that the distribution of sodium ions is similar to that in FAU,³⁵ the corresponding quantities are 12.8 wt % and 0.8 wt %. Thus, at least 93% of the crown ether molecules most likely exist as sodium complexes. In each case, the concentration of free crown ether appears to be below the detection limit of Raman spectroscopy (approximately 1 wt %), and only the predominant, sodium-complexed species is observed.

To investigate the conformation of crown ether molecules during faujasite crystallization, the syntheses of FAU and EMT were followed using Raman spectroscopy. Complexation of sodium by the crown ethers was observed immediately upon gel preparation. No further changes in the crown ether vibrations were observed during synthesis, suggesting that the crown ethers remain complexed to sodium throughout the crystallization process. Organic species were present in the wet gels but were not incorporated into the washed, dried solids until crystallinity was observed by XRD and by Raman spectroscopy (Raman band at 500–503 cm^{-1}). These results suggest that no preorganization of the solid phase around the crown ethers occurs prior to the formation of long-range structure. Thus, these Raman studies are inconclusive regarding the structure-directing role of the sodium/crown ether complexes.

Raman spectra of the wet synthesis gel during crystallization showed the presence of the same oligomeric silicate and aluminosilicate species (531–536 cm^{-1} ; 485–487 cm^{-1} ; 432–434 cm^{-1} ; 420–550 cm^{-1}) that have been observed previously in crown ether-free syntheses of FAU,³⁶⁻³⁹ and in syntheses of zeolite A,⁴⁰⁻⁴² ZSM-5,⁴³ and mordenite.⁴⁴ No differences

between the FAU and EMT syntheses were apparent and no unique inorganic moieties or intermediate structures were detected. Thus, Raman spectroscopy does not provide information regarding the factors that control the synthesis of either FAU or EMT.

Liquid-Phase Absorption of Crown Ethers

Absorption experiments demonstrate that 18-crown-6 cannot enter the void space of calcined EMT at synthesis temperature and pressure. The crown ether is excluded on the basis of steric size. This implies that 18-crown-6 is incorporated during structure formation, i.e., the crown ether molecules must be in the supercage sites as they form. This suggests the existence of a specific, stabilizing interaction between the crown ether and the growing inorganic structure, i.e., a structure-directing role for 18-crown-6 in the synthesis of EMT. 18-Crown-6 is also size-excluded from calcined FAU. This suggests that in the synthesis of FAU with 18-crown-6 in the presence of a higher sodium hydroxide concentration, an interaction (perhaps electrostatic) between the organic and inorganic species facilitates the observed stoichiometric incorporation of crown ether per supercage, although the crown ether does not provide the primary structure-determining influence.

In contrast to the absorption results with 18-crown-6, 15-crown-5 can be absorbed into calcined FAU at synthesis temperature and pressure as the sodium/crown ether complex, at an occupation of one molecule per supercage. The absence of a tight fit between the organic species and the zeolite structure suggests that a true structure-directing effect may not be present. However, the size of the cationic sodium/crown ether complex may be partially responsible for the observed increase in the Si/Al ratio of

the product (relative to FAU synthesized at higher sodium hydroxide concentration in the absence of crown ether). The observation that 15-crown-5 can be absorbed into calcined EMT suggests that the difference in size between 15-crown-5 and 18-crown-6 may be a factor in the relationship between the zeolite structures and organic agents. However, the differences in sodium binding affinity³⁴ and sodium complex conformation^{30,32} of 15-crown-5 and 18-crown-6 may also be significant.

NMR Spectroscopy

NMR spectroscopy was used in an attempt to examine the different environments experienced by crown ethers occluded in the supercages of FAU and EMT, particularly in evaluating the distribution of 18-crown-6 molecules in EMT. ^1H - ^{13}C CP MAS NMR spectra of the hydrated or dehydrated zeolites show a single, narrow, isotropic resonance for 15-crown-5 in FAU (69.4 ppm) and for 18-crown-6 in EMT (70.0 ppm), confirming that the crown ethers are intact within the zeolite supercages.^{5,6} A comparison of the chemical shifts of the sodium/crown ether complexes (69.4 ppm for $[\text{Na}^+/\text{15-crown-5}] \text{PF}_6^-$; 69.9 ppm for $[\text{Na}^+/\text{18-crown-6}] \text{PF}_6^-$) to that of the uncomplexed crown ethers (71.3 ppm for 15-crown-5;⁵ 72.6 ppm for 18-crown-6) supports the results obtained from Raman spectroscopy that the crown ethers are complexed to sodium. In the ^1H - ^{13}C CP MAS NMR spectra, the isotropic chemical shifts are sensitive only to the type of crown ether, and not to the zeolite supercage structure (69.3 ppm for 15-crown-5 in EMT; 69.9 ppm for 18-crown-6 in FAU). In low-temperature ^1H - ^{13}C CP MAS NMR studies of 18-crown-6⁴⁵ and of the sodium complex,⁴⁶ individual carbon environments can be resolved. However, in the current study, no splitting is observed in the low-

temperature spectra of hydrated FAU/15-crown-5 and EMT/18-crown-6; in each case, the crown ether resonance undergoes homogeneous broadening with no change in isotropic chemical shift as the temperature is decreased to 210 K. This observation suggests that crown ether motion within the zeolite supercages is appreciable, although somewhat slowed at low temperature.

Static ^1H - ^{13}C CP NMR spectra provide information about chemical shift anisotropies.⁴⁷ For neat 18-crown-6, a broad asymmetric powder pattern is observed (Figure 4.5). The sodium complexes of 18-crown-6 and 15-crown-5 have narrower, more symmetric resonances than 18-crown-6. Molecules occluded in zeolites can be more mobile than in the solid phase, which is reflected in the narrowness of static NMR spectra of organic species in zeolite hosts compared to static NMR spectra of the neat organic materials.⁴⁷ However, the NMR spectra of fully-hydrated faujasite samples do not provide useful information because the observed asymmetry of the powder patterns most likely results from multiple hydration environments. For dehydrated samples, differences become apparent. For 18-crown-6 in dehydrated EMT, a broad, asymmetric pattern is observed, while 18-crown-6 in FAU produces a symmetric lineshape (Figure 4.6). Asymmetry is also evident in the spectrum of 18-crown-6 in an intergrowth of EMT and FAU obtained from a synthesis with 18-crown-6 and a higher concentration of sodium nitrate (*vide infra*). The asymmetry persists as the ^1H - ^{13}C CP contact time is varied, or when ^1H decoupling is used without ^1H - ^{13}C CP. Similarly, 15-crown-5 in FAU produces one symmetric peak, while 15-crown-5 absorbed into EMT is broadened asymmetrically (Figure 4.7). This suggests that the asymmetry observed for crown ethers occluded in EMT does not arise from slowed or

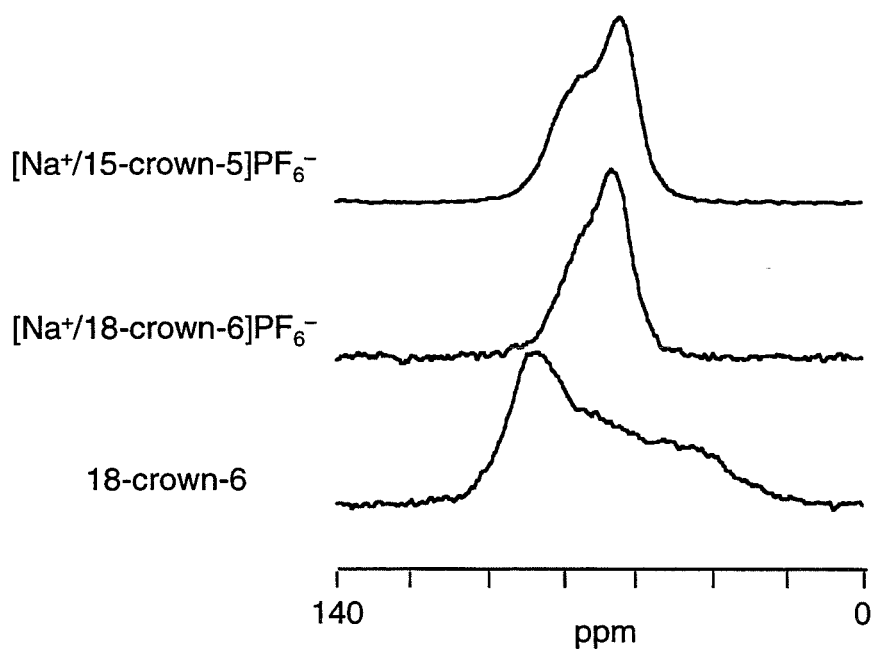


Figure 4.5. Static ^1H - ^{13}C CP NMR spectra of crown ethers.

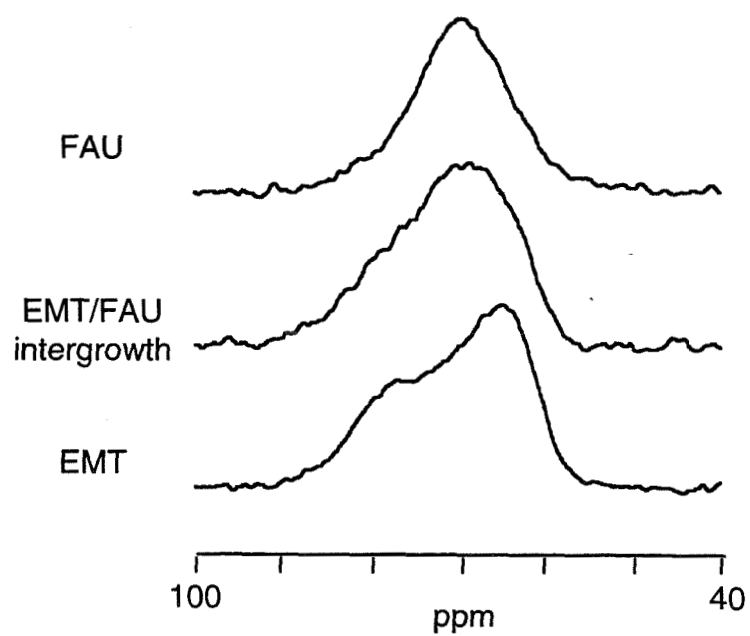


Figure 4.6. Static ^1H - ^{13}C CP NMR spectra of 18-crown-6 in dehydrated EMT and FAU.

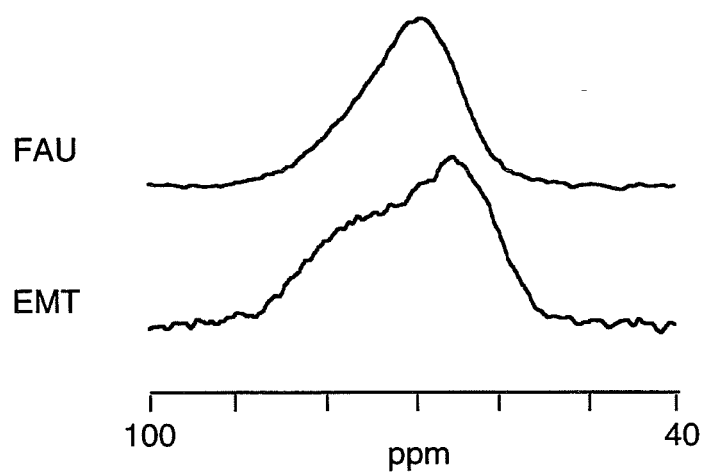


Figure 4.7. Static ^1H - ^{13}C CP NMR spectra of 15-crown-5 in dehydrated EMT and FAU.

restricted molecular motion (due to the fit of the organic molecule within the zeolite supercage) and is not unique to the 18-crown-6 molecule, but is instead due to the location of crown ethers in multiple environments.⁴⁸ Crown ethers occluded in FAU are exposed to a single supercage environment, while crown ethers in EMT can interact with more than one. The observation of asymmetry for 18-crown-6 in dehydrated EMT suggests that sodium/18-crown-6 complexes occupy both types of supercages in EMT. This conclusion was later confirmed by Rietveld refinement of the XRD pattern.⁴⁹

TGA, Raman, and NMR spectroscopies have demonstrated that the crown ether structure-directing agents in the synthesis of FAU and EMT are incorporated into the hydrated zeolite supercages as sodium/crown ether complexes, with one crown ether molecule in each supercage. The sodium/crown ether complexes are detected in the synthesis gels throughout the synthesis period but are not trapped in the solid material until long-range structure has been formed. In the synthesis of EMT, sodium/18-crown-6 molecules are incorporated into the crystalline product as the supercages are formed; for the 15-crown-5-mediated synthesis of FAU, a similar conclusion cannot be drawn. There are otherwise no detectable differences between the organic or inorganic components present in the crown ether-mediated syntheses of FAU and EMT. Thus, sodium/18-crown-6 complexes appear to serve as a structure-directing agent in the synthesis of EMT; the effect of sodium/15-crown-5 complexes on the structure-forming processes in the synthesis of FAU remains unclear.

Synthesis Variations

In order to investigate the roles of the organic and inorganic components in zeolite formation, syntheses involving systematic variation of these factors were performed. Variations included delayed times of addition of crown ethers, reduction of crown ether concentrations, the use of two crown ether structure-directing agents, the use of coronands and other macrocycles as organic additives, increases in sodium concentration, and the introduction of alkali metal ions other than sodium.

The time at which the crown ether was added to the synthesis gel was varied in order to determine whether structure direction occurs during gel aging, nucleation, or crystal growth. When 18-crown-6 was introduced after gel aging, nucleation and crystallization were not delayed: in the crown ether-mediated syntheses of FAU and EMT, crystals are first apparent by XRD after 2 days of heating, and crystallization is complete in 8 days. This suggests that the organic structure-directing agent is not involved in the aging process. However, when the crown ether was introduced after 1 or 2 days of heating of the organic-free gel (2.4 Na₂O), the onset of crystallization was delayed: EMT crystals were detected by XRD at 3 to 4 days of heating (2 days after crown ether addition), and crystallization was complete in 9 or 10 days (8 days after crown ether addition). After the addition of crown ether, crystal growth occurred at approximately the same rate as if the organic species were present during the entire heating period, and the products have the same chemical composition (Si/Al ratio and crown ether content). The delay in the onset of crystallization indicates that the crown ether is necessary for nucleation.

The roles of the crown ethers in the syntheses of FAU and EMT were investigated further through variations in the concentrations of the crown

ethers. Gel compositions that contained less than one equivalent of 15-crown-5 or 18-crown-6 (relative to Al_2O_3) gave the results summarized in Table 4.1. The amount of crown ether accommodated in fully-crystalline FAU or EMT with one crown ether molecule per supercage is 0.35 to 0.4 equivalents relative to Al_2O_3 in the gel (assuming 85–90% product yield). At crown ether concentrations of less than one equivalent, crystallization proceeded at the same rate and with the same product mass and Si/Al ratio until the concentration was slightly less than the threshold for one crown ether per supercage (0.3 equivalents). This result suggests that the presence of crown ether above the amount necessary for one molecule per supercage affects crystallization neither favorably nor adversely. At lower concentrations of crown ethers, different results were obtained. With 0.1 to 0.2 equivalents of 15-crown-5, crystallization of FAU was slowed. Using even lower concentrations of 15-crown-5, some FAU was synthesized, but the product contained some amorphous material; zeolite P (GIS) and an unidentified crystalline material were also produced. With 0.2 equivalents of 18-crown-6 (approximately half the amount necessary for one crown ether molecule per supercage), an intergrowth of FAU and EMT was crystallized at a slowed rate. A small amount of FAU was synthesized when 18-crown-6 was present at 0.1 equivalent or less, but an unidentified crystalline material and some amorphous material also resulted. The dependence on crown ether stoichiometry suggests that crown ethers play a critical role during crystal growth. The existence of a minimum amount of 15-crown-5 necessary for the synthesis of FAU ($2.4 \text{ Na}_2\text{O}$) suggests that the crown ether strongly influences structure formation. 18-Crown-6 appears to exhibit a structure-directing effect in the synthesis of EMT since in the absence of a sufficient concentration of 18-crown-6, a different yet

Table 4.1. Variations of Crown Ether Concentrations
in the Synthesis of FAU and EMT Zeolites

Gel Composition
x crown ether: 2.4 Na₂O: Al₂O₃: 10 SiO₂: 140 H₂O

<u>x</u>	<u>Product</u>	<u>Crystallization Time at 110 °C (days)</u>	<u>Wt % Crown Ether from TGA</u>	<u>Crown Ether Molecules Per Unit Cell</u>	<u>Si/Al ratio from ²⁹Si NMR Data</u>
15-crown-5					
1.0	FAU	8	13.5	8.0	3.6
0.8	FAU	12 ^a	14.6	8.0	3.7
0.6	FAU	12 ^a	15.0	8.0	3.7
0.4	FAU	12 ^a	9.2	7.2	3.5
0.3	FAU	12 ^a	10.4	8.0	3.5
0.2	FAU	15	8.2	6.2	3.6
0.1	FAU	30	6.4	—	—
0.05	FAU ^b	30	4.6	—	—
0.005	GIS ^{b,c}	45	—	—	—
0.0	GIS ^{b,c}	45	—	—	—
18-crown-6					
1.0	EMT	8	14.7	4.0	3.5
0.8	EMT	12 ^a	14.8	4.0	3.8
0.6	EMT	12 ^a	14.5	4.0	3.6
0.4	EMT	12 ^a	13.4	4.0	3.9
0.3	EMT	12 ^a	11.4	3.6	3.7
0.2	FAU ^d	25	9.1	2.9	—
0.1	FAU ^{b,c}	30	6.9	—	—
0.05	FAU ^{b,c}	30	—	—	—

^a Not analyzed prior to 12 days of heating.

^b Amorphous material present.

^c Small amount of an unidentified crystalline material.

^d Intergrowth containing a small amount of EMT.

related structure (FAU) is formed. Although the exact amount of 18-crown-6 needed for single occupation of the product supercages is not required for the synthesis of EMT, it is evident that in the presence of only half of this amount, no EMT is formed. The latter result suggests that both types of supercages must be occupied by 18-crown-6 molecules in order for EMT to be synthesized.

Systematic control of the relative amounts of the FAU and EMT end members present in intergrowths has been reported by several investigators.^{4,17,19,50} Intergrowths of varying domains of FAU and EMT can be obtained using synthesis mixtures containing different ratios of 15-crown-5 to 18-crown-6 at a total crown ether content of 1.0 equivalent (relative to Al_2O_3). The interpretation of these results is that 15-crown-5 and 18-crown-6 each preferentially stabilizes either the FAU or EMT structure; if there were no such preferences, a random stacking of faujasite sheets would be expected,¹⁷ but this is not observed experimentally. When the 15-crown-5 and 18-crown-6 structure-directing agents are not added simultaneously, rather one is present during the entire duration of the synthesis and the other is added after nucleation occurs, intergrowths of FAU and EMT are produced instead of the pure end members (Table 4.2). This result suggests that although some crown ether must be present in order for nucleation to occur, nucleation does not necessarily dictate the final structure of the product. Structure-directing agents are active during crystal growth as the inorganic units assemble to form the product structure.

The relative structure-directing efficacies of 15-crown-5 and 18-crown-6 have been noted: domains of EMT are observed by XRD only when 18-crown-6 constitutes at least half of the crown ether content of the

Table 4.2. Synthesis of Intergrowth Structures

Gel Composition
 X 15-crown-5: Y 18-crown-6: 2.4 Na₂O: Al₂O₃: 10 SiO₂: 140 H₂O^a

<u>(X+Y)</u>	<u>X</u>	<u>Y</u>	<u>Product</u>
0.2	0.1	0.1	FAU
0.4	0.2	0.2	FAU ^b
0.4	0.1	0.3	FAU ^b
0.6	0.3	0.3	FAU ^b
1.0 ^c	0.5	0.5	FAU+EMT ^d
1.0	0.5	0.5 ^e	FAU+EMT ^d
1.0	0.5 ^e	0.5	EMT+FAU ^d

a Heated for 12 days at 110 °C

b Intergrowth containing a small amount of EMT.

c Reference 19.

d Intergrowth; end members listed in order of decreasing amount present.

e Added after 4 days of heating.

gels containing a total crown ether content of 1.0 equivalent. At lower concentrations of 18-crown-6 (<0.5 equivalents), domains of a few unit cells of EMT may be present but are not detectable by XRD.^{17,19} In these systems it appears that there is a critical 18-crown-6 concentration threshold for the synthesis of EMT, similar to the syntheses involving low concentrations of a single crown ether species (*vide supra*). The use of less than one total equivalent of crown ether in mixed crown ether systems corroborates this idea (Table 4.2). In the absence of a sufficient amount of 18-crown-6 for the synthesis of domains of EMT, the effect of 15-crown-5 predominates. Only when 18-crown-6 is present in at least half the amount required for stoichiometric supercage occupation (>0.2 equivalents) is an appreciable domain of the EMT polymorph produced in an intergrowth. This result suggests the necessity of the presence of 18-crown-6 in both types of supercages for the synthesis of EMT.

In order to further investigate the physicochemical properties of 15-crown-5 and 18-crown-6 that are significant to structure direction, the influence of related organic molecules was also investigated. These species are divided into three categories: 1) heteroatom-substituted coronands such as S₆-18-crown-6, N₂-18-crown-6, and N₆-18-crown-6; 2) acyclic analogues of crown ethers such as TEGDME, TEG, and PEG; and 3) sodium-complexing agents such as dibenzo-18-crown-6,³⁴ α -cyclodextrin,⁵¹ and Kryptofix 2.2.2 cryptand.⁵² Delprato and coworkers report that S₆-18-crown-6, N₂-18-crown-6, N₆-18-crown-6, and Kryptofix 2.2.2 do not form FAU, EMT, or other crystalline products from a gel containing 2.4 Na₂O.^{4,5} Consequently, the approach taken in the current study was first to add the organic species to a gel containing a higher

concentration of sodium hydroxide (3.1 Na₂O) than that employed by Delprato and coworkers,⁵ which forms FAU in the absence of crown ether structure-directing agents. If the synthesis of FAU under these conditions was not disrupted by the presence of the organic species, the species was then added to a gel containing a lower sodium concentration (2.4 Na₂O) to determine whether it exhibits a structure-directing influence for FAU or EMT (Table 4.3).

Coronands such as S₆-18-crown-6, N₂-18-crown-6, and N₆-18-crown-6 do not form complexes with alkali metal ions.^{53,54} FAU was not formed from gels containing S₆-18-crown-6 or N₆-18-crown-6 (3.1 Na₂O), but FAU was crystallized from a similar gel when N₂-18-crown-6 was present (Table 4.3). The explanation for the differing results among the three organic species is not understood. However, from the results of Delprato and coworkers,⁵ it appears that structure direction does not simply result from shape and a space-filling effect of the organic species. Sodium complexation by the crown ether may be essential to its role in structure direction, due either to the effect of modulating the sodium concentration of the gel or to the establishment of an electrostatic attraction between the cationic structure-directing moiety and the anionic inorganic material.

Acyclic crown ether analogues (TEGDME, TEG, and PEG) were also used to probe the effects of shape and sodium-binding affinities of structure-directing agents. Acyclic ethers are less conformationally constrained than cyclic analogues and show only weak sodium binding affinities.⁵⁵⁻⁵⁷ The gels (3.1 Na₂O) containing acyclic ethers produced only small amounts of FAU with no occluded organic molecules (Table 4.3). The acyclic ethers appear to have disrupted the crystallization of FAU,

Table 4.3. Syntheses Involving Organic Components

Gel Composition					
R: (2.4+n) Na ₂ O: Al ₂ O ₃ : 10 SiO ₂ : 140 H ₂ O ^a					
<u>R</u>	<u>n</u>	Na ₂ O <u>Source</u>	<u>Product</u>	Wt % R <u>from TGA</u>	Si/Al ratio from ²⁹ Si <u>NMR Data</u>
No Organic Agent					
–	0	–	FAU, GME ^{b,c,d}	–	–
–	0.7	NaOH	FAU ^e	–	2.9
Crown Ether-Shaped Molecules					
S ₆ –18-crown-6 ^f	0	–	amorphous	–	–
S ₆ –18-crown-6	0.7	NaOH	GIS, GME ^b	0	–
N ₂ –18-crown-6 ^f	0	–	amorphous	–	–
N ₂ –18-crown-6	0.7	NaOH	FAU, GIS, GME ^b	4.9	–
N ₆ –18-crown-6 ^f	0	–	amorphous	–	–
N ₆ –18-crown-6	0.7	NaOH	amorphous	–	–
Acyclic Polyethylene Glycols					
TEGDME	0.7	NaOH	GIS, FAU, GME ^b	0	–
TEG	0.7	NaOH	FAU, GME, GIS ^b	0	–
PEG	0.7	NaOH	amorphous	–	–
Sodium-Binding Compounds					
Kryptofix 2.2.2	0	–	FAU	13.2	3.7
Kryptofix 2.2.2	0.7	NaOH	FAU	8.2	3.1
dibenzo–18-crown-6 ^f	0	–	amorphous	–	–
dibenzo–18-crown-6	0.7	NaOH	amorphous ^g	0	–
α-cyclodextrin	0	–	amorphous	–	–
α-cyclodextrin	0.7	NaOH	FAU	0	–

^a Heated for 12 days at 110 °C

^b Listed in order of decreasing amount present.

^c Amorphous material present.

^d Heated for 18 days at 110 °C.

^e Heated for 4 days at 110 °C.

^f Reference 5.

^g Small amount of unidentified crystalline material

perhaps due to interaction and interference of the long, flexible ether chain with the assembling inorganic units. The acyclic ethers are not occluded perhaps because they are not cationic species.

The question whether sodium complexation by an organic species is a sufficient condition for structure-directing ability was addressed through the use of sodium binding agents other than 15-crown-5 and 18-crown-6 (Table 4.3). Dibenzo-18-crown-6 appeared to interfere with the synthesis of FAU (3.1 Na₂O), perhaps due to size or to poor solubility in water. α -Cyclodextrin decomposed but did not perturb the synthesis of FAU (3.1 Na₂O). At a lower sodium concentration (2.4 Na₂O), α -cyclodextrin also decomposed and thus exhibited no structure-directing influence, and no crystalline material was produced. However, Kryptofix 2.2.2 did not interfere with the crystallization of FAU at a higher sodium concentration. In contrast to the results reported by Delprato and coworkers,⁵ the presence of Kryptofix 2.2.2 resulted in the synthesis of FAU at both the higher (3.1 Na₂O) and lower (2.4 Na₂O) concentrations of sodium, but no EMT was evident in the product. The Raman spectra in Figure 4.8 demonstrate that sodium/Kryptofix 2.2.2 complexes are incorporated into the supercages of FAU. TGA results indicate that 75% of the supercages in FAU synthesized at the lower sodium concentration are occupied by the cryptate complex, and that 45% of the supercages are occupied in FAU prepared at the higher sodium concentration. In contrast to the Raman results for 15-crown-5 and 18-crown-6, the position of the structurally-indicative 840–855 cm⁻¹ vibration of Kryptofix 2.2.2 in FAU corresponds most closely to that of the sodium/Kryptofix 2.2.2 complex, rather than to the aqueous sodium/Kryptofix 2.2.2 species. This result suggests that water molecules are not strongly associated with sodium/Kryptofix 2.2.2

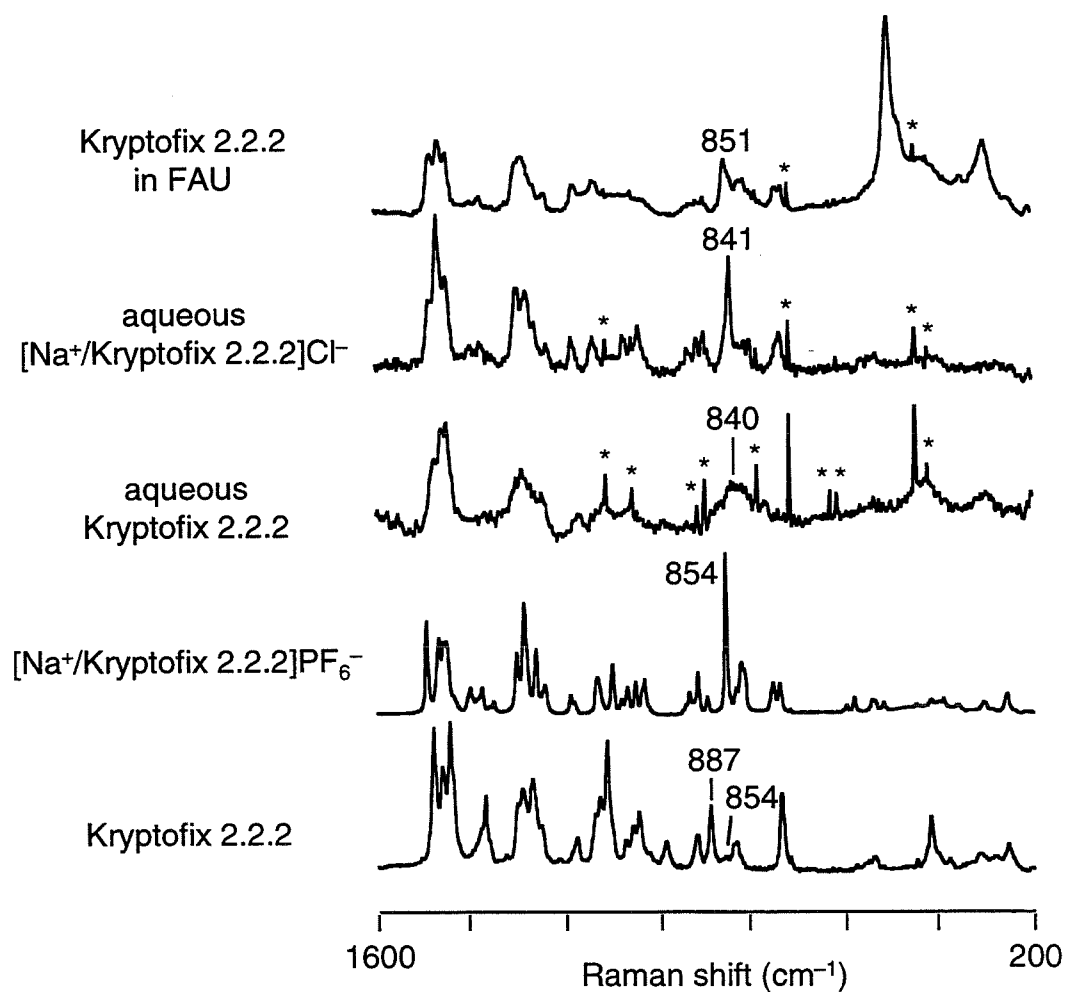


Figure 4.8. Raman spectra of Kryptofix 2.2.2 in various environments. The structurally-indicative ring-breathing mode is labeled in each spectrum (* indicates Raman laser lines).

complexes or are excluded from the supercages that are occupied by the cryptate, probably due to the size of the organic species. The similarity of Kryptofix 2.2.2 to 15-crown-5 and 18-crown-6 in sodium-binding affinity and in shape suggests that both of these factors are important in the synthesis of the polymorphs of faujasite. However, the observation that no EMT was synthesized in the presence of Kryptofix 2.2.2 suggests that the synthesis of EMT is specific to both the shape and the sodium-binding affinity of 18-crown-6.

The balance between the product-forming tendencies of the organic and inorganic components in the synthesis mixtures was investigated through competition experiments. Gels were formulated to contain both 18-crown-6 (1.0 equivalents) and sodium (3.1 Na₂O), each at a concentration sufficient to promote crystallization of EMT or FAU, respectively (Table 4.4). The structure-directing ability of sodium exhibits a counterion dependence, most likely due to changes in synthesis gel alkalinity (pH≈12 in the original synthesis gel). Consequently, the effect of a higher sodium concentration (i.e., in excess of 2.4 Na₂O) was examined using hydroxide or nitrate counterions. Sodium hydroxide was required as the source of additional sodium (3.1 Na₂O total) for the crystallization of FAU in the absence of 15-crown-5.^{5,6} When sodium nitrate was used in the absence of crown ether, a partially crystalline product that contained no faujasite was obtained.

When both 18-crown-6 and a higher sodium concentration (3.1 Na₂O) were present in the synthesis gel, the use of sodium hydroxide produced FAU with 18-crown-6 occluded at a level of one crown ether molecule per supercage (Table 4.4). Under these conditions, the tendency to form FAU (due to structure direction by sodium) masks the structure-directing effect

Table 4.4. Structure-Directing Effects of Sodium and Crown Ethers

Gel Composition R: (2.4+n) Na ₂ O: Al ₂ O ₃ : 10 SiO ₂ : 140 H ₂ O ^a					
<u>n</u>	Source of <u>n Na₂O</u>	<u>R</u>	<u>Product</u>	<u>Wt % R from TGA</u>	<u>Si/Al ratio from ²⁹Si NMR Data</u>
0	–	none	FAU, GME ^{b,c,d}	–	–
0	–	18-crown-6	EMT	14.7	3.5
0	–	15-crown-5	FAU	13.5	3.6
0.35	NaOH	18-crown-6	FAU+EMT ^e	16.5	3.3
0.35	NaNO ₃	18-crown-6	EMT	12.9	3.6
0.7	NaOH	none	FAU ^f	–	2.9
0.7	NaNO ₃	none	unidentified ^{c,d}	–	–
0.7	NaOH	18-crown-6	FAU	15.8	2.8
0.7	NaNO ₃	18-crown-6	FAU+EMT ^e	10.7	3.3
0.7	NaOH	15-crown-5	FAU	9.3	3.0
0.7	NaNO ₃	15-crown-5	FAU	12.2	>3.0
1.4	NaOH	18-crown-6	FAU	11.5	2.6

a Heated for 12 days at 110 °C

b Listed in order of decreasing amount present.

c Amorphous material present.

d Heated for 18 days at 110 °C.

e Intergrowth; end members listed in order of decreasing amount present.

f Heated for 4 days at 110 °C.

of 18-crown-6. The Si/Al ratio of the product correlates with the sodium concentration used; a higher concentration of sodium produces FAU with a lower Si/Al ratio. At an intermediate concentration of sodium hydroxide (2.75 Na₂O), the structure-directing effects of both sodium and 18-crown-6 were evident in the resulting intergrowth of FAU and EMT. An intergrowth containing FAU and EMT, with one 18-crown-6 molecule per supercage, was also obtained when sodium nitrate was the sodium source. The relative amount of FAU present in the intergrowth structure, as indicated qualitatively by the peak intensities in the $5^{\circ} \leq 2\theta \leq 7^{\circ}$ region of the XRD pattern, correlates with the amount of sodium used. Thus, at the gel alkalinities afforded by the use of non-hydroxide counterions, 18-crown-6 and sodium have similar efficacies in influencing product formation. There is a subtle competition between the tendency of sodium to produce FAU and the structure-directing effect of 18-crown-6 in the formation of EMT. EMT is synthesized only within narrow constraints of sodium concentration, gel alkalinity, and 18-crown-6 concentration. In most cases, the formation of FAU is favored.

When both 15-crown-5 and a high sodium concentration were present in the gel, the use of sodium hydroxide as the sodium source yielded FAU with 15-crown-5 occluded in each supercage (Table 4.4). With sodium nitrate as the sodium source, crystallization was slowed, but FAU with occluded 15-crown-5 was produced. Although the structure-directing influences of 15-crown-5 and sodium are indistinguishable in this case, it appears that there is an interaction between the organic species and the zeolite structure which facilitates incorporation of 15-crown-5 into the supercages of FAU, although the crown ether does not function as the sole structure-directing agent in this synthesis.

The effects of alkali metal ions on zeolite gel chemistry are well documented.^{14,58-61} These cations influence the aluminosilicate and silicate equilibria in the gel. Alkali metal ions also affect the structure of water within the gel: Li^+ and Na^+ are considered structure-forming relative to bulk water due to the small size and tight, hydrophilic hydration sphere; K^+ , Rb^+ , and Cs^+ are structure-breaking because of the less-ordered, hydrophilic hydration sphere. The effects of alkali metal ions on the chemistry of gels that contained 2.4 Na_2O are summarized in Table 4.5. The introduction of 0.7 K_2O , Rb_2O , or Cs_2O to the synthesis mixture significantly alters the gel chemistry such that the products formed are zeolites normally synthesized in the presence of these non-sodium alkali cations. In syntheses involving both 18-crown-6 and alkali metal ions, the crown ether does not act as a structure-directing agent. That is, the same zeolite products are formed as in the absence of 18-crown-6, and crown ether molecules are accommodated within the structure only if the cages are sufficiently large. The influence of the alkali metal ions dominates the gel chemistry, and the significance of the differences in conformation^{30,31} and strengths of ion binding³⁴ among the alkali metal ion/18-crown-6 complexes is not clear. The balance between inorganic and organic structure-directing factors in the syntheses of FAU and EMT is perturbed by the presence of alkali metal ions other than sodium; the structure-directing effects of these cations determine product formation.

Proposed Mechanism

15-Crown-5 and 18-crown-6 are involved in the nucleation and

Table 4.5. Structure-Directing Effects of Alkali Metal Ions and Crown Ethers

Gel Composition
R: 2.4 Na₂O: n M₂O: Al₂O₃: 10 SiO₂: 140 H₂O^a

<u>Source of M</u>	<u>n</u>	<u>R</u>	<u>Product</u>	<u>Wt % R from TGA</u>
LiOH	0.7	none	amorphous	—
LiCl	0.7	none	amorphous	—
LiOH	0.7	18-crown-6	amorphous	—
LiCl	0.7	18-crown-6	amorphous	—
KOH	0.7	none	CHA	—
KNO ₃	0.7	none	OFF	—
KOH	0.7	18-crown-6	CHA, OFF ^b	0
KNO ₃	0.7	18-crown-6	OFF	0
RbOH	0.7	none	OFF	—
RbNO ₃	0.7	none	OFF	—
RbOH	0.7	18-crown-6	OFF	0
Rb(CH ₃ CO ₂ ⁻)	0.7	18-crown-6	OFF	0
CsOH	0.7	none	ANA	—
CsNO ₃	0.7	none	RHO	—
CsOH	0.7	18-crown-6	ANA	0
CsNO ₃	0.7	18-crown-6	RHO	8.6
CsNO ₃	0.7	15-crown-5	RHO	6.3

^a Heated for 12 days at 110 °C

^b Listed in order of decreasing amount present.

crystallization processes in the syntheses of FAU and EMT. During crystallization of these polymorphs of faujasite, crown ether structure-directing agents are occluded into the hydrated zeolite supercages as sodium/crown ether complexes, at loadings of up to one crown ether molecule per supercage in both FAU and EMT. In order for FAU to be synthesized ($2.4 \text{ Na}_2\text{O}$), a small amount of 15-crown-5 (≥ 0.1 equivalent relative to Al_2O_3) must be present in the gel; the addition of Kryptofix 2.2.2 can also bring about the synthesis of FAU. However, for the synthesis of EMT, a larger amount of 18-crown-6 must be present: although EMT can be synthesized when slightly less 18-crown-6 than is sufficient for single occupation of the product supercages is present, reduction of the 18-crown-6 concentration to one molecule per two supercages results in no formation of EMT. These lower limits on crown ether concentration are also observed for the synthesis of intergrowths of FAU and EMT using both 15-crown-5 and 18-crown-6 as structure-directing agents. At lower crown ether concentrations, only a small amount of crystalline FAU and an unidentified material are produced.

The syntheses of FAU and EMT require the presence of sodium in the gel. Other alkali metal ions significantly alter the gel chemistry, resulting in products other than faujasite. The synthesis of pure EMT requires the presence of 18-crown-6 as the structure-directing agent; acyclic ethers appear to inhibit crystallization of FAU and EMT, while non-sodium-binding coronands and non-crown-shaped sodium-binding moieties do not produce any EMT. A delicate balance of the structure-directing effects of 18-crown-6 (EMT) and of high concentrations of sodium (FAU) is present, and intergrowths of the two end members can result from the presence of both structure-directing agents.

In a recent paper, Vaughan discusses the sheet and columnar structural relationships between sodium- and potassium-specific zeolite products, respectively.¹⁴ Among the products synthesized from gels of composition 2–4 Na₂O: 0–1 M₂O: 1 Al₂O₃: 6–15 SiO₂: 100–200 H₂O (M=alkali metal or alkylammonium ion), Vaughan identifies the faujasite sheet as the common structural feature. The inversion center between faujasite sheets within the FAU structure is related to the mirror plane in the EMT structure by a 60° rotation of one faujasite sheet. The ABCABC stacking of faujasite sheets in FAU seems to be favored in the absence of another strong structure-directing influence. The presence of large cations such as Cs⁺ or hydrated Li⁺ appears to cause a high incidence of twinned sheets, which produces small domains of the EMT structure.

Vaughan's analysis provides a context in which to evaluate the present synthesis results. The large, cationic sodium/18-crown-6 complex may serve to systematically disrupt the arrangement of faujasite sheets from the otherwise more favored FAU arrangement to form the EMT structure. The repeated twinning of faujasite sheets in the EMT structure could be facilitated by a specific stabilizing interaction between the sodium/18-crown-6 complex and the anionic surface of the growing crystallite, which would result in the presence of the crown ether complexes in the supercage sites as the latter are formed. The observation by Lievens and coworkers that "pure" EMT contains small domains of FAU is consistent with a finite probability of sheet mis-stacking.³⁵ In view of the evidence from static ¹H–¹³C CP NMR (and later confirmed by Rietveld refinement of the XRD pattern)⁴⁹ that there is one 18-crown-6 molecule in every supercage of EMT, and from the observed dependence of synthesis on 18-crown-6 concentration, it is proposed that the presence of

the sodium/18-crown-6 complex in the smaller supercage site is essential to the synthesis of EMT. Molecular modeling of this species in the smaller supercage demonstrates that the supercage is of sufficient size to accommodate the crown ether complex (Figure 4.9). Additionally, the ring of six oxygen atoms in the crown ether and the six T-atom oxide ring in the smaller EMT supercage are of similar size, and may suggest a mode of interaction of the sodium/18-crown-6 complex as a sandwich-like complex with the zeolite surface during crystal growth. Results from the Rietveld refinement of the XRD pattern provide support for this model.⁴⁹

Although FAU can be synthesized in the absence of crown ether, formation of this structure appears to be facilitated by the sodium complex of 15-crown-5 or of Kryptofix 2.2.2. The most notable difference between FAU synthesized with an organic structure-directing agent and FAU synthesized in the presence of a higher sodium hydroxide concentration is the higher Si/Al ratio of the former. This trend is consistent with previous work in the synthesis of silicon-rich zeolites using alkylammonium ions.¹ However, an additional influence such as a stabilizing interaction of the 15-crown-5 with the growing FAU crystal must be considered in order to explain the observed dependence on 15-crown-5 concentration. Despite the evidence from liquid-phase absorption and static ^1H - ^{13}C CP NMR that there is not a tight fit between 15-crown-5 and the FAU supercage, it appears that there is some structural specificity of 15-crown-5 to the synthesis of FAU: the large domains of the FAU and EMT end members present in the mixed crown ether intergrowth structures vary systematically with the ratio of crown ethers. If sheet stacking were random, the XRD patterns of the intergrowth structures would exhibit only two reflections in the $5^\circ \leq 2\theta \leq 7^\circ$ region, rather than the observed three

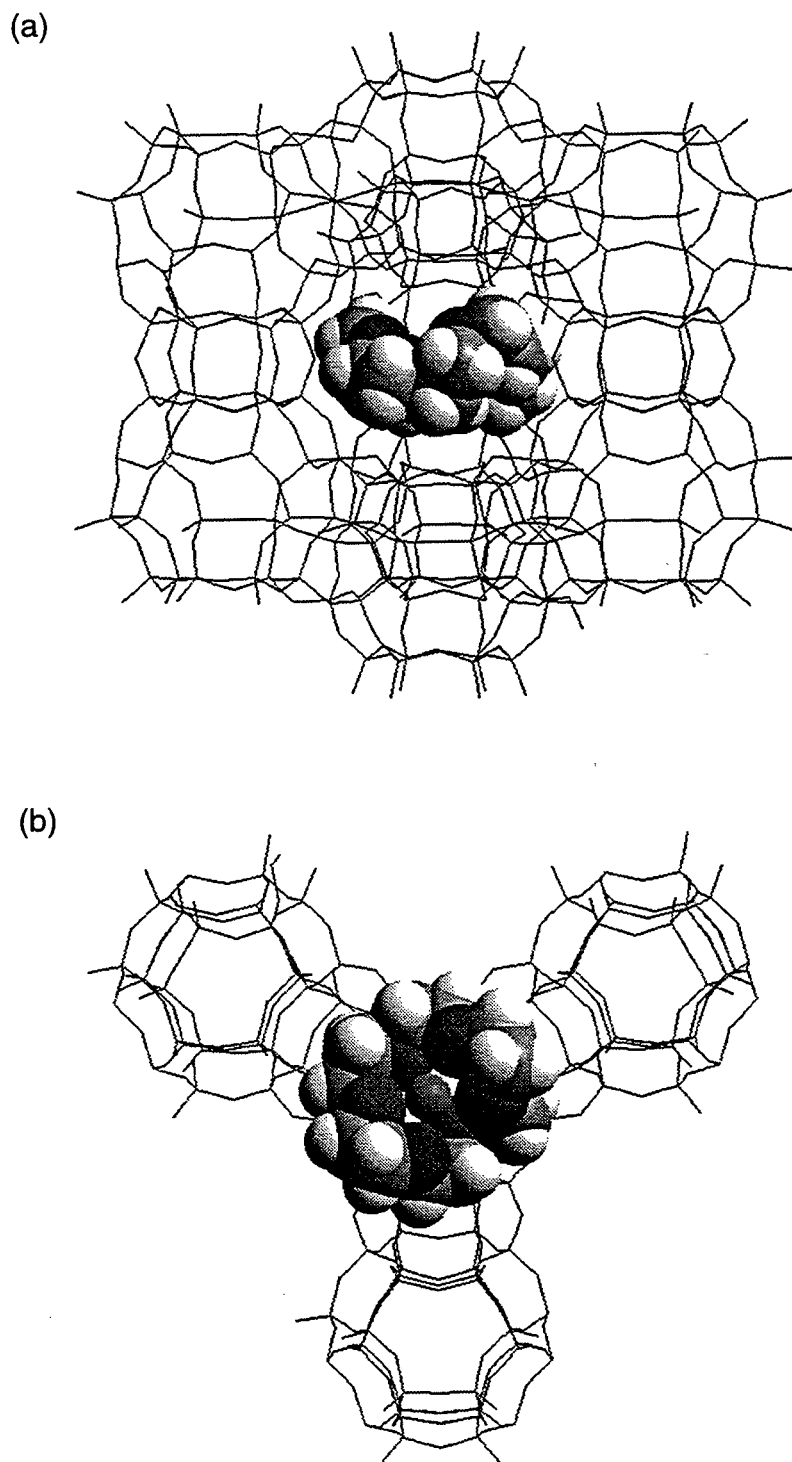


Figure 4.9. Sodium/18-crown-6 complex in the smaller supercage of EMT. View from an adjacent larger supercage through the elliptical aperture (a); view from the top of the supercage (b).

overlapping reflections of FAU and EMT.^{17,19} Thus, it appears that both the cationic nature and the shape of the organic species are important for structure direction in the faujasite system.

In the present interpretation, it is implied that crystallization of FAU and EMT occurs as a layer-by-layer stacking of pre-formed faujasite sheets or ordered aluminosilicate network structures. Structures on the length scale of 10–100 Å are not detectable by conventional techniques such as NMR, Raman spectroscopy, or X-ray diffraction.⁶² Some evidence for the existence of extended structures has been provided by small-angle neutron scattering (SANS) studies on the synthesis of ZSM-5 via a solid hydrogel transformation mechanism.⁶² However, Vaughan suggests that extended structures may not be observed in a system that involves synthesis by solution-mediated transport (such as faujasite)⁶³ since these structures may be consumed immediately upon formation.¹⁴ However, extended structures have also been observed by small-angle X-ray scattering (SAXS) early in the synthesis of zeolite A, which occurs by a solution-mediated process.⁶⁴ Investigation of faujasite synthesis by SANS or SAXS techniques remains to be undertaken. However, these techniques can only demonstrate the existence of extended structures, and cannot determine their identity.

A mechanism involving the assembly of extended structures is thus proposed for the crown ether-mediated syntheses of FAU and EMT; however, these structures are not necessarily faujasite sheets. The sodium/crown ether complexes facilitate the arrangement of sodium-templated, aluminosilicate networks into the FAU and EMT structures. An interaction of the sodium/15-crown-5 complex or the sodium/ 18-crown-6 complex with the surfaces of growing FAU or EMT crystals is

implicated. For the synthesis of EMT in particular, a sandwich-like interaction between the sodium/18-crown-6 complex and the six T-atom oxide ring in the smaller supercage of EMT is postulated. Only when a majority of the surface sites are occupied by sodium/18-crown-6 complexes is the EMT stacking of faujasite sheets favored; otherwise, the FAU stacking is the preferred arrangement. The present results are consistent with the proposed mechanism, although faujasite sheets and crown ether complex interactions with the crystallite surface have not been observed directly.

References

- (1) Barrer, R. M.; Denny, P. J. *J. Chem. Soc.* **1961**, 971.
- (2) Davis, M. E.; Lobo, R. F. *Chem. Mater.* **1992**, *4*, 756.
- (3) Lok, B. M.; Cannan, T. R.; Messina, C. A. *Zeolites* **1983**, *3*, 282.
- (4) Delprato, F.; Guth, J. L.; Anglerot, D.; Zivkov, C. (S. N. E. A.). Eur. Patent 364 352 A1, 1989; *Chem. Abstr.* **1990**, *113*, P66294g.
- (5) Delprato, F.; Delmotte, L.; Guth, J. L.; Huve, L. *Zeolites* **1990**, *10*, 546.
- (6) Annen, M. J.; Young, D.; Arhancet, J. P.; Davis, M. E.; Schramm, S. *Zeolites* **1991**, *11*, 98.
- (7) Moore, P. B.; Smith, J. V. *Mineral. Mag. J. Mineral. Soc.* **1964**, *34*, 1008.
- (8) Kokotailo, G. T.; Ciric, J. In *Molecular Sieve Zeolites I*; E. M. Flanigen and L. B. Sand, Eds.; American Chemical Society: Washington, DC, 1971; pp 109.
- (9) Ernst, S.; Kokotailo, G. T.; Weitkamp, J. *Zeolites* **1987**, *7*, 180.
- (10) Newsam, J. M.; Treacy, M. M. J.; Vaughan, D. E. W.; Strohmaier, K. G.; Mortier, W. J. *J. Chem. Soc., Chem. Commun.* **1989**, 493.
- (11) Ciric, J. (Mobil Oil Corp.). U.S. Patent 3 411 874, 1968; *Chem. Abstr.* **1969**, *70*, P21412w.
- (12) Ciric, J. (Mobil Oil Corp.). U.S. Patent 3 692 470, 1972; *Chem. Abstr.* **1973**, *78*, P6032u.
- (13) Baerlocher, C. *Acta Crystallogr., Sect. A* **1990**, *46*, C177.
- (14) Vaughan, D. E. W. In *Catalysis and Adsorption by Zeolites*; G. Ohlmann, Ed.; Elsevier: Amsterdam, 1991; pp 275.
- (15) Thomas, J. M.; Audier, M.; Klinowski, J. *J. Chem. Soc., Chem. Commun.* **1981**, 1221.

- (16) Audier, M.; Thomas, J. M.; Klinowski, J.; Jefferson, D. A.; Bursill, L. *A. J. Phys. Chem.* **1982**, *86*, 581.
- (17) Anderson, M. W.; Pachis, K. S.; Prébin, F.; Carr, S. W.; Terasaki, O.; Ohsuna, T.; Alfreddson, V. *J. Chem. Soc., Chem. Commun.* **1991**, 1660.
- (18) Vaughan, D. E. W.; Treacy, M. M. J.; Newsam, J. M.; Strohmaier, K. G.; Mortier, W. J. In *Zeolite Synthesis*; M. L. Occelli and H. E. Robson, Eds.; American Chemical Society: Washington, DC, 1989; pp 544.
- (19) Arhancet, J. P.; Davis, M. E. *Chem. Mater.* **1991**, *3*, 567.
- (20) Dutta, P. K.; Shieh, D. C.; Puri, M. *Zeolites* **1988**, *8*, 306.
- (21) Dutta, P. K.; Rao, K. M.; Park, J. Y. *J. Phys. Chem.* **1991**, *95*, 6654.
- (22) Fukuhara, K.; Ikeda, K.; Matusuura, H. *J. Mol. Struct.* **1990**, *224*, 203.
- (23) Sato, H.; Kusumoto, Y. *Chem. Lett.* **1978**, 635.
- (24) Takeuchi, H.; Arai, T.; Harada, I. *J. Mol. Struct.* **1986**, *146*, 197.
- (25) Miyazawa, M.; Fukushima, K.; Oe, S. *J. Mol. Struct.* **1989**, *195*, 271.
- (26) Zhelyaskov, V.; Georgiev, S.; Nickolov, C.; Miteva, M. *Spectrosc. Lett.* **1989**, *22*, 15.
- (27) Fukushima, K.; Ito, M.; Sakurada, K.; Shiraishi, S. *Chem. Lett.* **1988**, 323.
- (28) Matsuura, H.; Fukuhara, K.; Ikeda, K.; Tachikake, M. *J. Chem. Soc., Chem. Commun.* **1989**, 1814.
- (29) Dunitz, J. D.; Seiler, P. *Acta Crystallogr., Sect. B* **1974**, *30*, 2739.
- (30) Dobler, M.; Dunitz, J. D.; Seiler, P. *Acta Crystallogr., Sect. B* **1974**, *30*, 2741.
- (31) Seiler, P.; Dobler, M.; Dunitz, J. D. *Acta Crystallogr., Sect. B* **1974**, *30*, 2744.
- (32) Groth, P. *Acta Chem. Scand. A* **1981**, *35*, 721.
- (33) Wipff, G.; Weiner, P.; Kollman, P. *J. Am. Chem. Soc.* **1982**, *104*, 3249.

- (34) Izatt, R. M.; Terry, R. E.; Haymore, B. L.; Hansen, L. D.; Dalley, N. K.; Avondet, A. G.; Christensen, J. J. *J. Am. Chem. Soc.* **1976**, *98*, 7620.
- (35) Lievens, J. L.; Verduijn, J. P.; Bons, A. J.; Mortier, W. J. *Zeolites* **1992**, *12*, 698.
- (36) Dutta, P. K.; Shieh, D. C. *Appl. Spectrosc.* **1985**, *39*, 343.
- (37) Dutta, P. K.; Shieh, D. C.; Puri, M. *J. Phys. Chem.* **1987**, *91*, 2332.
- (38) Dutta, P. K.; Twu, J. *J. Phys. Chem.* **1991**, *95*, 2498.
- (39) Twu, J.; Dutta, P. K.; Kresge, C. T. *Zeolites* **1991**, *11*, 672.
- (40) Angell, C. L.; Flank, W. H. In *Molecular Sieves II*; J. R. Katzer, Ed.; American Chemical Society: Washington, DC, 1977; pp 194.
- (41) Dutta, P. K.; Shieh, D. C. *J. Phys. Chem.* **1986**, *90*, 2331.
- (42) Dutta, P. K.; Del Barco, B. *J. Phys. Chem.* **1988**, *92*, 354.
- (43) Dutta, P. K.; Puri, M. *J. Phys. Chem.* **1987**, *91*, 4329.
- (44) Twu, J.; Dutta, P. K.; Kresge, C. T. *J. Phys. Chem.* **1991**, *95*, 5267.
- (45) Buchanan, G. W.; Kirby, R. A.; Ripmeester, J. A.; Ratcliffe, C. I. *Tetrahedron Lett.* **1987**, *28*, 4783.
- (46) Buchanan, G. W.; Khan, M. Z.; Ripmeester, J. A.; Bovenkamp, J. W.; Rodrigue, A. *Can. J. Chem.* **1987**, *65*, 2564.
- (47) den Ouden, C. J. J.; Datema, K. P.; Visser, F.; Mackay, M.; Post, M. F. *M. Zeolites* **1991**, *11*, 418.
- (48) Hayashi, S.; Suzuki, K.; Shin, S.; Hayamizu, K.; Yamamoto, O. *Chem. Phys. Lett.* **1985**, *113*, 368.
- (49) Baerlocher, C.; McCusker, L. B.; Chiappetta, R. *Microporous Mater.* **1994**, *2*, 269.
- (50) Dognier, F.; Patarin, J.; Guth, J. L.; Anglerot, D. *Zeolites* **1992**, *12*, 160.
- (51) Saenger, W. *Angew. Chem. Int. Ed. Engl.* **1980**, *19*, 344.

- (52) Lehn, J. -M.; Montavon, F. *Helv. Chim. Acta* **1978**, *61*, 67.
- (53) Kodama, M.; Kimura, E.; Yamaguchi, S. *J. Chem. Soc., Dalton Trans.* **1980**, 2536.
- (54) Sekido, E.; Kawahara, H.; Tsuji, K. *Bull. Chem. Soc. Jpn.* **1988**, *61*, 1587.
- (55) Haymore, B. L.; Lamb, J. D.; Izatt, R. M.; Christensen, J. J. *Inorg. Chem.* **1982**, *21*, 1598.
- (56) Kasatani, K.; Sato, H. *Chem. Lett.* **1986**, 991.
- (57) Buncel, E.; Shin, H. S.; van Truong, N.; Bannard, R. A. B.; Purdon, J. G. *J. Phys. Chem.* **1988**, *92*, 4176.
- (58) Gabelica, Z.; Blom, N.; Derouane, E. G. *Appl. Catal.* **1983**, *5*, 227.
- (59) Aiello, R.; Crea, F.; Nastro, A.; Subotic, B.; Testa, F. *Zeolites* **1991**, *11*, 767.
- (60) de Ruiter, R.; Jansen, J. C.; van Bekkum, H. *Zeolites* **1992**, *12*, 56.
- (61) Gilson, J. -P. In *Zeolite Microporous Solids: Synthesis, Structure, and Reactivity*; E. G. Derouane, F. Lemos, C. Naccache and F. R. Ribeiro, Eds.; Kluwer Academic: Dordrecht, 1992; pp 19.
- (62) Iton, L. E.; Trouw, F.; Brun, T. O.; Epperson, J. E.; White, J. W.; Henderson, S. J. *Langmuir* **1992**, *8*, 1045.
- (63) Bodart, P.; Nagy, J. B.; Gabelica, Z.; Derouane, E. G. *J. Chim. Phys.* **1986**, *83*, 777.
- (64) Wijnen, P. W. J. G.; Beelen, T. P. M.; van Santen, R. A. In *Expanded Clays and Other Microporous Solids*; M. L. Ocelli and H. E. Robson, Eds.; Van Nostrand Reinhold: New York, 1992; pp 341.

Chapter Five

Towards the “Rational Synthesis” of Zeolites

In the investigations of the mechanisms of structure direction and self-assembly in the syntheses of Si-ZSM-5 and EMT and FAU, the common theme is the organization of extended silicate or aluminosilicate structures, i.e., on the length scale of 10–200 Å, by organic structure-directing agents as the essential process in zeolite nucleation and crystal growth. However, the nature of the extended structures and the means by which the organic species participates in their formation and the assembly into the final product are different for the two systems investigated. In the synthesis of Si-ZSM-5 in the presence of either tetrapropylammonium (TPA) or 1,6-hexanediamine, the formation of composite silicate–organic structures is determined initially by favorable overlap of the hydrophobic hydration spheres of the organic and silicate species. Subsequent optimization of intermolecular, inorganic–organic van der Waals interactions provides the essential structure-directing influence. By contrast, in the syntheses of EMT and FAU, the inorganic gel composition alone may determine the types of extended, aluminosilicate structures that are formed (in particular, each alkali metal ion favors the formation of certain structural types), while the organic species influence the orientation in which these structures assemble to create the long-range order within the crystalline zeolite. The formation of a sandwich-like complex via ion–dipole interactions between the sodium/18-crown-6 complex and the ring of six oxygen atoms in the smaller supercage of EMT is proposed as the key step in structure direction. In both cases, weak, non-covalent interactions between the organic and inorganic components that are easily masked by the influence of stronger structure-directing species, e.g., high concentrations of alkali metal cations, provide the essential intermolecular forces through which structure direction occurs.

The significance of extended structures in zeolite synthesis underscores the conceptual connection between the processes involved in zeolite self-assembly and the hierarchy of organization in self-assembled structures in biological systems.¹ Molecules spontaneously assemble into composite structures of increasing larger length scales. In both zeolite synthesis and biological systems, weak, non-covalent interactions, e.g., van der Waals interactions and ion–dipole forces, play a significant role in the multipoint molecular recognition processes that occur at the different levels of organization. For example, hydrophobic hydration and hydrophobic interactions provide important contributions to protein folding and to the formation of lipid bilayer membranes; these organized structures provide the subunits for larger architectures.

The primary difficulty in investigating the nature and extent of organization within the extended structures involved in zeolite synthesis is the absence of techniques suited to direct characterization of structures on this length scale. Small-angle neutron scattering (SANS) and small-angle X-ray scattering (SAXS) data can demonstrate the existence of structures on the order of approximately 20–1000 Å but cannot be used to probe the molecular composition or organization within the extended structures.² Complementary techniques such as NMR and IR spectroscopy can provide evidence for short-range interactions, e.g., the observation of van der Waals contacts between TPA and silicate species by ¹H–²⁹Si CP MAS NMR in the synthesis of Si–ZSM-5, thus allowing some characterization of the extended structures. NMR spectroscopy and systematic variations in synthesis composition in combination with the SANS and SAXS studies from other researchers²⁻⁷ provide strong evidence for the proposed structures and compositions of the extended structures implicated in the mechanisms of

structure direction in the syntheses of Si-ZSM-5 and EMT described in this thesis. Additional indirect evidence for the mechanism of structure direction proposed for Si-ZSM-5 might be provided by a ^1H - ^{29}Si CP MAS NMR study of the synthesis of Si-ZSM-5 using a siloxane-functionalized tetrabutylammonium structure-directing agent (Figure 5.1).⁸ If close contact between the alkyl groups (non-siloxane) of the organic species and the silicate species (similar to that observed by ^1H - ^{29}Si CP MAS NMR in the tetrapropylammonium-mediated synthesis of Si-ZSM-5) is established simultaneously with covalent linkage of the siloxane moiety to the condensed silicate structure (monitored by ^{29}Si MAS NMR), this would suggest that the proposed inorganic-organic composite structures are formed.

The proposed mechanism for the synthesis of Si-ZSM-5 can likely be generalized to other examples of structure direction in the synthesis of high-silica and pure-silica zeolites. The primary impetus for developing a mechanistic understanding of zeolite synthesis is the ultimate goal of the “rational design” and synthesis of novel zeolite pore architectures. The true test of the validity of the newly-found insights and understanding of the role of inorganic-organic interactions in zeolite synthesis (particularly for the synthesis of high-silica materials) lies in their applicability to the synthesis of new zeolites and molecular sieves. Although it may not be possible to control the precise atomic arrangements required to construct a particular structure, parameters such as the type of void space (one-dimensional channels, intersecting channels, isolated cages, or interconnected cage networks), the size and shape of the void spaces and the intervening apertures, and the arrangement of the void spaces relative to each other within the crystal unit cell should be amenable to the

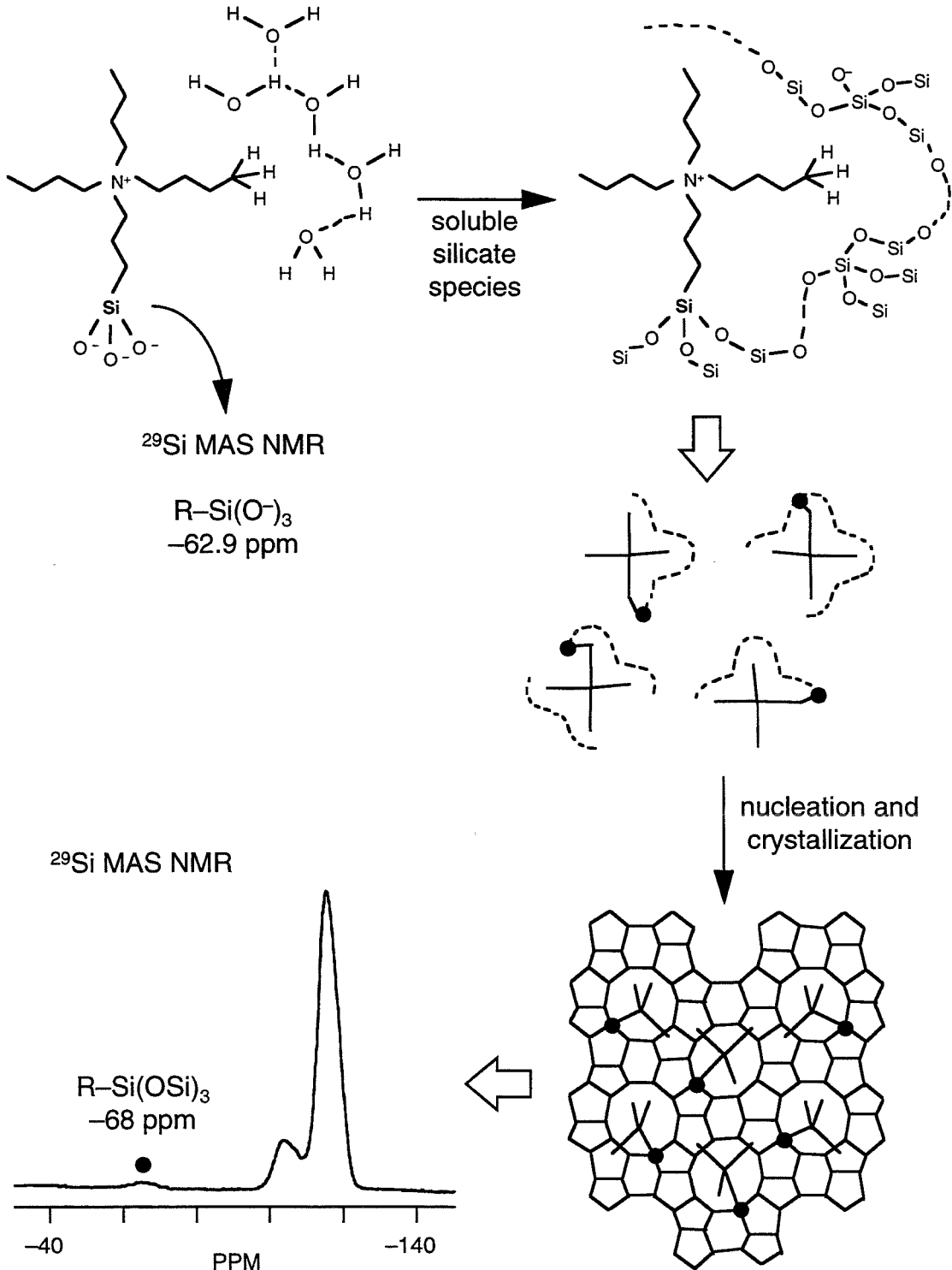


Figure 5.1. Proposed mechanism of structure direction in the synthesis of Si-ZSM-5 using siloxane-functionalized tetrabutylammonium.

influence of organic structure-directing agents. Many different topologies should be accessible to a pure-silica tetrahedral network because of the flexibility of the Si–O–Si bond⁹ and because the thermodynamic preference for the formation of dense phases, i.e., quartz or amorphous silica, versus microporous materials is small ($\approx 2\text{--}3$ kcal mol⁻¹).¹⁰ The presence of aluminum in the tetrahedral network appears to favor certain structural features, such as intersecting channels and pores,¹¹ and small amounts of aluminum can apparently be tolerated within a synthesis gel while remaining amenable to the influence of organic structure-directing agents. Low concentrations of alkali metal ions, particularly sodium, may facilitate zeolite synthesis, whereas high concentrations may mask or eliminate the relatively weak influence of the organic species. As observed for the two zeolite syntheses investigated here, it may be possible to control the formation of inorganic–organic composite structures and thus the van der Waals interactions that lead to structural specificity in high-silica systems. By contrast, in aluminum-rich synthesis mixtures it may only be possible to influence the orientation in which preorganized inorganic structures, determined by the inorganic gel composition, assemble to form the product structure.

Zones and coworkers have recently demonstrated the first example of zeolite synthesis by a priori design in the synthesis of SSZ-26.^{11,12} With the goal of making a novel zeolite containing a multidimensional channel system with large-pore (twelve-ring, or >7 Å in diameter) intersections, a diquatery ammonium propellane species was chosen based on geometric considerations (Figure 5.2). Conceptually, this compound is derived from a bicyclic, diquatery ammonium species that has a linear axis and has been used in the syntheses of ZSM-12 and EU-1,¹¹ both

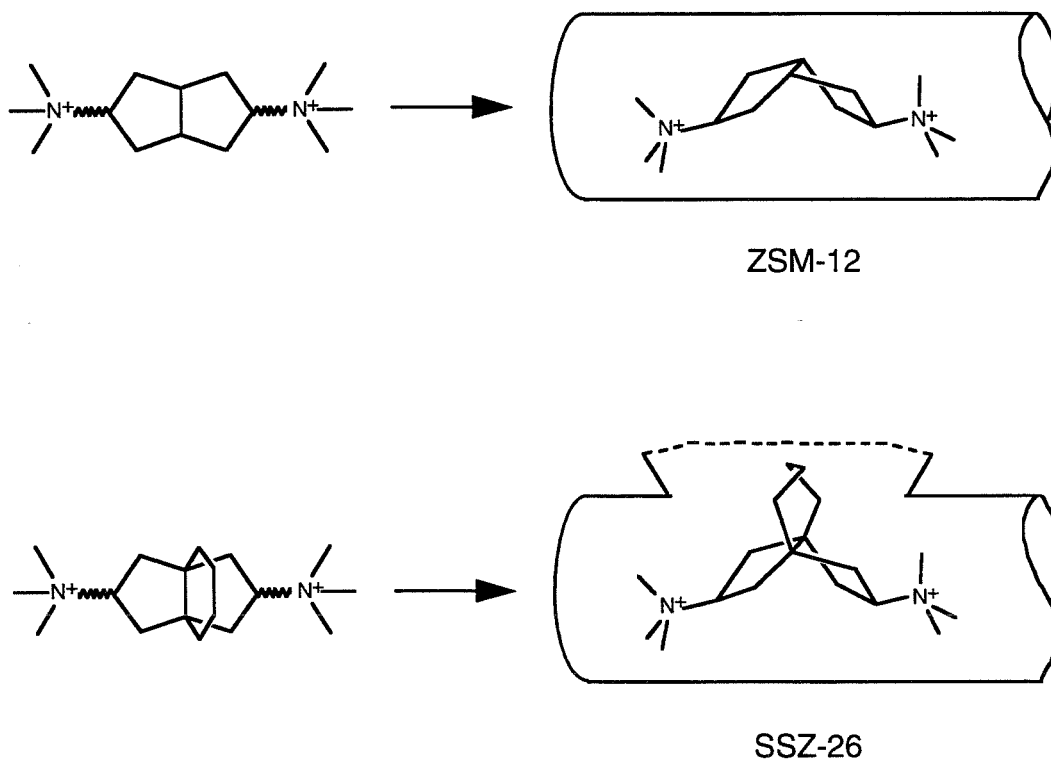


Figure 5.2. Representation of how a dicationic ammonium propellane species might disrupt the formation of a linear channel structure in SSZ-26.¹¹

one-dimensional channel structures. Introduction of the fused cyclohexane ring generates a molecule that is too large to be contained within a one-dimensional channel or an isolated cage. Thus, the diquatery, bicyclic portion of the organic molecule may direct the formation of a channel structure while the third ring may disrupt the one-dimensional channel such that an intersection might be created. The resulting high-silica zeolite, SSZ-26, is composed of intersecting ten-ring and twelve-ring channels (or, more correctly, an intergrowth of two related polymorphs, each composed of these intersecting channels), with one molecule of the organic structure-directing agent immobilized at each channel intersection, as anticipated.¹³

Among all of the properties of the organic agents used, e.g., charge, chemical character, size, and geometry, structure direction appears to be most dependent on the geometry of the organic molecule, as suggested by the examples of EMT (Chapter Four) and SSZ-26. For high-silica syntheses, the structure-directing effect of the organic species is exhibited primarily via optimized van der Waals interactions with the inorganic species; it is through these interactions in the formation of composite species that the shape of the organic molecule can be translated into the zeolite pore architecture. As demonstrated by the NMR results from the TPA-mediated synthesis of Si-ZSM-5 and from the series of tetraalkylammonium ions described in Chapters Two and Three, the hydrophobic character of the organic species also makes a significant contribution to the structure-directing ability. The origin of the higher degree of structural specificity present in examples of templating, i.e., the close correspondence between the contour of the zeolite pore and the geometry of the organic molecule, remains to be elucidated, and is likely

due to the distribution of hydrophilic and hydrophobic domains within the multiply-charged organic templates such as those used in the synthesis of ZSM-18. A better understanding of the hydrophobic hydration behavior of quaternary alkylammonium species may provide insight into the design of new structure-directing agents. If the organic species exhibits the appropriate balance of hydrophobic and hydrophilic character, a sufficient extent of hydrophobic hydration can occur in solution such that the formation of inorganic–organic composite species is favored. It may be possible to screen potential organic structure-directing agents by observing their interactions with silicate species via the ^1H – ^{29}Si CP MAS NMR technique. Thus, by considering issues such as the hydrophobic hydration behavior and the optimization of inorganic–organic van der Waals interactions, the successful design of organic structure-directing agents and templates for the synthesis of new zeolite structures may be possible.

References

- (1) Mann, S.; Archibald, D. A.; Didymus, J. M.; Douglas, T.; Heywood, B. R.; Meldrum, F. C.; Reeves, N. J. *Science* **1993**, *261*, 1286.
- (2) Dokter, W. H.; Beelen, T. P. M.; van Garderen, H. F.; Rummens, C. P. J.; van Santen, R. A.; Ramsay, J. D. F. *Colloids Surfaces A* **1994**, *85*, 89.
- (3) Henderson, S. J.; White, J. W. *J. Appl. Cryst.* **1988**, *21*, 744.
- (4) Iton, L. E.; Trouw, F.; Brun, T. O.; Epperson, J. E.; White, J. W.; Henderson, S. J. *Langmuir* **1992**, *8*, 1045.
- (5) Wijnen, P. W. J. G.; Beelen, T. P. M.; van Santen, R. A. In *Expanded Clays and Other Microporous Solids*; M. L. Ocelli and H. E. Robson, Eds.; Van Nostrand Reinhold: New York, 1992; pp 341.
- (6) Regev, O.; Cohen, Y.; Kehat, E.; Talmon, Y. *J. Phys. IV (Orsay, Fr.)* **1993**, *C8*, 397.
- (7) Regev, O.; Cohen, Y.; Kehat, E.; Talmon, Y. *Zeolites* **1994**, *14*, 314.
- (8) Li, H. -X.; Cambor, M. A.; Davis, M. E. *Microporous Mater.* **1994**, *3*, 117.
- (9) Giesinger, K. L.; Gibbs, G. V.; Navrotsky, A. *Phys. Chem. Minerals* **1985**, *11*, 266.
- (10) Petrovic, I.; Navrotsky, A.; Davis, M. E.; Zones, S. I. *Chem. Mater.* **1993**, *5*, 1805.
- (11) Zones, S. I.; Santilli, D. S. In *Proceedings of the Ninth International Zeolite Conference, Montreal, 1992*; R. Von Ballmoos, J. B. Higgins and M. M. J. Treacy, Eds.; Butterworth-Heinemann: Boston, 1993; pp 171.
- (12) Zones, S. I.; Olmstead, M. M.; Santilli, D. S. *J. Am. Chem. Soc.* **1992**, *114*, 4195.

- (13) Lobo, R. F.; Pan, M.; Chan, I.; Li, H. -X.; Medrud, R. C.; Zones, S. I.; Crozier, P. A.; Davis, M. E. *Science* **1993**, *262*, 1543.